



# The intestine under stress

*Effects of chemotherapy on the intestinal epithelium*

The intestine under stress

*Effects of chemotherapy on the intestinal epithelium*

Melissa Verburg

Thesis, Erasmus University – with references – with a summary in Dutch

ISBN 90-9017040-5

Printed in The Netherlands

© 2003 Melissa Verburg, Amsterdam, The Netherlands.

All rights reserved. No part of this thesis may be reproduced or transmitted in any form, by any means, electronic or mechanical, without prior written permission of the author.

# The intestine under stress

Melissa Verburg

*Effects of chemotherapy on the intestinal epithelium*

## De darm onder stress

*Gevolgen van chemotherapie voor het darmepitheel*

## Proefschrift

ter verkrijging van de graad van doctor aan de  
Erasmus Universiteit Rotterdam

op gezag van de

Rector Magnificus

Prof.dr.ir. J.H. van Bommel

en volgens besluit van het College voor Promoties.

De openbare verdediging zal plaatsvinden op  
woensdag 25 juni 2003 om 9.45 uur  
door

Melissa Verburg

geboren te Amsterdam

Promotiecommissie

Promotor(en): Prof.dr. H.A. Büller

Overige leden: Prof.dr. E.J. Kuipers  
Prof.dr. D. Tibboel  
Prof.dr. R. Pieters

Copromotor(en): Dr. A.W.C. Einerhand  
Dr. J. Dekker

The first part of the work described in this thesis was performed at the laboratory of Pediatric Gastroenterology & Nutrition of the Academic Medical Center, Amsterdam, The Netherlands. It was continued and completed at the Laboratory of Pediatrics, Pediatric Gastroenterology & Nutrition of the Erasmus Medical Center, Rotterdam, The Netherlands. Part of this project was financially supported by Numico bv, Zoetermeer, The Netherlands.

Publication of this thesis was financially supported by Sectie Experimentele Gastroenterologie van de Nederlandse Vereniging voor Gastroenterologie, The Netherlands and by Nutricia Nederland bv, The Netherlands.

## List of abbreviations

AP	alkaline phosphatase
BAC	benzalkonium chloride
BrdU	bromodeoxyuridine
CPS	carbamoylphosphate synthase
EGF	epidermal growth factor
EGF-R	epidermal growth factor receptor
ENS	enteric nervous system
ER	endoplasmatic reticulum
FABP	fatty acid binding protein
M-FABP	membrane bound fatty acid binding protein
FAT	fatty acid translocase (CD 36)
FATP	fatty acid transporter protein
I-FABP	intestinal fatty acid binding protein
L-FABP	liver fatty acid binding protein
FITC	fluorescein isothiocyanate
GALT	gut associated lymphoid tissue
GLP-2	glucacon-like peptide 2
GLUT2	glucose transporter 2
GLUT5	glucose transporter 5
HE	hematoxilin & eosin
IGF	insuline-like growth factor
IL	interleukin
LAC	lactase
LCFA	long chain fatty acids
LYS	lysozyme
MAT	matrilysin
MUC2	mucin 2
PCNA	proliferating cell nuclear antigen
PP	Peyer's patch
SCFA	short chain fatty acids
SI	sucrase-isomaltase
SGLT 1	sodium glucose transporter 1
TJ	tight junctions
TFF3	intestinal trefoil factor
TGF $\alpha/\beta$	transforming growth factor alfa/beta
TNF $\alpha$	tumor necrosis factor alfa
TUNEL	terminal transferase deoxyuridine nick-end labeling

# Contents

<b>Scope of this Thesis</b>	<b>8</b>
<b>1 Introduction</b>	
Structure of the Small Intestinal Epithelium	10
<i>Cell types of the small intestinal epithelium</i>	
<i>Epithelial Cell Renewal</i>	
<i>Crypt dynamics</i>	
<i>Stem Cells</i>	
<i>Markers of Epithelial Proliferation</i>	
<i>Apoptosis</i>	
Nutrient Degradation & Absorption	15
<i>Enterocytes</i>	
<i>Dietary Carbohydrates</i>	
<i>Dietary Lipids</i>	
<i>Fatty Acid Binding Proteins</i>	
<i>Intestinal Alkaline Phosphatase</i>	
The Intestinal Epithelial Barrier	17
<i>Goblet Cells</i>	
<i>Paneth Cells</i>	
<i>Gut-Associated Lymphoid Tissue (GALT)</i>	
The Enteric Nervous System	20
<i>Mast Cells</i>	
<i>Stress</i>	
Methotrexate as Chemotherapeutic Drug	23
<i>Mechanism of Action of MTX</i>	
<b>2 Aims and Outline of this Thesis</b>	<b>24</b>
<b>3 Selective sparing of goblet cells and Paneth Cells in the intestine of methotrexate-treated rats</b>	<b>28</b>
<i>Introduction</i>	
Materials and Methods	30
<i>Animals</i>	
<i>Morphology</i>	
<i>Immunohistochemistry</i>	
<i>Histochemistry</i>	
<i>Terminal transferase deoxyuridine nick-end labeling</i>	
<i>Northern blots</i>	
<i>Statistical analysis</i>	
Results	33
<i>Clinical symptoms</i>	
<i>Proliferation</i>	
<i>Morphology</i>	
<i>MTX-induced apoptosis</i>	
<i>Epithelial gene expression during MTX-induced damage and regeneration</i>	
<i>Sparing of goblet cells and Paneth cells</i>	
Discussion	39

#### **4 Specific responses in rat small intestinal epithelial mRNA expression and protein levels during chemotherapeutic damage and regeneration**

<i>Introduction</i>	42
Materials and Methods	45
<i>Animals</i>	
<i>Morphology</i>	
<i>Immunohistochemistry</i>	
<i>Histochemistry</i>	
<i>Terminal transferase deoxyuridine nick-end labeling</i>	
<i>Northern blots</i>	
<i>Statistical analysis</i>	
Results	47
<i>The model</i>	
<i>Enterocytes</i>	
<i>Goblet and Paneth cells</i>	
<i>Expression of enterocyte-specific mRNAs</i>	
<i>Expression of goblet and Paneth cell-specific mRNAs</i>	
<i>Expression levels of epithelial proteins</i>	
Discussion	52

#### **5 Protection of the Peyer's patch-associated crypt and villus epithelium against methotrexate-induced damage is based on its distinct regulation of proliferation**

<i>Introduction</i>	56
Materials and Methods	57
<i>Animals</i>	
<i>Experimental design</i>	
<i>Histology</i>	
<i>Immunohistochemistry</i>	
<i>In situ hybridization</i>	
<i>Probe preparation</i>	
<i>Statistical analysis</i>	
Results	61
<i>Histological evaluation</i>	
<i>Epithelial proliferation</i>	
<i>Epithelial apoptosis</i>	
<i>Enterocyte-specific gene expression</i>	
<i>Goblet cell-specific gene expression</i>	
<i>Paneth cell-specific gene expression</i>	
Discussion	63

#### **Colour illustrations to chapters 3-6**

67

#### **6 Isolation stress increases small intestinal sensitivity to chemotherapy in rats**

<i>Introduction</i>	76
Materials and Methods	77
<i>Animals</i>	
<i>Immunohistochemistry</i>	
<i>Scoring of epithelial damage</i>	
<i>Mast cell staining</i>	
Results	81
<i>Isolation of rats increases the MTX-induced inhibition of epithelial proliferation</i>	
<i>Isolation of rats increases the MTX-induced crypt damage</i>	
<i>Changes in epithelial protein expression are dose and stress dependent</i>	
<i>Mucosal mast cells</i>	
Discussion	85

#### **7 Summarizing discussion**

90

<i>Epithelial cytoprotection has priority over digestive function</i>
<i>Local regulation of the intestinal epithelial proliferation and differentiation</i>
<i>Intestinal damage and stress</i>
<i>Possible interventions</i>
<i>Concluding remarks</i>

#### **8 Nederlandse samenvatting**

96

References	101
Curriculum Vitae	107
List of Publications	108
Acknowledgements\ Dankwoord	109

# Scope of this thesis

Every year, around 500 new pediatric and 60.000 new adult cancer patients are identified in the Netherlands, divided over some 50 different clinical diagnoses. Yearly, in the Netherlands around 30.000 cancer patients die. Thanks to extensive research in the last decennia and newly implemented treatment protocols, more and more cancer patients can currently be cured. Besides operative removal of the tumors and their metastasis, which is only effective in a minority of the cancers, treatment most often consists of a combination of irradiation and chemotherapy. Until today, anti-cancer treatments are often long-lasting and painful. The intensity of the therapy needs to be carefully monitored in order to prevent toxic side effects from becoming a life-threatening problem.

Besides the bone marrow, a major dose-limiting organ in anti-cancer treatments is the intestine. Malfunctioning of the small intestine, through the application of anti-cancer drugs and local irradiation therapy, is clinically manifested by abdominal pain, malabsorption, malnutrition, anorexia, dehydration, weight loss and diarrhea. This syndrome is caused by a dysfunction of the intestinal epithelial cells, which are responsible for the degradation and absorption of nutrients as well as the protection against pathogens and other substances in the intestinal lumen.

The intestine is a relative large organ. Starting at the stomach and ending at the anus, the intestine is divided in two parts with different functions. The first and longest part is called the small intestine due to its relative narrow circumference. This part is indispensable for the digestion and absorption of nutrients, such as carbohydrates, fatty acids, proteins and vitamins. The second part is the colon. Here, the remaining bulk is further degraded by residing micro-organisms. Useful products such as short chain fatty acids, vitamin B, bile acids and other sterols, can be absorbed. The colon is also the part where the faeces is formed, through resorption of water. At the



transition from small intestine to colon, humans have a rudimentary appendix with no apparent function which is analogous to the coecum in rodents. In contrast to the appendix, the coecum is continuous with the rest of the intestine and functional as part of the colon.

The life-time of the epithelial cells in the small intestine is in the order of days. To remain healthy, the small intestinal epithelium is continuously producing new cells. Because of the relative high cell turnover, the epithelium of the small intestine is very sensitive for the action of anti-cancer drugs, such as methotrexate, which inhibit cell proliferation. Effective concentrations of this drug in anti-cancer treatments lead to a reduction in the numbers of intestinal epithelial cells within days. It can be easily imagined that during this decrease in cell numbers the ability of the epithelium to absorb sufficient amounts of nutrients is under great pressure. Similarly, the cytoprotective capacity is likely to be reduced, thereby rendering the epithelium more sensitive to damage, and allowing unwanted substances and organisms to enter the body more freely.

Most research in analyzing the consequences for intestinal epithelial functions has focussed on morphological changes. Much less is known about the functions of the various types of intestinal epithelial cells. For further improvement in effective treatment of cancer patients, a better understanding of intestinal physiology during chemotherapy is essential. Insight in the functional changes and failures of the intestine in response to anti-cancer treatment would allow to offer protection and repair to this indispensable organ. In addition, it could also lead the way for development of clinical diets that could assist in the prevention of malnutrition in, especially pediatric, cancer patients.

In studying the effects of cytostatic drugs on intestinal function, the use of experimental animals is indispensable. Only they permit a detailed analysis of the entire organ in time,

allowing each study of each phase of the disease. This would be both unethical and technically very difficult to perform in biopsies of human patients, especially in cancer patients who are already suffering from both disease and treatment. In our studies, the rat was chosen as a model, because of the similarities to humans in intestinal physiology and the availability of techniques and tools.

In this thesis, attention was focussed on the absorptive and defensive functions of the intestine during damage and regeneration induced by the cytostatic drug methotrexate (MTX). MTX was chosen among the various cytostatic drugs available, because of the considerable knowledge about its pharmacology and its way of action in humans and animal species. As folic acid analogue, MTX directly seizes the proliferative machinery of the intestine, thereby disturbing the normal cell turnover of the epithelium.

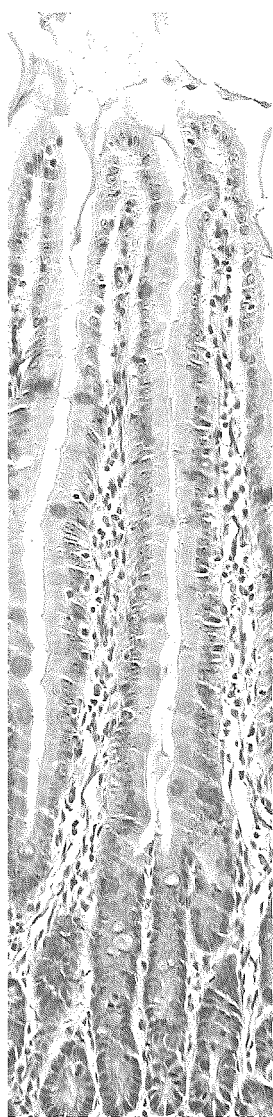


Figure 1.1  
Alcian blue/nuclear fast red  
staining of rat small intestinal  
epithelium. Stem cells and  
proliferating cells are localized  
in the crypts (c). Along the  
crypt-villus axis, the epithelium  
is populated by enterocytes  
(white), goblet cells (blue),  
entero-endocrine cells (arrow)  
and Paneth cells (arrowhead).

Structure of the Small  
Intestinal Epithelium

The small intestinal epithelium is formed by a monolayer of cells with numerous invaginations (crypts) and finger-like folded structures (villi). This highly folded structure covers the entire intestinal mucosa and separates the exterior (i.e. the intestinal lumen) from the bodies interior. Figure 1.1 shows a cross-section of rat small intestinal epithelium with its characteristic crypt-villus organization.

Cell types of the small intestinal epithelium  
Along the crypt-villus axis, the epithelium is populated by four differentiated cell types: enterocytes, goblet cells, entero-endocrine cells and Paneth cells, each with specific functions. Detailed accounts of the numbers of each cell type in the small intestine of adult mice on tissue sections showed a regional variations in the population of each cell type (Table 1.1). On average, about 88% of the cells are enterocytes, 4% are goblet cells, 0.5% are entero-endocrine cells and 7.5% are Paneth cells (Cheng and Leblond 1974a). In rats and humans, the frequencies of these cell types are similar to those found in mice.

The epithelium functions as a highly selective barrier in all regions of the small intestine, to prevent the entrance of toxins and noxes into the body's interior. At the same time, the epithelium orchestrates the dynamic processes of nutrient degradation and absorption. To this end, the intestinal epithelial cells express a wide range of specific enzymes and transporter proteins. The absorptive and defensive functions are under the control of both

Table 1.1  
Cell types in the crypts and villi of the small intestine of adult mice, calculated as the percentage of total cells. Data are from: Cheng and Leblond, 1974a.

	Duodenum		Jejunum		Ileum	
	crypts	villi	crypts	villi	crypts	villi
Enterocytes	92,4	97,3	86,0	95,0	84,1	87,6
Goblet cells	3,7	2,5	5,9	4,6	8,9	12,1
Entero-endocrine cells	0,6	0,2	0,6	0,4	0,4	0,3
Paneth cells	3,3	-	7,5	-	6,6	-

autonomous and environmental signals during normal as well as during pathological conditions, such as after chemotherapy.

Along the proximal-to-distal axis, the small intestine is divided into three regions. The first part is the duodenum and is about 12 cm long in adult rats. It continues into the jejunum that extends for about 70 cm, and ends in the ileum that measures about 15 cm in rat. There are morphological and functional differences along the proximal-to-distal axis of the small intestine. For instance, the length of the villi and the proliferation rate in the crypts decrease towards the distal end of the small intestine. Furthermore, the digestive functions of the small intestinal epithelium in duodenum, jejunum and ileum are overlapping but not the same. There is a region-specific expression of genes that mediate the different epithelial functions along the proximal-to-distal axis of the small intestine (Gordon 1993, 1989; Traber 1994).

#### Epithelial Cell Renewal

The small intestinal epithelium has one of the most rapid cell turnover rates among mammalian tissues. Cells are produced by stem cells and proliferating daughter cells in the lower half of the crypts of Lieberkühn (Figure 1.1). Most of the newly produced cells migrate as a cohort in a rapid, orderly way out of the crypts and up to the villus tip. During migration these cells differentiate into functional enterocytes, entero-endocrine cells, or goblet cells. The journey takes about 3 days in rodents and 5 days in humans, then the epithelial cells are removed from the villus tip by either apoptosis or shedding into the lumen (Potten et al. 1997b). The cells that migrate to the base of the crypts differentiate into Paneth cells. These cells reside below the stem cell level (Figure 1.1). Paneth cells have a relative long life-time of about 3 weeks in humans and rodents before undergoing apoptosis.

Despite the high turnover of the epithelium, its integrity is remarkably stable, which is

reflected by the very low incidence of small intestinal cancers. From all malignancies in the gastrointestinal tract only 2% are situated in the small intestine, which predominantly arise in the smooth muscular tissue but not in the epithelium (Blanchard et al. 2000). Of all malignant tumors in the small intestine, 30%-50% are adenocarcinomas. The majority of which arise in the proximal duodenum and jejunum (Gill et al. 2001). Remarkably, site with the highest risk of developing tumors is the duodenum (65%), despite the fact that it contributes only 4% of the overall length of the small intestine (Hutchins et al. 2001).

Because of the high cell turnover, intestinal epithelial cells are highly sensitive for chemotherapeutic drugs such as methotrexate (MTX), which inhibit epithelial proliferation. Until today, the detailed consequences of such an inhibition of proliferation for the function of the different intestinal epithelial cells remains unclear.

#### Crypt Dynamics

The most detailed studies of gut epithelial renewal have been performed in mice. An average crypt in adult mouse small intestine contains about 250 cells (Table 1.2). When viewed in longitudinal cross section, crypts are approximately 22 cells in height with 16 cells forming an average circumference at the widest point (Bach et al. 2000). Incorporation studies of tritiated thymidine or bromodeoxyuridine indicate that between 50-80% of all crypt cells are proliferative of which 150-160 are in rapid cycle, whereas 75 of these are in S-phase at any one time (Bach et al. 2000).

Table 1.2

*Estimates of small-intestine epithelial cell dynamics in the crypt-villus units of mice and humans. Data are from: Potten et al. 1997b; Wright and Irwin 1982.*

	Mouse	Human
Cells/crypt	250	450
Cell cycle	10-18 h	20-73 h
Stem cell cycle	~24 h	>36 h
Stem cells/crypt	4-16	unknown
Transit cell generations	4-6	>4-6
Crypts/villus	6-14	~6
Cells/villus	2000-8000	unknown
Crypts/intestine	1-3 x 10 <sup>6</sup>	unknown

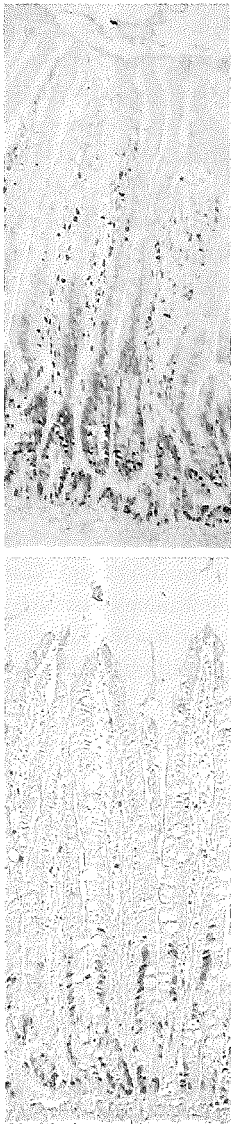


*Figure 1.2*  
*In rat and human small intestine, PCNA expression is localized in epithelial cells in the crypt compartment and in stromal lymphocytes (A). Like PCNA, BrdU-positive cells can be visualized on tissue sections with the use of immunohistochemistry (B).*

Radio-label dilution studies have shown that cells in the upper region of the crypt have only limited division potential. The number of mitotic divisions increases toward lower cell positions and is maximal at positions 6-9 from the crypt base, where the cells have an average cell cycle time of 12-13 h (Potten et al. 1997a).

#### Stem cells

Eventually, all epithelial cells are derived from epithelial stem cells. The numbers of stem cells that are present in a small intestinal crypt was investigated by different research groups. Based on indirect evidence from studies in mice, the number of stem cells ranges between four and sixteen (Loeffler et al. 1997). In mice, stem cells divide on average once every 24 h. Each crypt produces about 12 cells per hour or about 300 new cells per day (Potten and Loeffler 1990). In humans, the cell cycle times of stem cells are less well defined; studies in the colon indicate that they are between four and eight times longer, compared with mice (Bach et al. 2000). Through studies on the migration velocity of tritiated thymidine-labeled crypt cells, e.g. in cell positions per unit of time, the actual stem cells appear to be positioned at about 4-6 cell positions from the crypt base in the small intestine (Potten et al. 1997a). The actual stem cells as well as first, 2nd and 3rd generation of clonogenic daughter cells are all localized within the first 7 cell positions from the base of the crypt (Figure 1.1).

The undifferentiated nature of these cells makes it impossible to recognize them in situ using specific labeling protocols. Stem cells can only be defined by their functions. They are capable of proliferation, thereby producing many different progeny. Furthermore, they allow regeneration of the tissue after injury (Potten et al. 1997a). The proliferation of stem cells is inhibited by the action of anti-cancer drugs, such as MTX.

According to Potten and colleagues, stem cells are organized in an hierarchic manner. There findings in regenerating chimeric mice,

following irradiation or drugs that reduce stem cell numbers, together with the positional analysis of apoptosis in small intestinal crypts, suggest that three apparently distinct categories of stem cells can be distinguished (Potten and Hendry 1995). The actual stem cells are the less differentiated ones, being very sensitive to DNA damage and unable to repair such damage. These cells are irreversibly damaged and die through apoptosis within about 6 h after 1 Gy of gamma-radiation. By committing suicide following injury, these cells execute the ultimate form of protection. The use of computer modeling indicates the presence of approximately 4-6 actual stem cells in a normal steady state adult mouse small intestinal crypt (Potten and Loeffler 1990).

A supposed second category of stem cells appears to consist of 6 clonogenic cells per crypt with lower sensitivity toward gamma-radiation. These 6 daughter cells are derived after division of one or more actual stem cells and normally become dividing transit cells and subsequently differentiated epithelial cells. However, at this early stage they have the ability to repair their DNA and retain stem cell properties (Roberts et al. 1995). Hence, in a situation where the actual stem cells are killed, such as by local radiation or chemotherapy, these cells may repopulate the crypt stem cell niche.

A third category of 16-24 stem cells is being recruited as the level of damage increases and the first two stem cell types have been killed. This has been demonstrated in highly cytotoxic radiation studies using above 9 Gy of gamma-radiation, in which the small intestinal crypts recruited about 30-40 clonogenic cells during regeneration (Potten et al. 1997a). Thus, as the level of damage increased, the crypts called upon more and more clonogenic cells. All together the crypts had the ability to call upon about 36 (28-42) clonogenic cells to ensure crypt survival. It is therefore proposed that there is a hierarchical loss of stemness over two cell divisions, without loss of the ability to repopulate the crypt (Potten et al. 1997a).

The potency of crypts to regenerate following damage is solely attributed to stem cells, and not to other lineages of the proliferative zone. Evidence for this comes from studies in mice and rat in which the small intestinal crypts were damaged with large doses of radiation (Al-Dewachi et al. 1980, 1977; Potten et al. 1990). The regeneration of the damaged crypts initiated at the position that is attributed to stem cells (i.e. upto 7 cell positions from the crypt base), whereas the mid- and upper crypts did not have the capacity to regenerate. Similarly, crypts could be sterilized by a dose of irradiation that spared the mid- and upper crypts, which contain undifferentiated proliferating daughter cells (Hendry et al. 1989).

Markers of Epithelial Proliferation  
Proliferating cell nuclear antigen (PCNA) and 5-bromo-2'-deoxyuridine (BrdU) are commonly used markers to assess proliferation in human and animal tissues. PCNA, or DNA polymerase  $\delta$ -associated antigen, is an evolutionary highly conserved acidic nuclear protein of 35 kD, previously known as cyclin (Mathews et al. 1984). The expression of PCNA is essential for DNA replication in eukaryote cells (Waseem and Lane 1990). PCNA can be demonstrated by immunohistochemistry on routinely processed and embedded tissues (Hall et al. 1990). In rat and human small intestine, PCNA expression is localized in epithelial cells in the crypt compartment and in stromal lymphocytes (Figure 1.2 a). The half-life of PCNA is relative long, about 20 h (Bravo and Macdonald-Bravo 1987). Therefore, immunohistochemical detection is not restricted to cells in S-phase.

The uridine-analogue BrdU can be used *in vivo* for the analysis of proliferation, through a pulse-labeling of proliferating cells. When injected in substantial amounts (50 mg/kg body weight.) in rodents, BrdU will be incorporated into the DNA of cells during S-phase. Like PCNA, BrdU-positive cells can be visualized on tissue sections with the use of immunohistochemistry (Figure 1.2 b).

### Apoptosis

Apoptosis is a form of genetically controlled cell death. The control of cell death is of major importance for maintenance of homeostasis in rapidly dividing tissues such as the small intestine (Potten et al. 1997b). In the crypts, apoptosis serves to remove mutated or superfluous (stem) cells. Apoptosis in the small intestine occurs predominantly in cells that have reached the villus tip. As an alternative mechanism these cells can also be removed through shedding. Under conditions that lead to DNA damage or disturbances in DNA synthesis, like irradiation or cytostatic drugs, apoptosis is induced in the proliferative crypt cells.

A classical apoptotic cell has a very distinctive morphology which has well been described in literature. Initially, the cell cytoplasm shrinks and the cell becomes detached from its neighbors. The nucleolus disappears and the chromatin becomes condensed around the nuclear membrane. At a light microscopical level, these shrinking cells can be recognized on tissue sections stained with haematoxylin and eosin (HE). After fragmentation of the cell into smaller membrane-bound vesicles, these so-called apoptotic bodies are phagocytosed by neighboring cells. Unlike necrosis, the organized packaging of the dying cell into smaller fragments and their uptake by neighboring cells may very well be to save energy.

During the process of apoptosis the cell activates a variety of caspases, such as caspase-3, which can be used to identify these cells with immunohistochemical methods (Grossmann et al. 1998). Caspase-3 is such a apoptose-linked protease and responsible for the cleavage of poly (ADP-ribose) polymerase. The enzyme, also known as apopain, is composed of two subunits of relative molecular mass 17K and 12K that are derived from a common pro-enzyme, identified as CPP32. Cleavage of the two subunits is required to obtain proteolytic activity and subsequent induction of apoptosis. The suitability of cleaved caspase-3 in the detection

of apoptotic cells has been demonstrated in the small intestine of mice, where radiation significantly induced cleaved caspase-3 staining in the crypts and not on the villi (Marshman et al. 2001).

## Nutrient Degradation and Absorption

### Enterocytes

Most of the small intestinal epithelial cells differentiate into enterocytes. Enterocytes are highly specialized polarized cells, responsible for the degradation and absorption of nutritional compounds. At the same time these cells play a role in intestinal mucosal immunity and maintenance of the barrier. In the crypts and on the villi, enterocytes have distinct functions. In the crypts, secretory functions of the enterocytes predominate, whereas the enterocytes of the villi have mainly hydrolytic and absorptive functions.

Degradation and absorption of ingested carbohydrates, proteins and lipids, as well as vitamins, minerals, and trace elements occurs in the apical membrane of villus enterocytes. This highly folded membrane domain, named brush border, harbors a whole range of enzymes and proteins, including lactase, sucrase-isomaltase, sodium glucose cotransporter 1, glucose transporter 5, and alkaline phosphatase. Intra-cellularly, enterocytes contain binding proteins, such as fatty acid binding proteins, which are needed for the transport of specific substrates to the basolateral membrane. At the basolateral side, these substrates are transported to the blood. All degradation and absorption processes are highly specific and the expression of metabolic enzymes is tightly regulated. The consequences of chemotherapy for the function of enterocytes is thus far not well understood.

### Dietary Carbohydrates

Dietary carbohydrates include mono-, di-, and polysaccharides. Disaccharides, such as lactose and sucrose, as well as polysaccharides, such as starch, are degraded in the intestinal

lumen into mono-saccharides before they can be taken up by enterocytes (Dekker et al. 2002a). The small intestinal epithelium contains several glycohydrolases that are indispensable in degrading the more complex carbohydrates into absorbable mono-saccharides.

In newborns, the sole source of carbohydrate is lactose, present in mammalian milk. This disaccharide is exclusively hydrolyzed by lactase in the small intestine. Mature lactase is 160 kDa and expressed in the apical membrane of villus enterocytes. The mean functional residence time of lactase was estimated 7.8 h in *in vivo* experiments in adult rat (Dudley et al. 1993). Lactase is responsible for hydrolysis of the disaccharide lactose, into glucose and galactose.

The more complex carbohydrates, consumed at later age, are degraded in the small intestine primarily by sucrase-isomaltase (SI). SI consists of 2 subunits, which are both encoded by the SI gene and cleaved after translation by pancreatic proteinases into a 120 kDa sucrase subunit and a 140 kDa isomaltase subunit (Van Beers et al. 1995). SI is localized in the apical membrane of villus enterocytes and has its active sucrase and maltase domains in the intestinal lumen. The mean residence time of functional SI is 5.8 h in rat (Dudley et al. 1993). SI is responsible for hydrolysis of the disaccharide sucrose into glucose and fructose. Sucrose is found in many fruits and some vegetables. Importantly, SI is particularly important for the degradation of maltose, which is the main degradation product of starch. The maltose is split by either of the two subunits of SI in two glucose residues, which can be absorbed by the intestine.

In mammalian intestine, absorption of degraded carbohydrates is mediated via selective transporter proteins, specific for one or more hexoses or pentoses. The most important proteins for digestion and absorption of carbohydrates are schematically represented in Figure 1.3.

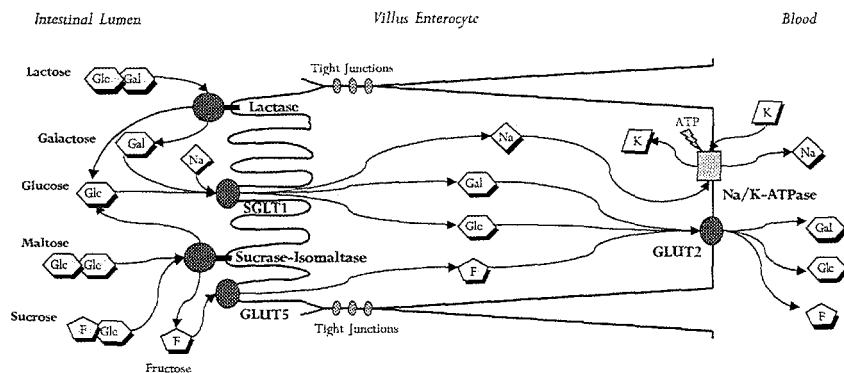
The major transporter involved in glucose absorption in humans and rodents is the sodium ( $\text{Na}^+$ )-coupled glucose transporter (SGLT1). SGLT1 is localized in the apical membrane of enterocytes and actively takes up glucose (and galactose), in combination with sodium ( $\text{Na}^+$ ) (Figure 1.3). Most glucose is derived from dietary starch. Another important carbohydrate transporter is GLUT5. GLUT5 passively takes up fructose through facilitated diffusion. GLUT5 is localized in the apical membrane of enterocytes (Figure 1.3). Its activity is driven by the concentration gradient of fructose over the plasma membrane. Fructose is present for instance in processed apple juice. Since the uptake of fructose can be relatively easily saturated, high amounts of fructose in the diet may in fact lead to malabsorption symptoms, and may be one of the causes of 'toddlers diarrhea' in children. At the basolateral side of the enterocyte, fructose as well as glucose and galactose are passed to the blood through the facilitative hexose transporter GLUT2 (Figure 1.3).

Figure 1.3

Hexose and pentose transport through enterocytes. From: (Dekker et al. 2002a) Schematic representation of a small intestinal enterocyte showing the most important compounds of the carbohydrate hydrolysis and absorption system. The enterocyte is shown with its apical membrane to the left, and the basolateral membrane to the right. These plasmamembrane domains are separated by the tight junctions, which also serve to seal off the intestinal luminal compartment from the bodies interior. Indicated are the most important glycohydrolases, lactase and sucrase-isomaltase, and the three most important monosaccharide transporter proteins, SGLT1, GLUT2, and GLUT5. Also indicated is the sodium/potassium ATPase ( $\text{Na}^+/\text{K}^+$ -ATPase) that is responsible for the sodium (and potassium) gradient over the apical brushborder membrane, which is essential for the active uptake of glucose and galactose over this membrane. Glc, glucose; Gal, galactose; F, fructose; Na, sodium; K, potassium. From: (Dekker et al. 2002a)

#### Dietary Lipids

Dietary lipids (triacylglycerols) are mainly composed of long-chain fatty acids ( $>\text{C}_{16}$ ). These are liberated from lipid droplets in the proximal part of the small intestine by pancreatic lipases and bile acids. These liberated fatty acids form mixed micelles with bile acids to increase their solubility. Other dietary lipids are cholesterol esters and phospholipids. Although lipophilic molecules can passively diffuse across cell membranes, enterocytes are supplied with lipid transporters at the apical membrane to absorb





long chain fatty acids from the lumen (Abumrad et al. 1999; Abumrad et al. 2000). The conditions for lipid absorption can be favored by lowering the pH microclimate in the jejunum, which results in an enhanced dissociation of the mixed micelles and a higher fatty acid uptake (Shiau 1990).

Genes involved in mammalian lipid absorption are FABPM, FAT/CD36 and FATP (Dutta-Roy 2000). In the small intestine, the fatty acid translocase FAT is an abundant protein for uptake of long chain fatty acids (LCFAs). FAT is localized in enterocytes of the upper two-third of the small intestinal villi (Poirier et al. 1996). In addition, the fatty acid transporter protein FATP4 has been identified as the major intestine-specific isoform of fatty acid transporters (Stahl et al. 1999). Fatty acids are transported intracellularly to the endoplasmic reticulum (ER) to be re-esterified and, depending on the hydrophobicity, either or not incorporated into chylomicrons, and transported to the basolateral membrane. Basolaterally secreted chylomicrons are taken up by the lymphatic system. In contrast, medium-chain and short-chain fatty acids, which are less hydrophobic compared to LCFAs, are essentially found in the blood bound to albumin (Stahl et al. 1999).

#### Fatty acid binding proteins

The intracellular transport processes of fatty acids is mediated by fatty acid binding proteins (FABPs). They are members of a family of 14-15 kDa proteins (Storch and Thumser 2000). Two FABPs are known to be expressed in mammalian enterocytes, e.g. intestinal- (I-) and liver (L-) FABP. Studies with fluorescent fatty acids and model membranes suggest that I-FABP may be involved in uptake and specific targeting of fatty acids to subcellular membrane sites, whereas L-FABP may serve as cytosolic buffer to balance unbound fatty acid concentrations within the cell (Storch 1990). The use of specific antibodies and immunohistochemical methods have shown a co-expression of these proteins in rodent small intestine (Shields et al. 1986). Expression of

I-FABP but not L-FABP, is regulated by the cytokine TGF-beta, as shown in studies using TGF-beta knockout mice (Fontaine et al. 1996).

Intestinal alkaline phosphatase  
Intestinal alkaline phosphatase (I-AP) is a membrane-bound enzyme at the apical membranes of enterocytes in the intestinal epithelium which can dephosphorylate various phosphorylated substrates. The natural substrate of I-AP is not known but endotoxin is a likely candidate (Poelstra et al. 1997). In one study, I-AP was capable of inactivating endotoxins in vivo (Poelstra et al. 1997). Through the inactivation of bacteria, I-AP contributes to protection of the intestinal epithelium. In rats it was shown that I-AP expression and localization is regulated by dietary triacylglycerols (Zhang et al. 1996). Movement of I-AP from the apical membrane to the supra-nuclear Golgi region, in response to triacylglycerols, suggest that I-AP plays a role in fat absorption.

#### The Intestinal Epithelial Barrier

There are several factors that contribute to the maintenance of the epithelial barrier. An important structural component is formed by the tight junctions. These are highly organized membrane networks between adjacent cells (Nusrat et al. 2000; Powell 1981). Another important component serving protection against infiltrating noxes and pathogens is formed by the mucus layer (Dekker et al. 1999). Mucus mainly consists of gel-forming mucins, which cover the luminal side of the epithelium (Van Klinken et al. 1997). The gel structure of mucins also forms a specific anchorage for micro-organisms. It has been described that the intestinal lumen serves as a host for some 400 different bacterial species in humans (Bry et al. 1996). By their permanent residence as symbiotic organisms this so-called microflora prevents that unwanted prokaryotes invade the epithelium.

#### Goblet cells

Goblet cells constitute 4-20 % of the epithelial cells depending on their position along the

duodenal- colonic axis. Goblet cells contribute to the epithelial barrier through the expression of mucins. Mucins are large glycoproteins with a molecular weight of  $>1,000$  kD. There are at least 18 different epithelial mucins identified (Dekker et al. 2002b). These mucins are expressed in a tissue-specific manner, of which MUC2 is the most prominent mucin in the small and large intestine (Van Klinken et al. 1997).

In addition to mucin, goblet cells of the small and large intestine also constitutively express and secrete trefoil peptides. Trefoil peptides are small molecules and extremely protease-resistant. They are expressed in the gut and important for epithelial protection. There is a region-specificity leading to expression of TFF1 and TFF2 in the stomach and TFF3 in the small and large intestine. Expression of intestinal trefoil factor (TFF3) is induced in damaged intestinal mucosa, where it enhances repair through induction of epithelial restitution (Dignass et al. 1994). Restitution is a rapid process by which differentiated intestinal epithelial cells migrate over denuded connective tissue to reseal superficial wounds. The movement of cells requires rearrangements in the cells cytoskeleton. In cell lines it was shown that TFF3 promotes migration through its effects on E-cadherin, APC and catenin expression (Efsthathiou et al. 1998). The purpose of restitution is to prevent the formation of gaps in the epithelial barrier.



**Figure 1.4**  
*Alcian blue/nuclear fast red staining of a tissue section containing a Peyer's patch in rat small intestinal epithelium. Immune cells, which regulate the immune response, are localized inside the lymphoid nodules (domes).*

#### Paneth cells

Deep down in the base of the crypts of the small intestine lie the Paneth cells. Paneth cells are thought to perform antibacterial functions. Their extensive endoplasmic reticulum and secretory granules allow them to secrete large quantities of peptides and proteins, such as lysozyme, TNF alpha, and cryptdins, which contribute to the local immunity (Ouellette 1999). Their position, in the base of the crypts, allow Paneth cells to offer protection to the epithelial stem cells. The genetic information that lies in these cells is endlessly passed through to daughter cells during proliferation. To maintain a healthy

epithelium, stem cell integrity is vital. Paneth cells are capable of preserving the viability of stem cells by protecting crypts from bacterial overgrowth (Ouellette 1997). Interestingly, certain species such as dog and pig appear to lack Paneth cells, which contradicts their supposed essential function in crypt immunity (Potten et al. 1997a).

Morphologically, the activation of Paneth cell defense is characterized by an increase in the numbers of cells and an enlargement of the intracellular granules, as observed using electron microscopy (Brennan et al. 1998; Jeynes and Altmann 1978; Sulikowska and Lewicki 1990). Studies in mice showed that activated Paneth cells release a whole series of cryptdins. At least some of these cryptdins need to be activated before their bactericidal activity becomes functional. This activation is done by the protease matrilysin, which is also expressed and secreted by Paneth cells (Lopez-Boado et al. 2000; Wilson et al. 1995; Wilson et al. 1997; Wilson et al. 1999). Matrilysin secretion is induced in response to bacteria, both in vitro and in vivo. Furthermore, it is not detectable in germ-free animals, unless they are inoculated with bacteria such as *Bacteroides thetaiotaomicron* (Lopez-Boado et al. 2000). An important antibacterial enzyme secreted by Paneth cells is lysozyme. This enzyme breaks down the peptidoglycan of bacteria and thus contributes to the maintenance of local immunity.

#### Gut-Associated Lymphoid Tissue (GALT)

The lumen of the gastrointestinal tract is continuous with the outside of the body and much of it is heavily populated with potentially pathogenic microorganisms. It is thus important that the immune system establishes and maintains a strong representation at this mucosal boundary. Indeed, the intestinal mucosa is heavily laden with lymphocytes, macrophages and other cells that participate in immune responses.

Aside from all of its other functions, the gastrointestinal tract is a lymphoid organ, and the lymphoid tissue within it is collectively

referred to as the gut-associated lymphoid tissue or GALT. Lymphocytes of the GALT can, based on location, be distributed in three populations:

- 1 Peyer's Patches: These are lymphoid follicles similar in many ways to lymph nodes, located in the mucosa and extend into the submucosa of the small intestine, especially the ileum (Figure 1.4).
- 2 Lamina propria lymphocytes: These are lymphocytes scattered in the lamina propria of the mucosa. A majority of these cells are IgA-secreting B cells.
- 3 Intraepithelial lymphocytes: These are lymphocytes that are positioned in the basolateral spaces between luminal epithelial cells, beneath the tight junctions.

Another important component of the gastrointestinal immune system is the M or microfold cell. M cells are localized in the intestinal epithelium that endocytose a variety of protein and peptide antigens. Instead of digesting these proteins, M cells transport them into the underlying tissue, where they are taken up by macrophages. Macrophages that receive antigens from M cells present them to T cells in the GALT, leading ultimately to appearance of immunoglobulin A-secreting plasma cells in the mucosa. The secretory IgA is transported through the epithelial cells into the lumen, where, for example, it interferes with adhesion and invasion of bacteria. T cells exposed to antigen in Peyer's patches also migrate into the lamina propria and the epithelium, where they mature to cytotoxic T cells, providing another mechanism of epithelial defense.

#### The Enteric Nervous System

The nervous system exerts a profound influence on all digestive processes, namely motility, ion transport (associated with secretion and absorption), and gastrointestinal blood flow. Some of this control emanates

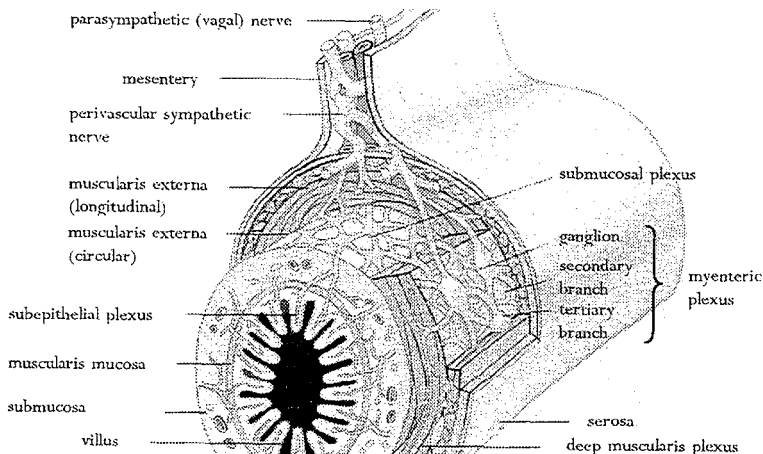
from connections between the digestive system and central nervous system (CNS) via parasympathetic and sympathetic nerves. Besides the CNS, the digestive system is endowed with its own, local nervous system, the enteric nervous system (ENS). With a collection of 108 neurons, it has the ability to innervate the intestinal muscles in response to mechanical stimulation from the lumen, independently of input from the brain or spinal cord. Anatomically, the ENS is organized in 2 plexuses of ganglia: the submucosal (Meissner's) plexus and the myenteric (Auerbach's) plexus, both of which are embedded in the wall of the digestive tract (Figure 1.5).

Figure 1.5

*The enteric nervous system is composed of two ganglionated plexuses. The larger myenteric plexuses, situated between the circular and the longitudinal layers of the muscularis externa, contains the neurons responsible for motility and for mediating the enzyme output of adjacent organs. The smaller submucosal plexus contains sensory cells that 'talk' to the motor neurons of the myenteric plexus, as well as motor fibers that stimulate secretion from epithelial crypt cells into the gut lumen. Other anatomical landmarks of note include parasympathetic (vagal) fibers entering the bowel in the mesentery, perivascular sympathetic input to the gut, and the subepithelial plexus of nerve fibers in the lamina propria of the mucosa.*

The myenteric plexus is located between the longitudinal and circular layers of muscle in the tunica muscularis and exerts control primarily over digestive tract motility. The submucosal plexus is buried in the submucosa. Its principal role is in sensing the environment within the lumen, regulating gastrointestinal blood flow and controlling a variety of epithelial functions. In addition to the two major enteric nerve plexuses, there are minor plexuses beneath the serosa, within the circular smooth muscle and in the mucosa.

Within enteric plexuses are three types of neurons:



1 Sensory neurons receive information from sensory receptors in the mucosa and muscles. Chemoreceptors sensitive to acid, glucose and amino acids have been demonstrated which, in essence, allows 'tasting' of luminal contents. Sensory receptors in muscle respond to stretch and tension. Collectively, enteric sensory neurons compile a comprehensive battery of information on gut contents and the state of the gastrointestinal wall.

2 Motor neurons within the enteric plexuses control gastrointestinal motility and secretion, and possibly absorption. In performing these functions, motor neurons act directly on a large number of effector cells, including smooth muscle, secretory cells (chief-, parietal-, mucous-, pancreatic exocrine cells, and enterocytes) and gastrointestinal endocrine cells.

3 Interneurons are largely responsible for integrating information from sensory neurons and providing this information to enteric motor neurons.

In addition to neurons, the ENS also contains interstitial cells of Cajal (ICC), localized between the two layers of the muscularis externa and in the muscularis plexus. ICC's have been identified as intestinal pacemaker cells. Abnormalities in ICC are increasingly recognized in a number of disorders such as infantile hypertrophic pyloric stenosis, Hirschsprung's disease, inflammatory bowel diseases, slow transit constipation, and chronic intestinal pseudo-obstruction.

Enteric neurons secrete an array of neurotransmitters, such as acetylcholine, 5-HT, substance P, and many neuropeptides (e.g. vasoactive intestinal polypeptide (VIP), neuropeptide  $\gamma$ , somatostatin). One major neurotransmitter produced by enteric neurons is acetylcholine. In general, neurons that secrete acetylcholine are excitatory, stimulating smooth muscle contraction, increases in intestinal secretions, release of enteric hormones and dilation of blood

vessels. Norepinephrine is also used extensively for neurotransmission in the gastrointestinal tract, but it derives from extrinsic sympathetic neurons; the effect of norepinephrine is almost always inhibitory and opposite that of acetylcholine.

Autonomic innervation by the ENS is involved in cell division and migration in the intestinal epithelium. For instance, the chemical or electrical stimulation of the cholinergic receptors was shown to have stimulatory effects on intestinal epithelial proliferation, whereas both chemical and surgical sympathectomy inhibited crypt cell proliferation in rats (Tutton and Helme 1974; Tutton 1975a; Tutton 1975b).

#### Mast cells

There are two types of mast cell populations in the intestinal mucosa. The mucosal mast cells, in the lamina propria, and the connective tissue mast cells, in the submucosa. They are both recruited from mast cell precursors in the bone marrow (Wershil 2000). Mucosal mast cells are localized in close proximity to nerves in the human gastrointestinal mucosa (Stead et al. 1989). Mast cells secrete a variety of regulatory mediators and cytokines such as biogenic amines, proteoglycans, proteases and TNF- $\alpha$  (Yu and Perdue 2001).

Mucosal mast cells serve both transport and barrier functions in the intestinal mucosa. For instance, mucosal mast cells have direct effects on intestinal epithelial permeability (Scudamore 1998) and mucin secretion (Castagliuolo et al. 1996). In mast cell-deficient rats it was further shown that mast cells enhance fluid secretion and neutrophil infiltration in endotoxin-mediated enteritis in mice (Wershil et al. 1998). Also the vascular permeability is regulated by the mucosal mast cells, such as during delayed type hypersensitivity reactions in the rat (Kranefeld et al. 1998).

In rats mucosal mast cells can be histochemically stained on tissue sections with the use of specific antibodies directed against rat

mast cell protease (Kimura 1998), as well as with alcian blue or toluidine blue (Stead 1987).

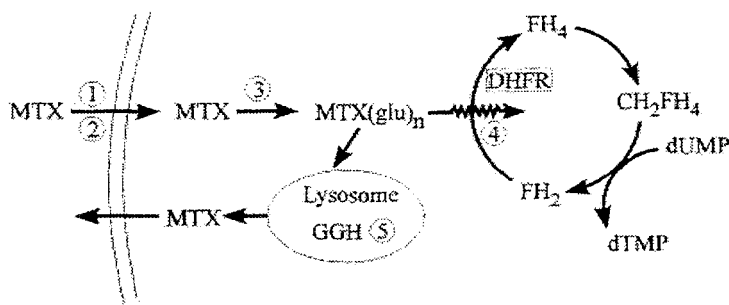
### Stress

Stress is known to induce a variety of physiological responses in the intestine. Two types of stress can be discriminated, the chronic and the acute form, which have different consequences for intestinal epithelial functioning. Chronic stress is based on the long-term effects of a physiological stressors, such as the repetitive appliance of an electrical shock, or immobilization, or removal of drinking water to laboratory animals. This type of stress results in decreased intestinal epithelial proliferation (Tutton and Helme 1973; Greant et al. 1988), increased intestinal ion secretion (Saunders et al. 1994), and increased intestinal epithelial permeability (Kiliaan et al. 1998) as well as endothelial permeability (Wilson and Baldwin 1998).

Figure 1.6

Sites of action of MTX and MTX polyglutamates (MTX(glu)<sub>n</sub>). MTX enters cells by either the reduced-folate carrier (1) or the membrane folate binding protein (2). MTX is then polyglutamylated by the enzyme folypolyglutamate synthetase (3). MTX(glu)<sub>n</sub> is a potent inhibitor of dihydrofolate reductase (DHFR) (4). MTX polyglutamates are hydrolyzed to MTX in the lysosome by gamma-glutamyl hydrolase (GGH) (5). FH<sub>2</sub> = dihydrofolate; FH<sub>4</sub> = tetrahydrofolate; CH<sub>2</sub>FH<sub>4</sub> = N<sup>5</sup>, N<sup>10</sup>-methylene tetrahydrofolate; dUMP = deoxyuridylate; dTMP = thymidine monophosphate; GGH = gamma-glutamyl hydrolase.

Studies in rats showed that sensory neurons (Ren et al. 2000), mast cells (Wilson and Baldwin 1999), and adrenal glucocorticoids (Meddings and Swain 2000) can be involved in the mechanism of chronic stress-induced mucosal changes. Much less is known about the effects of acute stress for intestinal epithelial functions.



## Methotrexate as Chemotherapeutic Drug

The folate antagonist MTX is widely used in (pediatric) cancer patients to kill neoplastic cells. The use of MTX to treat cancer patients has been extensively described. MTX is given either alone, or in combination with other chemotherapeutic agents. High doses of this anti-cancer drug lead to severe side effects in the small intestine and cause symptoms like abdominal pain, diarrhea, weight loss, mal-absorption, or even malnutrition. As a rescue therapy for proliferating epithelial cells after exposure to high concentrations of MTX, the reduced folate pools can be restored through by-passing the MTX-induced enzymatic block with leucovorin. This 'classical' combination therapy is successfully used in (childhood) leukemia. Also in cancer-bearing rats, primary tumor eradication can be realized through this combination of MTX and leucovorin (Poligeorgis et al. 1993).

### Mechanism of action of MTX

Methotrexate is an inhibitor of dihydrofolate reductase (DHFR), a key enzyme in the synthesis of thymidylate, and therefore, of DNA. Dihydrofolate reductase is responsible for the reduction of dihydrofolates to tetrahydrofolates (Figure 1.6). These reactions are essential in the biosynthesis of thymidilic acid, a DNA-specific nucleotide, and inosinic acid, a purine precursor. Binding of MTX to DHFR leads to a decrease in tetrahydrofolate-pools and thus to decreased thymidylate biosynthesis.

Although the response of the intestinal epithelium to MTX has been well described, the functions of the epithelial cell types during damage and regeneration are not well understood. From studies in human and rat it is known that MTX induces apoptosis in the proliferative compartment of the epithelium. It is described that the loss of epithelial crypts induces crypt loss, crypt atrophy and villus atrophy (Taminiau et al. 1980; Pinkerton et al. 1982; Altmann 1974; Trier 1962). With the use of biochemical and

histochemical methods, MTX treatment has been shown to lead to reduced expression of si and lactase enzyme activities in rat and mice small intestine (Taminiau 1980).

## 2 Aims & outline of this thesis

A well known side-effect of the use of the chemotherapeutic drug MTX in anti-cancer treatments is the inhibition of intestinal epithelial cell proliferation, which leads to villus atrophy in the small intestine. This side-effect is dose-limiting but the consequence of chemotherapeutic damage for intestinal epithelial functions remains largely obscure. We aimed to study the intestinal epithelial functions in response to chemotherapy with the use of an in vivo model, in which rats are injected intravenously with the cytostatic drug methotrexate (MTX). In this model we investigate epithelial functions in intestinal tissue segments during different stages of damage and regeneration. To this end, rats are sacrificed every 24 h after the administration of the drug until regeneration is complete. The reproducibility of our model will be tested using various concentrations of MTX ranging from 30-60 mg/kg. These will be given either as a single dose, or as a fractionated dose on two consecutive days. In the different drug-administration protocols we will analyze the inhibition of epithelial proliferation, the development of epithelial damage, the implications for intestinal epithelial functions and the regeneration of the intestinal epithelium.

In our study we will pay attention to possible region-specific differences in MTX sensitivity, since it is not known whether the severity of intestinal epithelial damage, provoked by cytostatic drugs, is dependent on the position along the horizontal axis and whether it can be modulated by local factors. To this end, we will carefully study intestinal epithelial morphology and function in different regions of the small intestine during damage and regeneration. And, since very little is known about the effects of cytostatic drugs on colonic functions, we also aim to study epithelial functions in the colon. To assess a possible role of local immuno-modulatory factors in the development of damage we will also focus on the epithelium in close proximity to Peyer's patches, which are known to contain immuno-regulatory T cells and B cells.



The inhibitory action of MTX on epithelial proliferation will be evaluated on tissue sections through detection of incorporated BrdU into the DNA of proliferating epithelial cells, which is injected 24 h before sacrificing the animals. The 24 h-interval between BrdU-administration and analysis of the tissue allows analysis of both proliferation and migration of the epithelial cells. As second, independent marker of proliferation we will localize the expression of proliferating cell nuclear antigen (PCNA). Both markers can be detected in situ using immunohistochemical methods.

To investigate the intensity of direct damage in proliferative cells of the epithelium, we qualitatively evaluate the induction of apoptosis on tissue sections. Apoptotic cells are stained on tissue sections using the TUNEL method. In addition, cells expressing cleaved caspase-3 are stained as second, independent marker of apoptosis. Identification of apoptotic cells with the use of these specific detection methods will be evaluated through comparison with morphological signs of apoptosis, such as cell shrinkage and appearance of apoptotic bodies, which can be observed on HE-stained tissue sections.

Epithelial functions will be studied through analysis of epithelial gene expression. The use of cell type-specific differentiation markers allows us to discriminate between the different cell types of the intestinal epithelium, i.e. enterocytes, goblet cells and Paneth cells. Through analysis of gene expression at mRNA and protein levels, insight will be obtained in regulatory events. Knowledge thus gathered regarding changes in epithelial functions during damage and regeneration could contribute to the development of specific diets, either via providing epithelial protection or by preventing malnutrition.

Enterocytes with their unique functions in nutrient-metabolism will be investigated through expression of a range of markers. Sucrase-isomaltase (SI), lactase (Lac), sodium-glucose cotransporter1 (SGLT1), and

the facilitative glucose transporter5 (GLUT5), will be used as characteristics for carbohydrate metabolism. Lipid metabolism will be screened via intestinal alkaline phosphatase (I-AP), intestinal fatty acid binding protein (I-FABP) and liver type fatty acid binding protein (L-FABP).

Goblet cell functions will be evaluated with the use of mucin (MUC2) and intestinal trefoil factor (TFF3) as markers. Both gene products are important for the barrier function of the epithelium. Loss of MUC2 expression will increase the vulnerability of the epithelium through an impairment of the mucus layer. Likewise, loss of TFF3 could lead to decreased intestinal repair, in particular via decreased ability for restitution.

The defensive functions of Paneth cells will be studied through analysis of the expression of lysozyme (LYS). Loss of lysozyme expression is potentially harmful and could contribute to a colonization of bacteria, especially in the crypts where these cells are localized. On the other hand, an increased expression of this protein could be important during phases of increased vulnerability. The specificity of changes in the expression of lysozyme will be evaluated by the use of matrilysin (MAT), a protease needed for cryptdin activation in mice, as second marker of Paneth cell function.

Intestinal epithelial regeneration is studied through analysis of a recovery of crypt-villus morphology in the small intestine and crypt morphology in the colon, as well as the recovery in cell type-specific gene expression in the small intestine and colon. Through comparison of gene expression patterns, in time and per cell type, insight is provided in regulatory mechanisms that control epithelial functions. In Chapter 3, three regions of the small intestine, i.e. duodenum, jejunum, and ileum, and the proximal part of the colon were studied to investigate possible region-specific differences in MTX-sensitivity. Morphological data are presented about changes in crypt- and

villus heights and changes in the population of functional epithelial cells during 4 phases of damage and repair. Furthermore, data are presented which indicate that not all cell types are equally sensitive for damage in the small intestine induced by MTX. The relative resistance of goblet cells and Paneth cells is demonstrated, compared to enterocytes, towards MTX-induced changes in epithelial differentiation with the use of immunohistochemical and biochemical methods. Also, preliminary data are presented on colonic changes in epithelial proliferation and morphology. Since the general effects of MTX on epithelial proliferation and morphology were similar along the horizontal axis, later chapters only describe the effects of MTX in the jejunum as representative for the entire small intestine.

In Chapter 4, a detailed analysis of the MTX - induced changes in epithelial mRNA and protein expression is presented during the 4 phases of damage and regeneration which could be discriminated in this model. With the use of statistical analysis, the specificity is shown of quantitative changes in mRNA and protein expression during these 4 phases of damage and regeneration. The presence of correlations between some, but not all, gene products of the same cell type is demonstrated, as well as the absence of correlations between gene products of different cell types. The mRNA and protein expression patterns in the MTX -treated rats, which are expressed as relative percentages of those seen in saline-injected controls, indicate a preference for fatty acid metabolism in contrast to carbohydrate metabolism during damage. Furthermore, the maintenance is demonstrated of defensive goblet cell functions during damage via expression of mucin (MUC2) and trefoil factor molecules (TFF3). And, with the use of statistical analysis the independent regulation of these genes during damage and regeneration is shown. Furthermore, the maintenance of Paneth cell function in epithelial protection during MTX -induced damage is demonstrated in Chapter 4 via the specific increased expression of lysozyme. All quantitative data

are underscored by immunohistochemical data, which are also presented in this Chapter.

In Chapter 5, the protection of intestinal epithelium in close proximity to Peyer's patches (PP) is described, compared to non-patch (NP) epithelium towards MTX. (Immuno) histochemical data are presented which show a reduced inhibition of proliferation in PP epithelia relative to NP epithelium, but equal induction of apoptosis in response to MTX. The absence of damage in PP epithelium, in contrast to NP epithelium, was demonstrated by a lack of changes in epithelial mRNA and protein expression using in situ hybridization and immuno-histochemical methods.

A possible role for the Central Nervous System in the development of intestinal damage is presented in Chapter 6, where the impact of stress during chemotherapy is demonstrated. Through the use of various concentrations and administration schedules of MTX in combination with different housing-conditions, a doubling is shown of small intestinal dysfunction under stressful circumstances.

### 3 Selective sparing of goblet cells and Paneth cells in the intestine of methotrexate-treated rats

Proliferation, differentiation and cell death were studied in the small intestinal and colonic epithelium of rats after a 2-days treatment with methotrexate. Days 1-2 after the final dose were characterized by decreased proliferation, increased apoptosis and decreased numbers and depths of small intestinal crypts, in a proximal-to-distal decreasing gradient along the small intestine. The remaining crypt epithelium appeared flattened, except for the Paneth cells, in which lysozyme protein and mRNA expression was increased. Regeneration through increased proliferation, during days 3-4, coincided with villus atrophy, showing decreased numbers of villus enterocytes and decreased expression of the enterocyte-specific genes *SI* and *CPS1*. Remarkably, goblet cells were spared at villus tips and remained functional in *MUC2* and *TFF3* gene expression. On days 8-10, all parameters had returned to normal in the whole small intestine. No methotrexate-induced changes were seen in epithelial morphology, proliferation, apoptosis, *MUC2* and *TFF3* immunostaining in the colon. The observed small intestinal sparing of Paneth cells and goblet cells following exposure to methotrexate, is likely to contribute to epithelial defensive during increased vulnerability of the intestinal epithelium.

Published as:

Melissa Verburg, Ingrid B. Renes, Helen P. Meijer, Jan A.J.M. Taminiau, Hans A. Büller, Alexandra W.C. Einerhand and Jan Dekker. 'Selective sparing of goblet cells and Paneth cells in the intestine of methotrexate-treated rats' in *Am J. Physiol Gastrointest Liver Physiol* 2000; 279: G1037-G1047.

#### Acknowledgements

We thank Prof D.K. Podolsky for kindly providing us with the rat *TFF3* probe and the *WE9*- and anti-rat *TFF3* antibodies. We are also grateful to Prof Dr R. Charles for providing us with both the anti-rat *CPS1* antibody and the rat *CPS1* probe. The anti-rat-sucrase-isomaltase antibody was a kind gift from Dr H.P. Hauri. Furthermore, we thank Dr W.S. Sly, for providing us with the anti-rat *CA1* antibody. We also thank Dr S. Krasinski, who kindly gave us the anti-rat-sucrase-isomaltase probe and Dr J. Power, for his donation of the rat lysozyme probe.

## Introduction

The intestinal epithelium forms a dynamic system of continuous proliferation, differentiation and cell death. In the crypt compartment, stem cells and proliferating cells produce new epithelial cells. During migration from the proliferative compartment towards the crypt base, villus tips (small intestine) or surface epithelium (colon), epithelial cells differentiate into distinct cell types, that can be identified using morphological criteria and through expression of specific genes. At villus tips and at the surface epithelium, cells are shed into the lumen or become phagocytosed after apoptosis (Hall et al. 1994).

Enterocytes form the largest population of epithelial cells. They express highly selective enzymes and transporter proteins that regulate nutrient uptake and fluid housekeeping in a well-orchestrated manner. Specific differences exist in the functions of enterocytes along the proximal-to-distal axis of the intestine, which are reflected in the regulated expression of region-specific genes (Walters et al. 1997). The vulnerable epithelium is protected against mechanical stress, luminal substances and pathological micro-organisms through the secretion of mucus. The mucus barrier consists mainly of mucins, which are large glycoproteins that are secreted by goblet cells (Tytgat et al. 1995a, Van Klinken et al. 1995). The relative numbers of goblet cells increase along the proximal-to-distal axis, constituting only a few percent in the duodenum but up to about 20 percent of the cells in the colon. Paneth cells, only present in the small intestine, are localized at the very base of the crypts and secrete anti-microbial polypeptides, like lysozyme, and growth factors into the lumen. In contrast to the enterocytes and goblet cells, which have lifespan of only 3 days in rat, the Paneth cells have a slower turnover resulting in a lifespan of about 3 weeks (Cheng 1974). Another small group of slowly renewing cells is formed by the enteroendocrine cells, specialized in the primarily mucosal secretion of hormonal peptides (Cheng and Leblond

1974b). Collectively, the epithelial cells maintain a high barrier function, principally through the presence of a tight junctional network between their plasma membranes, to separate the luminal content from the body's interior (Westcarr 1999).

The use of the cytostatic drug methotrexate (MTX) in anti-cancer treatments may severely impair intestinal epithelial function and therefore constitutes a dose-limiting factor in treatment schedules (Pinkerton et al. 1982). Like other chemotherapeutics it induces diarrhea and anorexia, accompanied with malabsorption, malnutrition and dehydration. Research has been performed on the effects of cytostatic drugs, including MTX, on the epithelium of the small intestine in animals. The use of animal experiments allows the analysis of the effects of a specific drug in time in all regions of the intestine, which would be impossible to perform in humans. Previously, it was shown in rats that MTX inhibited intestinal epithelial proliferation, which was followed by villus atrophy in the rat small intestine (Taminiau et al. 1980). Furthermore, during damage the levels of glycohydrolase enzyme activities strongly decreased in rat jejunum (Taminiau et al. 1980), suggesting enterocyte malfunction. In other studies using the cytostatic drug 5-fluorouracil (5-FU), expression of the aminopeptidase transporter 1 (PEPT1) appeared resistant to similar mucosal injury in rat ileum (Tanaka et al. 1998). In each study, the epithelium was able to fully regenerate. During regeneration, the epithelial cells increased in number and the enterocytes regained their degradative and absorptive functions. In several studies, the prophylactic or therapeutic administration of particular growth factors, vitamins or inhibitors of apoptosis could enhance the regenerative capacities of the epithelium in vivo (Farrell et al. 1998, Howarth et al. 1998, Howarth et al. 1996, Kanauchi et al. 1998, Logvinova et al. 1999, Nagai et al. 1993).

Despite numerous investigations, very little is known about the fate of the individual epithelial

lial cell types after exposure to cytostatic drugs. Also, little attention was paid to the response of the large intestine to MTX or other cytostatics. Knowledge of cell type-specific and region-specific variation in MTX sensitivity is still lacking, that is essential for the development of oral treatments in humans that could maintain or enhance intestinal epithelial cell functions during and after exposure to cytostatic drugs. In this study, we investigated in rats the mechanism of intestinal epithelial damage and regeneration in all regions of the small intestine and in the proximal colon using specific (immuno-) histochemical stainings for proliferating cells, enterocytes, goblet cells, Paneth cells and apoptotic cells. Furthermore, we quantified the expression of cell type-specific differentiation markers at the mRNA level. This will give us insight in the functional capacities of the epithelium during each phase of MTX-induced damage and subsequent regeneration.

## Materials and Methods

Unless otherwise indicated, chemicals and enzymes were obtained from the following manufacturers: Merck (Darmstadt, Germany); Sigma (St Louis, MO, USA); BDH (Poole, Dorset, UK); Boehringer Mannheim (Mannheim, Germany); Vector Laboratories (Burlingame, CA, USA); Dako (Glostrup, Denmark); Amerham (Buckinghamshire, UK) and Gibco-Bethesda Research Laboratories (Gaithersburg, MD, USA).

### Animals

Male Wag/Rij rats (Broekman, Utrecht, The Netherlands), aged 6 weeks (120–140 gram), were kept in conventional cages (3 rats per cage) in a specific-pathogen-free environment under controlled humidity and 12 h light/dark cycle (light: 7am–7pm) with free access to defined semisynthetic chow (1 mg/kg folic acid, Hope Farms, Woerden, The Netherlands) and water. The dosage schedule of MTX-treatment leading to intestinal damage and regeneration without causing death was obtained from pilot studies. At 10 am (Day –1), 20 mg/kg body

weight methotrexate (MTX, Ledertrexate SP forte, Cyanamid Benelux, Etten-Leur, The Netherlands) was injected intravenously under light anesthesia. Twenty-four h later (Day 0), a second injection of 10 mg/kg body weight MTX was given. Control animals received equivalent volumes of 0.9% sodium chloride solution both times. During the experiment, food intake, body weight, diarrhea and malaise were recorded daily. At days 1, 2, 3, 4, 5, 6, 8, and 10, the MTX-treated rats were sacrificed by decapitation. Control animals were sacrificed at day 8. To analyse epithelial proliferation, 50 mg/kg body weight bromodeoxyuridine (BrdU, Sigma), dissolved in sterile phosphate-buffered saline, pH 7.4 (PBS), was injected intraperitoneally 24 h prior to decapitation. Rats that were sacrificed at day 1 were injected with BrdU 17 h before decapitation. Segments of duodenum (proximal 3 cm of the small intestine), jejunum (anatomical middle of the small intestine), ileum (distal 3 cm of the small intestine) and proximal colon (proximal 3 cm of the colon) were rinsed in PBS, fixed in 4% formaldehyde (Merck) dissolved in PBS, dehydrated and embedded in Paraplast Plus (Sherwood Medical, Den Bosch, The Netherlands) according to standard procedures for (immuno-)histochemistry. In addition, small segments of the jejunum (0.5 cm) of each animal were frozen in liquid nitrogen and further stored at  $-80^{\circ}\text{C}$  for RNA-isolation.

#### Morphology

Epithelial morphology and apoptosis were analyzed on 6  $\mu\text{m}$  thick tissue sections after standard histochemical staining methods using either alcian blue (BDH) and nuclear fast red (Merck) or hematoxylin (Vector Laboratories) and eosin (Merck) (HE-stain). Crypt depth and villus height were measured manually in well-orientated sections (5 measurements per region per rat) using a micrometer (Nikon, Bunnik, The Netherlands) mounted in an Eclipse E800 Microscope (Nikon, Japan).

#### Immunohistochemistry

Proliferation and antigen expression were

detected using immunohistochemistry. Tissue sections were deparaffinized with xylene (Merck), rehydrated in graded ethanol solutions and treated with 1.5% (v/v) hydrogenperoxide (Merck) in PBS for 30 min at room temperature to remove endogenous peroxidase activity. Antigen unmasking was carried out by heating the sections for 10 min in 0.01 M sodium citrate (Merck, pH 6.0) at  $100^{\circ}\text{C}$ . For the anti-BrdU antibodies, all sections were incubated using 20 mg/ml proteinase K (Boehringer) in PBS for 7.5 min and colonic sections were additionally treated with 2 N HCl (Merck) for 90 min before incubation with the protease. Non-specific protein binding was blocked using a buffer containing 10 mM Tris (Merck), 5 mM EDTA (Merck), 0.15 M NaCl (Merck), 0.25% gelatin (Sigma), 0.05% Tween-20 (Merck), pH 8.0. All sections were incubated overnight ( $4^{\circ}\text{C}$ ) using the primary mouse monoclonal antibodies, anti-BrdU (Boehringer, 1:100-400), anti-human proliferating cell nuclear antigen (PCNA, Boehringer, 1:2500), anti-human MUC2 (WE9 (Tytgat et al. 1995b), 1:100) or the rabbit polyclonal antibodies anti-human lysozyme (Dako, 1:50), anti-calf alkaline phosphatase (Dako, 1:1500), anti-rat carbamoylphosphate synthase 1 (Gaasbeek Janzen et al. 1984) (1:5000), anti-rat sucrase-isomaltase (Yeh et al. 1991) (1:6000), anti-rat trefoil factor 3 (1:6000) or anti-rat carbonic anhydrase 1 (CA1, 1:6000). Immunodetection was performed using Vectastain elite ABC kit, peroxidase-conjugated (Vector Laboratories) and 0.5 mg/ml 3,3'-diaminobenzidine (Sigma) in imidazole buffer containing 30 mM imidazole (Merck) and 1 mM EDTA (Merck), pH 7.0. Sections were counterstained using ready-to-use hematoxylin (Vector Laboratories), mounted in Entellan (Merck) and analyzed under an Eclipse E800 Microscope (Nikon). To investigate whether the observed sparing of goblet cells during villus atrophy was statistically significant, MUC2-positive cells were counted in villi of the jejunum until day 4 after MTX. Ten crypt-villus axes were chosen per animal in well-orientated sections. The number and ratio of

MUC2-positive cells in the lower- and upper half of the villi of control and MTX-treated rats were compared using the Mann-Whitney *u* test. Similarly, the number of lysozyme-positive cells were counted in 10 jejunal crypts per animal, until day 4, to investigate the MTX-resistance of Paneth cells.

#### Histochemistry

Differentiated enterocytes expressing alkaline phosphatase activity were localized on deparaffinized, rehydrated tissue sections in an one step assay using 50  $\mu$ l nitroblue tetrazolium solution (NBT, Vector Laboratories) and 37.5  $\mu$ l bromo-chloro-indolyl phosphate solution (BCIP, Vector Laboratories) in 10 ml Tris (pH 9.5) as described by the manufacturer. After a 12 min incubation at room temperature, the reaction was stopped in distilled water. After mounting in Entellan (Merck), brush border staining was analyzed under an Eclipse E800 microscope (Nikon).

#### Terminal transferase deoxy-uridine nick-end labeling (tunel)

For the detection of apoptotic cells, the TUNEL method was used as described previously, with slight modifications (Moss et al. 1996). Briefly, following deparaffinization and rehydration, sections were incubated for 7.5 min with 20 mg/ $\mu$ l proteinase K (Merck) at room temperature. After rinsing in PBS and removal of endogenous peroxidase activity for 20 min using 1.5% (v/v)  $H_2O_2$  in PBS, sections were pre-incubated in 25 mM Tris, pH 6.6, 200 mM potassium cacodylate, 0.2 mM EDTA, 0.25 mg/ml bovine serum albumine (BSA) for 10 min. Subsequently, new buffer was added including 1 mM cobalt chloride, 0.4 pM digoxigenin-11-deoxyuridine triphosphate (Boehringer) and 25 U/ml terminal transferase (Boehringer) for a 90 min incubation at 37°C. Negative controls were included by omitting terminal transferase. Positive controls were incubated in 0.5 U/ml DNase (Boehringer) containing buffer, including 50 mM Tris (Merck, pH 9.2), 14 mM ammonium sulfate (Merck), 20% (v/v) dimethylsulfoxide (Merck), 0.3% (v/v) Tween-20 (Merck), 50

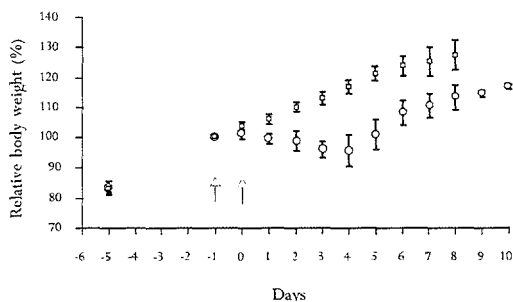


Figure 3.1

MTX-induced effects on body weight. For each rat, its body weight at the onset of treatment (day -1) was set arbitrarily at 100%. Rats of the control group ( $\circ$ ) and the MTX-treated group ( $\square$ ) were injected intravenously using NaCl or MTX, respectively at day -1 and day 0 (arrows). Individual changes in body weight relative to day -1 were recorded daily and averaged per group. Standard deviations are given in percentages of absolute weights. Rats of the MTX-treated group were sacrificed sequentially until day 10. Control rats were sacrificed at day 8.



mm MgCl<sub>2</sub> (Boehringer) and 100 mM CaCl<sub>2</sub> (Boehringer), prior to incubation with the terminal transferase. The reaction was stopped for 15 min using 300 mM NaCl and 30 mM sodium citrate and subsequently blocked for 10 min with 2% BSA in PBS. After rinsing in PBS, the sections were incubated overnight at 4°C using peroxidase conjugated Fab fragments (1:2000, Boehringer) in PBS. Binding of Fab fragments was visualized using 0.5 mg/ml 3,3'-diaminobenzidine, dissolved in imidazole buffer. Serial sections were stained using HE for comparison of TUNEL reaction with the known morphological criteria (nuclear shrinkage, apoptotic bodies) (Hall et al. 1994).

#### Northern Blots

Total RNA was isolated from frozen jejunal segments (0.5 cm) using Trizol Reagent (Gibco). Cell type-specific mRNA expression was quantified on both Northern- and Northern spot blots. For the detection of MUC2 and CPSI mRNA, 2 mg total RNA was spotted directly onto nylon membranes (HybondN+, Amersham) using a BioRad spot blot device (BioRad, Hercules, CA, USA). To detect SI, TFF3 and lysozyme mRNA, 10 mg total RNA was separated on 1-1.2% agarose gels (Boehringer) containing 3.5% glyoxal (Merck) before blotting. All blots were hybridized using specific <sup>32</sup>P-labeled cDNA probes. Hybridization signals were quantified using a PhosphorImager (Molecular Dynamics) after 1-3 days exposure time. The following probes were used: A 827 bp *ECOR*I-fragment of rat SI mRNA (Krasinski et al. 1994), a 1.9 kb *ECOR*I fragment of rat CPSI mRNA (Nyunoya et al. 1985), 1 kb of rat lysozyme mRNA (Yogalingam et al. 1996) and 438 bp of rat TFF3 mRNA (Suemori et al. 1991). For the construction of a rat MUC2 probe, RT-PCR was performed on colonic RNA using the following primers: ACC TGT CGA CTG GTA GAG GAG ATT ACC CCC AND GCT CTA GAT CAC ATG TGG TCA GGT TGC, based on the rat MUC2 coding sequence (Xu et al. 1992). 1.1 kb of rat MUC2 (bp 506-1560) was amplified and cloned in the *sal*I-*xb*aI sites of pBluescript SK+ (Promega

Biotech, Madison, WI, USA). Hybridized signals were corrected for glyceraldehyde-3-phosphate dehydrogenase (GAPDH) mRNA expression, to correct for the amount of loading, using 1.4 kb GAPDH mRNA as a probe.

#### Statistical analysis

Statistical analysis was performed on crypt depth, villus height, goblet cell- and Paneth cell numbers and mRNA expression using the Mann-Whitney-u test. Due to time-dependent intra-animal variations, data of 2 consecutive time points were pooled. A p-value of less than 0.05 was considered statistically significant.

## Results

#### Clinical symptoms

The intake of food and the gain in body weight decreased immediately after the first injection of MTX and lasted until day 4. In Figure 3.1, average changes in the body weight of control and MTX-treated rats are shown in time, relative to their individual weight at the onset of treatment at day-1. Food consumption in the MTX-treated group was minimal at days 2 and 3, when only 25% (i.e. 4 gram per rat) of the intake of control rats was observed (not shown). By then, the MTX-treated rats had lost 2-10% of their initial body weight. Partly, this weight loss was the result of dehydration as all MTX-treated rats developed diarrhea from day 2 until day 6. Recovery was seen from day 3 onwards, accompanied with regain of appetite and with increased gain in body weight when compared to the controls. During the experiment, no effect of MTX-treatment on water intake was observed (not shown).

#### Proliferation

The effects of MTX on intestinal epithelial proliferation were analyzed through detection of incorporated BrdU, injected the day before the rats were sacrificed. Because of the 24 h interval between injection and killing, BrdU-positive cells were not restricted to the crypts, but were also found up to one third of the length of the villi in all small intestinal regions

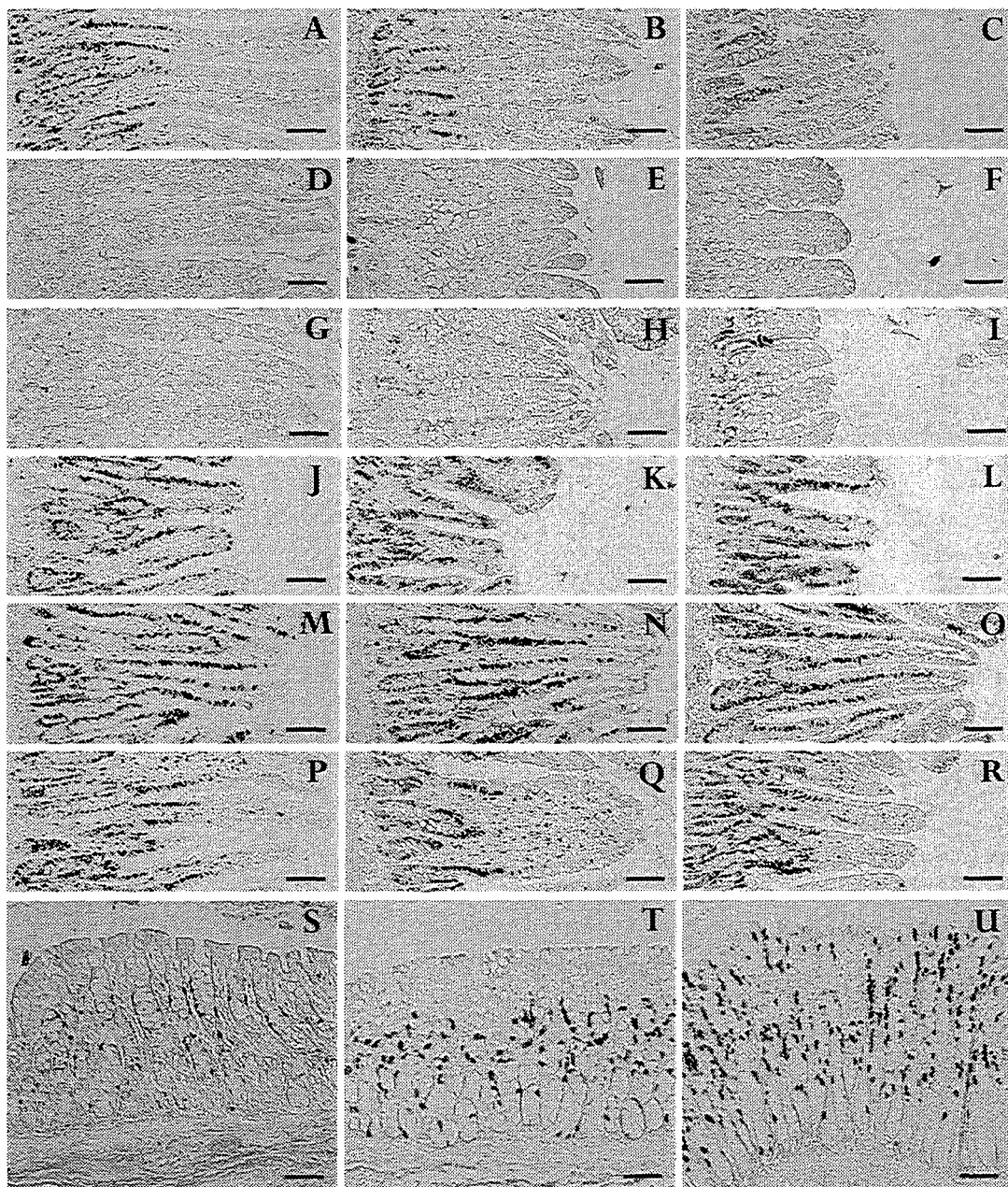


Figure 3.2

*Effects of MTX-treatment on epithelial proliferation. BrdU-incorporation was detected immunohistochemically in the duodenum (A, D, G, J, M, P), jejunum (B, E, H, K, N, Q), ileum (C, F, I, L, O, R) and the colon (S-U) of control and MTX-treated rats. In control rats, proliferation and migration resulted in BrdU-positive cells up to one third of the villi in the small intestine (A-C) and in the mid-crypts of the colon (S); After MTX-treatment, proliferation was absent at day 1 along the entire small intestine (D-F), and proliferation returned at first in the distal small intestine at day 2 (G-I). Maximal proliferation was seen at day 4 along the entire small intestine (J-L). Proliferation decreased gradually towards control patterns as seen at day 6 (M-O) and day 8 (P-R). No decrease in BrdU-staining was seen at day 1 in the colon (T). Hyperproliferation was seen in the colon of some rats at day 6 (U). Bars represent 100  $\mu$ m.*

of control rats due to migration of the cells (Figure 3.2A-C). In each small intestinal region, MTX completely inhibited epithelial proliferation, since Brdu injected 5 h after the final dose of MTX could not be detected in epithelial cells in any of the small intestinal regions (Figure 3.2D-F). An induction of epithelial proliferation in the small intestine occurred between 24 h and 48 h after the final dose of MTX in a region dependent way.

A minor increase in the amount of Brdu-staining was seen in duodenal crypts at day 2 (Figure 3.2G). Slightly more Brdu-labeled cells were seen in the jejunum at day 2 (Figure 3.2H), while highest induction of proliferation was seen in the ileum (Figure 3.2I). At day 3, Brdu-positive cells were abundantly covering the crypt epithelium and reached up to one third of the length of the villi in all small intestinal regions (not shown). The numbers of Brdu-positive cells were further increased at day 4 in each region of the small intestine such that labeling was seen along the entire crypt-villus axes (Figure 3.2J-L). Between day 5 and day 8 the numbers of Brdu-positive cells decreased towards control patterns in each of the small intestinal region (Figure 3.2M-R).

Inhibition of proliferation was not seen in the colon in the days following MTX-treatment since the detection of Brdu-positive cells at day 1-3 remained in the mid-crypt area very similar to controls (Figures 3.2S, T).

A remarkable induction of proliferation was observed in the colon between day 4-6, when Brdu-labeling occurred along the entire colonic crypt epithelium (Figure 3.2U). However, this colonic hyperproliferation was not seen in each animal. After day 6, the detection of Brdu in the colon of MTX-treated rats was comparable to the controls (not shown).

#### Morphology

Morphological damage and regeneration was analyzed on tissue sections through measurement of the length of the crypts and the villi in the small intestine and the colon. Due to time-dependent inter-animal variations in the

response to MTX-administration, measurements of 2 consecutive days were pooled in the quantitative analysis of crypt depth and villus height (Figure 3.3). Following the second MTX-injection, the crypt depths were decreased in all small intestinal regions at day 1 and day 2 when compared to controls. This decrease was only significant in duodenum and jejunum, where crypt depths were 80% and 60% of controls, respectively. In all small intestinal regions, the crypts were significantly elongated on days 3 and 4 when compared to days 1 and 2. The small intestinal crypts were further elongated on days 5 and 6 when compared to controls or to days 3 and 4. Between days 8 and 10, the crypt depth was comparable to controls in all small intestinal regions. In the colon, no significant changes occurred in the average crypt depth following MTX-administration (not shown).

Nevertheless, it is worth to mention that in some animals the colonic crypts were enlarged to 150% of control length between day 4-6, coinciding with increased Brdu-incorporation in these animals, as shown in Figure 3.2U.

The small intestinal villi progressively shortened between day 1 and day 4 following MTX-treatment, when compared to the length of the villi in controls. This villus atrophy was only significant in the jejunum (75% of control values) and less pronounced in duodenum (80% of control values) and ileum (85% of control values). Between day 5 and day 10, the villi regenerated to normal lengths in all small intestinal regions. However, during the regeneration phase at days 5 and 6, the ileal villi temporarily exceeded the lengths of normal ileal villi (140% of controls).

Next to MTX-induced changes in small intestinal crypt and villus sizes, a morphological characteristic of epithelial damage became apparent when judged on HE-stained sections. At days 1 and 2, epithelial damage in the small intestine was characterized by a reduction in the number of crypts. In the remaining crypts, the epithelial cells appeared flattened. This damage was most severe in the

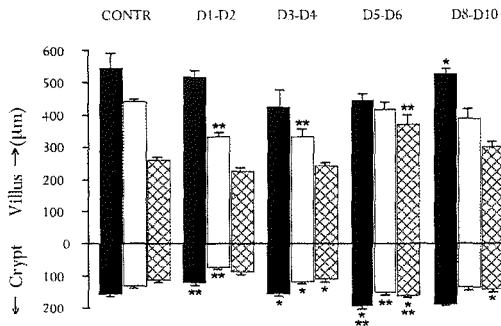


Figure 3.3

Effects of MTX-treatment on crypt depth and villus height in duodenum (filled bars), jejunum (open bars) and ileum (hatched bars). Mean crypt depth (downwards) and mean villus height (upwards) is shown per group per region. Crypt depth decreased in the small intestine until day 2. In the proximal regions this decrease was significant when compared to controls ( $p < 0.05$ ). During crypt regeneration on days 3 and 4, they were enlarged when compared to days 1 and 2 in all small intestinal regions ( $p < 0.05$ ). Crypt elongation continued on days 5 and 6, during which they even exceeded control values in duodenum and ileum. The length of the small intestinal villi decreased until day 4 after MTX. Only in the jejunum this decrease was significant ( $p < 0.05$ ). Small intestinal villi regenerated on days 5 and 6, during which they were elongated in the ileum when compared to controls. At days 8 and 10, the length of small intestinal crypts and villi returned within the range of controls. Filled bar: duodenum; open bars: jejunum; hatched bars: ileum. Error bars represent standard error of the mean. Statistically significant difference ( $p < 0.05$ ) from controls (\*\*) or to the previous group of the time course (\*) was analyzed using the Mann-Whitney U-Test.

duodenum (Figure 3.4A). Towards the ileum, epithelial damage in the crypts was less pronounced (Figures 3.4B and C), whereas in the colon morphological changes were absent (Figure 3.4D). Epithelial cell damage was also observed on the villi at later stages in all small intestinal regions. At days 3 and 4, the villi showed reduced numbers of epithelial cells and the remaining cells were flattened, e.g. day 4 of the jejunum (Figure 3.4E and F). Similar to the observed crypt damage, also villus damage was less severe towards the ileum (not shown). By day 5 and day 6, the villus epithelial cells appeared normal in number and in morphology in each small intestinal region (not shown).

#### MTX-induced apoptosis

In each of the small intestinal regions of controls, only an occasional crypt cell was TUNEL-positive, and most crypts were TUNEL-negative (Figure 3.5A). In MTX-treated rats, the amount of TUNEL-positive cells was markedly increased at day 1 and day 2 in the small intestinal crypts, but not on the villi (Figure 3.5B). MTX-induced TUNEL-positive cells occurred in the crypts in all small intestinal regions, suggesting enhanced apoptosis at days 1 and 2 along the entire small intestine. The induction of apoptosis in small intestinal crypts at day 1 and day 2 was further supported by the increased appearance of nuclear shrinkage and apoptotic bodies in serial HE-stained sections (not shown). In the colon, the number of TUNEL-positive cells was not altered in the crypts after MTX-treatment when compared to controls (not shown). Also on serial sections stained with HE, no signs of altered apoptosis were observed in the colon (not shown).

#### Epithelial gene expression during

MTX-induced damage and regeneration  
To localize differentiated enterocytes in the small intestine during epithelial damage, expression of alkaline phosphatase (AP) and sucrase-isomaltase (SI) was detected immuno-histochemically along the small intestine. In the jejunum of control small intestine, the

brush border of villus enterocytes were AP- and si-positive (not shown). During maximal villus atrophy and epithelial restitution (days 3-4), villus enterocytes were reduced in number but still AP- and si-positive (e.g. Figure 3.6G). To verify the functionality of AP during damage, its activity was localized on serial sections. The localization of AP activity in control jejunum was comparable to the immunohistochemical localization of the protein (dark blue, Figure 3.6A) and did not change during villus atrophy as shown on day 4 (Figure 3.6B). Similar results for AP and si were also obtained for the duodenum and the ileum (not shown). Interestingly, In control jejunum, intracellular staining of si precursor is restricted to villus enterocytes localized close to the crypt-villus junction (not shown). The late onset of enterocyte differentiation during villus regeneration is reflected by the detection of si in the Golgi region of enterocytes on villus tips on day 4 (Figure 3.6H, arrows).

The presence and the functionality of goblet cells during MTX-induced damage and regeneration was analyzed in each small intestinal region using alcian-blue staining of mucins in combination with the immunodetection of MUC2 and trefoil factor 3 (TFF3). In control small intestine, goblet cells increased in number towards the distal small intestine and were evenly distributed along the crypt-villus axis (light blue, Figure 3.6A). At days 1 and 2, the number of goblet cells was decreased in the small intestinal crypts, but not on the villi, as could be demonstrated using alcian blue-staining, and MUC2 or TFF3 immunostaining. This goblet cell depletion was most pronounced in the duodenum and was less pronounced towards the ileum (not shown). At days 3 and 4, goblet cells had returned in the crypts, and became increasingly abundant on the tops of the villi in each region of the small intestine (e.g. Figure 3.6B). These villus goblet cells, identified by alcian blue-staining, were never positive for BrdU in double stainings (Figure 3.6C). Apparently, the goblet cells but not the enterocytes were

spared from extrusion, at least in the 24 h period following BrdU-injection. This notion was confirmed using PCNA-immunostaining as proliferation marker (Figure 3.6D). The accumulating villus tip goblet cells were expressing both MUC2 (Figure 3.6E) and TFF3 (Figure 3.6F). To verify whether the increase in upper-villus goblet cells was statistically significant during villus atrophy, MUC2-positive cells were counted in 3 zones along the crypt villus axis of control- and MTX-treated jejunum, as a representative for the entire small intestine. In the jejunum of control animals, the goblet cells were almost evenly distributed along the crypt villus axis (Table 3.1). From day 5 onwards, the distribution pattern of goblet cells was normal in the small intestine (not shown).

Differentiated Paneth cells were identified in the base of the small intestinal crypts by their expression of lysozyme. Both in controls and in MTX-treated rats, a gradual increase in the number of Paneth cells per crypt was seen from the duodenum towards the ileum (not shown). At days 1 and 2 after MTX-treatment, the amount of lysozyme immunostaining was strongly increased in each of the small intestinal region when compared to controls, with a maximum at day 2 (Figure 3.6I and J). During regeneration of the small intestinal crypts, from day 3 to 4, lysozyme immunostaining returned to control level (not shown).

In the colon, no changes were observed in the amount and distribution of either alcian blue-, MUC2- or TFF3-positive goblet cells following MTX-treatment (not shown). Differentiated colonic enterocytes were stained by their expression of CAI, a bicarbonate-producing enzyme present in the cytosol of colonic surface enterocytes. MTX-treatment did not affect colonic CAI expression, except for some animals in which during the late regeneration phase on day 6 and 8, less CAI-positive cells were found in the colonic surface epithelium. Possibly, this decrease was related to colonic hyperproliferation mentioned earlier (not shown).

Table 3.1

*Numbers of goblet cells and Paneth cells in the jejunum of MTX-treated rats.*

	Control	Day 1-2	Day 3-4
Goblet cells:			
Villus tip	11.00 $\pm$ 1.70	5.60 $\pm$ 1.80 *	9.50 $\pm$ 2.50 **
Villus base	14.30 $\pm$ 0.70	7.70 $\pm$ 1.98	6.00 $\pm$ 2.80 *
Ratio (b:t)	1.36 $\pm$ 0.14	1.64 $\pm$ 0.43 *	0.68 $\pm$ 0.29 *(*)
Paneth cells	3.07 $\pm$ 0.23	3.52 $\pm$ 0.38	2.77 $\pm$ 0.20

*Average numbers of goblet cells and Paneth cells ( $\pm$  standard deviation) were determined in well-orientated tissue sections by counting 2-positive and lysozyme-positive cells, respectively. For goblet cells, 3 zones along the crypt-villus axis were discriminated (see materials and methods). Statistical analysis was performed using the Mann Whithney test. <0.05 was considered statistically different. \*: compared to control, \*\*: compared to Day 1-2.*

Sparing of goblet cells and Paneth cells  
To investigate whether the observed accumulation of goblet cells at villus tips was statistically significant, muc2-positive cells were counted along the crypt-villus axis, as described in Materials and Methods. The numbers and distribution of muc2-positive cells along the crypt-villus axis in the jejunum of controls, and at days 1-2 and days 3-4 after MTX-treatment, are summarized in Table 1. In the 2 days following MTX-treatment, the number of muc2-positive cells was about 50% reduced in both the upper half and the lower half of the villus (Table 3.1). In the lower half of the villi, the number of muc2-positive cells were still decreased on days 3-4, while in contrast, they had increased in villus tips, to numbers that differed not statistically from controls. This increase in muc2-positive cells on villu tips on days 3-4 was statistically significant compared to days 1-2, and supported the observation of goblet cell sparing at villus tips during MTX-induced villus atrophy (Figure 3.6).

The number of lysozyme-positive cells in the deeper crypts were counted on days 1-4 after MTX-treatment and compared with controls, to verify whether the amount of Paneth cells was affected by MTX (Table 3.1). However, the number of lysozyme positive Paneth cells on days 1-2 and days 3-4 were not statistically different from control values.

Quantitation of epithelial mRNA expression  
Morphological damage was compared with alterations in levels of mRNA expression in the jejunum of MTX-treated rats using quantitative

Northern blots. mRNA expression of CPSI and SI, markers for crypt and villus enterocytes, respectively, both decreased after MTX-treatment (Figure 3.7). CPSI decreased to 15% of control levels in 2 days and SI to 45% of control levels in 4 days. The mRNA expression of both enterocyte markers increased in days thereafter and reached control levels on days 5-6. On days 8 and 10, the expression of CPSI and SI mRNA had further increased to 150% of control levels.

Goblet cell-specific mRNA expression was quantified using TFF3 and MUC2 as markers. In contrast to the enterocyte markers, TFF3 and MUC2 mRNA levels were maintained during damage on days 1 and 2 (Figure 3.7). Lowest levels of TFF3 mRNA were seen during a period of extensive cell loss on days 3-4 (50% of control) and lowest levels of MUC2 mRNA during regeneration on days 5-6 (55% of control). Both TFF3 and MUC2 mRNA levels gradually increased to control levels on days 8-10.

Lysozyme mRNA expression was quantified to investigate Paneth cell function. In agreement with the observed increase in lysozyme immunostaining, lysozyme mRNA was increased to 165% of control levels during damage on days 1 and 2 (Figure 3.7). In the days thereafter, lysozyme mRNA expression was not statistically different from controls, except for a second phase of induction occurring on days 8-10.

## Discussion

The use of rats in this study allowed us to identify regional variation in intestinal epithelial sensitivity towards MTX and to gain insight in mechanisms of intestinal epithelial damage and regeneration after exposure to cytotoxic concentrations of MTX. These regional differences were reflected by a decrease in the degree of MTX-induced crypt damage along the proximal-to-distal axis of the intestine.

Analysis of epithelial proliferation after 2 consecutive days of MTX-administration, using

brdu-incorporation as a marker, demonstrated an inhibition of DNA synthesis in the epithelium of the entire small intestine, until at least 5 h after the final dose. Proliferation of the colonic epithelium on the other hand, was not inhibited when compared to controls. In the small intestine, proliferation re-occurred around 24 h after the final dose of MTX. This induction of proliferation was strongest in the ileum and decreased towards the duodenum. In vivo and in vitro proliferation studies in both human and rat have demonstrated a gradient of crypt cell production rates along the duodenal-colonic axis. In rat small intestine, the crypt cell production rate (cells/crypt/h) decreases from 28 in the duodenum to 12 in the ileum, whereas in the colon a decrease from 7.7 to 3 has been reported from proximal to distal (Al-Nafussi and Wright et al. 1982, Hall et al. 1992). The gradual decrease in crypt cell production rates from the duodenum towards the colon could explain the different sensitivity towards MTX.

Together with an inhibition of cell proliferation, MTX also induced apoptosis on day 1 and day 2 in the proliferative region of small intestinal crypts, as judged by morphological criteria and TUNEL-staining. In contrast, MTX-induced cell death was not observed in the colon. It is possible that the difference in apoptosis between small and large intestine is the result of regional differences in cell cycle control mechanisms, following cellular damage, for instance through the lower expression of p53 and the higher expression of bcl-2 in the colon when compared to the small intestine (Merritt et al. 1994). On the other hand, the colonic resistance to MTX-induced cell death could be directly related to the relative slow cell turnover in the colon, leading to only minor damage and less induction of cell death.

Morphological damage in the crypts of the small intestine paralleled increased apoptosis on days 1 and 2. The observed flattening of the remaining crypt cells most likely represents epithelial restitution, to prevent breaches in

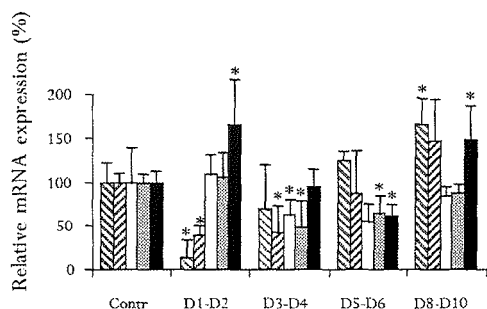


Figure 3.7

Intestinal epithelial mRNA expression in normal- and MTX-treated rats. mRNA expression of was quantified on Northern blots and corrected for the amount of glyceraldehyde-3-phosphate dehydrogenase mRNA. Expression of carbamoylphosphate synthase (cross-hatched bars) and S1 (hatched bars) mRNA through enterocytes decreased during damage and gradually increased during and after regeneration to levels higher than control on days 8 and 10. Expression of goblet cell-specific MUC2 (grey bars) and TFF3 (open bars) mRNA remained stable during crypt damage (days 1-2) but were temporarily decreased during extensive cell loss on the villi (days 3-4). Expression of both markers returned to normal in the next days. Lysozyme mRNA expression (filled bars) as marker for Paneth cell differentiation was increased during crypt damage and during late regeneration. \* $P < 0.05$  vs. control by Mann-Whitney U-Test.

the epithelial barrier. During crypt damage, CPSI mRNA expression was 6-fold decreased in the jejunum, indicating the loss of crypt enterocyte function. Regeneration of the atrophic crypts started on day 3 in the small intestine, via hyperproliferation and hyperplasia.

During MTX-induced villus atrophy (days 3 and 4), epithelial restitution was observed on the villi. Furthermore, S1 mRNA expression was 3-fold decreased in the jejunum and paralleled the loss of villus enterocytes. Previously it has been shown that during MTX-induced villus atrophy, activities of the brush border glycohydrolytic enzymes sucrase-isomaltase and lactase are strongly down-regulated in the small intestine (Taminiau et al. 1980). The absence of glycohydrolases indicates enterocyte malfunctioning with regard to the degradation and absorption of nutrients during villus atrophy. In contrast to the glycohydrolases, no decrease in the enterocytic expression of alkaline phosphatase protein and enzyme activity was found during villus atrophy. Poelstra et al have indicated a role for AP in host defense against endotoxins (Poelstra et al. 1997). Possibly, expression of this protein is selectively maintained after MTX-treatment, to assist in the maintenance of the epithelial integrity. Especially during epithelial damage, as induced by MTX, epithelial defense is of vital importance for survival of the animal.

During regeneration, the lengths of the villi returned to normal in duodenum and jejunum. However, in the ileum villus elongation continued and on day 5-6 abnormally long villi (370  $\mu$ m) were seen when compared to controls (260  $\mu$ m). It is not clear why hyperplasia in the distal small intestine is more extensive than in the proximal small intestine. Also in other studies, describing the regeneration of intestinal villi following small bowel resection, increased villus lengths have been reported (McDermott and Roudnew 1977). It is possible that the feedback mechanisms, involved in balanced cell proliferation, are less controlled in the ileum when compared to the proximal regions of the small intestine, as



during regeneration not only the villi, but also the crypts, were over 40% longer compared to controls.

As in other studies (Xian et al. 1999), MTX induced a mild goblet cell depletion in the small intestine during a 4-day period of epithelial damage. Immunohistochemistry demonstrated that the MTX-induced goblet cell depletion mainly affected the villus base, while a remarkable sparing of goblet cells was observed at villus tips during the days of maximal villus atrophy (Days 3-4). Furthermore, these accumulating cells were not labeled with BrdU and were PCNA-negative. Apparently, these cells were spared from extrusion via an adaptive mechanism. Selective sparing of goblet cells could very well serve a protective function in epithelial defense via their secretion of mucins and trefoil factors (Mashimo et al. 1996, Tytgat et al. 1995, Van Klinken et al. 1995). Indeed, during early damage (days 1-2), small intestinal mRNA levels of MUC2 and TFF3 remained unchanged, although the number of goblet cells was 50% reduced along the villi. Only during severe villus atrophy, when the amount of epithelial cells was minimal, the expression of MUC2 and TFF3 mRNA was decreased. Apparently, goblet cell function is very important during MTX-induced damage and therefore maintained. Another cell type with a pertinent role in epithelial defense is the Paneth cell. During crypt damage, they express 160% of normal lysozyme mRNA levels and show increased intensity of lysozyme immunostaining. The phenomenon of Paneth cell hyperplasia through MTX-treatment was described morphologically in electron microscopical studies. (Jeynes and Altmann 1978) Most likely, the slowly renewing Paneth cells not only have an advantage to the more shortly lived cell types in survival, but importantly the increased amounts of lysozyme expression indicate an increase in secretory capacity that very likely contributes to protection of the damaged mucosa.

In the colon, no significant changes could be observed in epithelial morphology and differentiation during the time course studied. The hyperproliferation and crypt elongation observed in some animals between days 4 and 6 were possibly secondary effects in the response to MTX. For example, enhanced small intestinal repair mechanisms could lead to an increase in the amount of inductive signals, such as carbohydrates, fatty acids, bile salts, growth factors and trefoil factors in the intestinal lumen that could potentially stimulate proliferation in the downstream compartments.

In summary, MTX was shown to inhibit intestinal epithelial proliferation in the small intestine but not in the colon. Subsequent crypt damage was most severe in the duodenum, but regeneration through hyperproliferation was strongest in the distal small intestine. Interestingly, although severe damage could be induced in the small intestine using MTX, both Paneth cells, goblet cells, and enterocytes were all able to contribute to epithelial defense mechanisms. First, a direct increase of antimicrobial lysozyme expression was seen in Paneth cells, which remained high until crypt integrity was fully restored. Second, the goblet cells remained functional during early damage, were selectively spared from undergoing cell death, and accumulated at villus tips during villus atrophy allowing secretion of the protective mucin and trefoil factor molecules. And third, despite the MTX-induced reduction in enterocyte numbers and SI and CPS1 gene expression during villus atrophy, the putative detoxifier of endotoxins AP remained actively expressed in the small intestinal brush border. To gain further insight in regulatory mechanisms of epithelial defense and enterocyte function during MTX-induced damage and regeneration, additional studies are needed that allow a quantitative analysis of cell type specific gene expression. This insight is necessary to develop further clinical relevant strategies to protect cancer patients from intestinal damage during chemotherapeutic therapy.

## 4 Specific responses in rat small intestinal epithelial mRNA expression and protein levels during chemotherapeutic damage and regeneration

The rapidly dividing small intestinal epithelium is very sensitive to the cytostatic drug methotrexate. We investigated the regulation of epithelial gene expression in rat jejunum during methotrexate-induced damage and regeneration. Ten differentiation markers were localized on tissue sections and quantified at mRNA and protein levels relative to control levels. We analyzed correlations in temporal expression patterns between markers. MessengerRNA expression of enterocyte and goblet cell markers decreased significantly during damage for a specific period. Of these, sucrase-isomaltase (-62%) and CPS (-82%) were correlated. Correlations were also found between lactase (-76%) and SGLT1 (-77%), between I-FABP (-52%) and L-FABP (-45%). Decreases in GLUT5 (-53%), MUC2 (-43%), and TFF3 (-54%) mRNAs occurred independently to any of the other markers. In contrast, lysozyme mRNA present in Paneth cells increased (+76%). At the protein level, qualitative and quantitative changes were in agreement with mRNA expression, except for MUC2 (+115%) and TFF3 (+81%), which increased significantly during damage, following independent patterns. During regeneration, expression of each marker returned to control levels. The enhanced expression of cytoprotective molecules (MUC2, TFF3, lysozyme) during damage represents maintenance of goblet cell and Paneth cell functions, most likely to protect the epithelium. Decreased expression of enterocyte-specific markers represents decreased enterocyte function, of which fatty acid transporters were least affected.

Published as:

Melissa Verburg, Ingrid B. Renes, Danielle J.P.M. van Nispen, Sacha Ferdinandusse, Marieke Jorritsma, Hans A. Büller, Alexandra W.C. Einerhand and Jan Dekker. 'Specific responses in rat small intestinal epithelial mRNA expression and protein levels during chemotherapeutic damage and regeneration' in *J Histochem Cytochem* 2002; 50: 1525-1536.

### Acknowledgements

Dr W.H. Lamers is thanked for the CPS 1 probe and antibodies, and Dr S. Krasinsky is acknowledged for providing the sucrase-isomaltase probe. Dr K. Y. Yeh and Dr A. Quaroni are gratefully acknowledged for supplying anti-sucrase antibodies. Furthermore, we thank Dr C.F. Burant for kindly providing SGLT 1 and GLUT5 probes, as well as Dr B. Hirayama for his valued SGLT 1 antibodies. Dr D. Yver kindly provided anti-GLUT5 antibodies. The intestinal FABP and liver FABP probes and antibodies were a generous gift from Dr J.I. Gordon. Dr D.K. Podolsky is acknowledged for providing both the TFF3 probe and the anti-TFF3 antibodies and Dr J.H. Power for providing the lysozyme probe. We also thank Dr K. Redekop for statistical advice and support.

## Introduction

The use of the cytostatic drug methotrexate (MTX) in anti-cancer treatments severely impairs intestinal epithelial function, which constitutes a major dose-limiting factor in treatment schedules (Fata et al. 1999; Kohout et al. 1999). Like gamma-irradiation, this drug induces diarrhea and anorexia, which is associated with malabsorption, malnutrition and dehydration (Pinkerton et al. 1982). It is of great importance to unravel the response of the small intestinal epithelium to cytostatic agents at the biochemical level, to gain insight in the functional properties of the epithelial cells during damage and subsequent regeneration.

As folic acid analogue, the action of MTX primarily inhibits DNA synthesis through binding to the enzyme dihydrofolate reductase (Werkheiser 1961). This leads to an inhibition of proliferation in the crypts of the small intestine (Goldman and Matherly 1985). It has been demonstrated in biopsies of human cancer patients that epithelial damage in the small intestine through chemotherapy could be identified via increases in apoptosis in the crypts, epithelial changes in cell height and crypt height and the manifestation of villus atrophy (Keefe et al. 2000).

In our rat model of chemotherapeutic damage and regeneration in the small intestinal epithelium, 4 phases could be discriminated following the 2-dose administration (i.v.) of 20 mg/kg plus 10 mg/kg bodyweight MTX (Verburg et al. 2000). In this model, day 1 and 2 represented damage in the crypt epithelium, which was characterized by increased apoptosis as well as decreased crypt depth and cell height. Day 3 and 4 represented a phase of prominent damage to the villus epithelium, marked by reduced cell and villus heights as well as accumulating goblet cells at the tips of the small intestinal villi. Day 5 and 6 represented a phase of regeneration via increased proliferation during which the morphological appearance of the epithelial cells returned to normal. Day 8 and 10 represented a phase of

regenerated small intestinal epithelium, which was indistinguishable from untreated rats (Verburg et al. 2000).

Studies have been performed with the use of particular growth factors, such as TGF (Booth et al. 2000), KGF (Booth and Potten 2001), EGF (Hirano et al. 1995; Petschow et al. 1993) and IGF (Howarth et al. 1998) that aimed to protect the small intestinal epithelium against radiation injury or damage through cytostatic drugs. For example, the prophylactic administration of transforming growth factor beta (TGF $\beta$ ) was able to decrease proliferation in the stem cell region prior to radiation injury, which resulted in enhanced crypt survival and enhanced recovery in mice (Booth et al. 2000). Also, the therapeutic administration, but not the prophylactic administration, of epidermal growth factor (EGF), insulin-like growth factor (IGF-1), and TGF $\beta$  has been shown to stimulate epithelial proliferation in the regeneration phase following radiation- or MTX-induced injury in mice (Hirano et al. 1995; Howarth et al. 1998; Petschow et al. 1993; Potten et al. 1995). Thus, although these growth factors are important for an enhanced recovery of the small intestinal epithelium, they fail to prevent or reduce the development of the initial damage.

The functions of intestinal epithelial cells are reflected by the expression of cell type-specific genes. Very little is known about the absorptive and protective functions of epithelial cells during damage and regeneration induced by chemotherapy. Sucrase-isomaltase and lactase, responsible for intestinal disaccharidase activities, were decreased during MTX-induced damage in rat small intestine (Kralovanszky and Prajda 1985; Taminiau et al. 1980). In contrast, the amino acid transporter Pept1 appeared resistant to damage in the ileum of 5'-fluorouracil (5-FU) treated rats (Tanaka et al. 1998). Furthermore, MTX-treatment appeared to affect the various populations of epithelial cell types differently. Relative to enterocytes, epithelial goblet and Paneth cells were shown to be spared from cell death in

rat small intestine following MTX-treatment (Verburg et al. 2000). Very little is known about the contribution of these specialized cell types to epithelial protection during such a response.

In the present study, the functional capacities of the epithelial cells were investigated during MTX-induced damage and repair, through analysis of the expression of a range of differentiation markers. The following markers were used for enterocytes: carbamoyl-phosphate synthase (CPS), sucrase-isomaltase (SI), lactase, glucose transporter-5 (GLUT5), sodium glucose co-transporter 1 (SGLT1), intestinal- and liver fatty acid binding protein (I-FABP, and L-FABP, respectively). For goblet cells the markers mucin (MUC2) and trefoil factor 3 (TFF3) were investigated and lysozyme was used to study Paneth cell function.

The jejunum was chosen as a representative for the small intestine, since morphology and proliferation were similarly affected along the small intestinal axis in this model (Verburg et al. 2000). Epithelial gene expression was quantified at the mRNA and protein level, and compared with the immunohistochemical localization of the protein, at sequential days after MTX-treatment.

Table 4.1  
Antibodies to detect intestinal epithelial proteins

Antigen	Dilution		Type
	W-Blots	IHC	
rat CPS	1:1000	1:5000	r-polyclonal (Gaasbeek Janzen et al. 1984)
rat SI*)	-	1:6000	r-polyclonal (Yeh et al. 1991)
rat SI*)	1:100	-	m-monoclonal (Quaroni and Isselbacher 1985)
rat GLUT5	1:500	1:1000	r-polyclonal (Rand et al. 1993)
rat I-FABP	1:1000	1:4000	r-polyclonal (Rubin et al. 1989)
rat L-FABP	1:1000	1:4000	r-polyclonal (Rubin et al. 1989)
rabbit SGLT1	-	1:1000	m-monoclonal (Hwang et al. 1991)
rat MUC2*)	1:1000	-	r-polyclonal (Tytgat et al. 1995b)
human MUC2*)	-	1:100	m-monoclonal (Podolsky et al. 1986)
rat TFF3	1:200	1:6000	r-polyclonal (Suemori et al. 1991)
human lysozyme	-	1:50	r-polyclonal (This study)

Each antibody was shown to be specific in rat. \*) Except for SI and MUC2, the same antibodies were used for both Western blot and immunohistochemistry. r: rabbit, m: mouse.

## Materials and Methods

### Animals

Six-weeks old male Wag/Rij rats (Broekman, Utrecht, The Netherlands) were kept under specific pathogen free conditions with free access to water and defined semi-synthetic chow (Hope Farms, Woerden, The Netherlands). Glucose, starch and cellulose constitute the carbohydrates in the food: 424 g/kg, 140 g/kg, and 45 g/kg, respectively. Upon analysis no other carbohydrates were found. The folic acid content was 0.98 mg/kg. The dosage schedule of MTX-treatment was defined during pilot studies. At day -1, 20 mg/kg body weight methotrexate (MTX, Ledertrexate SP forte, Cyanamid Benelux, Etten-Leur, The Netherlands) was injected intravenously under light anesthesia. Twenty-four h later (day 0), a second injection of 10 mg/kg body weight MTX was given. Control animals received equivalent volumes of 0.9% (wt/vol.) sodium chloride solution both times. At days 1, 2, 3, 4, 5, 6, 8, and 10 after the second dose of MTX, 3 rats were sacrificed by decapitation after anesthesia. Three control animals were sacrificed at day 8. The experiments were performed with permission of the Animal Ethics Committee of our institution. Jejunal segments (anatomical middle of the small intestine) were rinsed in PBS, fixed in 4% (wt/vol.) paraformaldehyde (Merck, Darmstadt, Germany) in PBS, and processed for immunohistochemistry according to standard procedures (Verburg et al. 2000). In addition, adjacent intestinal segments (0.5 cm long) were frozen in liquid nitrogen and stored at -80°C for quantitative mRNA and protein analysis.

### Immunohistochemistry

Expression and localization of protein was detected using immunohistochemistry according to standard procedures (Verburg et al. 2000). Antigen unmasking was carried out by heating the sections for 10 min in 0.01 M sodium citrate (pH 6.0) at 100°C. Endogenous peroxidase activity was blocked by treatment with 1.5% H<sub>2</sub>O<sub>2</sub> in PBS for 30 min. Non-

specific protein binding was blocked using a buffer containing 10 mM Tris (pH 8.0), 5 mM ethylenediamine tetraacetic acid (Merck), 0.15 M NaCl (Fluka Chemie, Zwijndrecht, The Netherlands), 0.25% (wt/vol.) gelatin (Merck) and 0.05% (wt/vol.) Tween-20 (Merck). All sections were incubated overnight at 4°C using one of the primary antibodies diluted in PBS. (Table 4.1). The antibodies raised against human SGLT-1 (Yoshida et al. 1995), human MUC2 (Tytgat et al. 1995a; Tytgat et al. 1995b) and human lysozyme (Dako, Glostrup, Denmark) were shown to be specific in rat. Antibody binding was visualized using biotin-labeled secondary antibodies and Vectastain®, an avidin-biotin peroxidase complex detection kit, according to the manufacturer (Vector Laboratories, Burlingame, CA). All sections were recorded and analyzed using a CCD camera (Sony, The Netherlands) and an Eclipse E800 Microscope (Nikon, Japan). Appropriate control staining was performed, leaving out each of the primary antibodies, which resulted in complete absence of staining in for each separate antibody at the dilutions as used in our experiments (Table 4.1).

### Messenger RNA quantitation

Total RNA was isolated from frozen tissue using Trizol® reagent (Gibco-BRL, Gaithersburg MD). Ten µg of total RNA was run on 1% or 1.2% (wt/vol.) agarose gels containing 0.5 M glyoxal (Boehringer Mannheim, Mannheim, Germany) and blotted overnight onto Hybond-N+ membranes (Amersham, Buckinghamshire, UK). Serial dilutions of each RNA sample were analysed to ensure that the mRNA quantification, of each marker mRNA using its cognate cDNA probe, was performed within the linear range of this technique. All blots were baked for 2 h at 80°C and hybridized using rat-specific,  $\alpha$  [<sup>32</sup>P]-dATP-labeled, cDNA probes. The following rat specific cDNA probes were used, CPS (Nyunoya et al. 1985), SI (Krasinski et al. 1994), lactase (Büller et al. 1990), SGLT1 (Burant et al. 1994), GLUT5 (Rand et al. 1993), I-FABP (Alpers et al. 1984), L-FABP (Gordon et al. 1983), MUC2 (Verburg et al.

2000), TFF3 (Suemori et al. 1991), and lysozyme (Yogalingam et al. 1996). Each probe hybridized to a mRNA band of the appropriate molecular weight as originally described for the respective probes. Moreover all bands were clear and discrete, and no signs of RNA degradation were observed. Following exposure for 1 or 2 days to PhosphorImager plates, the hybridization signals were quantified using a PhosphorImager and ImageQuant software (Molecular Dynamics/Amersham, Roosendaal, The Netherlands). Expression was corrected for the amount of glyceraldehyde-3-phosphate dehydrogenase (GAPDH) mRNA, which served as internal standard.

#### Protein quantitation

Changes in epithelial protein expression were determined in tissue homogenates using quantitative Western blotting. Tissue was homogenized in HEPES buffer (20 mM HEPES (Merck) pH 7.5, 20 mM NaCl (Boehringer), 0.5% (wt/vol.) Triton X-100® (BDH, Poole, UK) containing 10 µg/ml Pepstatin A (Sigma, St Louis, MO), 10 µg/ml Leupeptin (Sigma), 1 mM phenylmethylsulphonyl fluoride (Sigma) and 0.38 U/ml Aprotinin (Sigma) as protease inhibitors, using a Polytron (Kinematica AG, Basel, Swiss). Ten µg of total protein was separated on 7 or 15% (wt/vol.) SDS-PAGE and blotted for 1 h on to Hybond+ membranes. Serial dilution series of the protein samples were analysed to ensure that the quantification of each protein by its cognate antibody was performed in the linear range of this technique. Routine staining of the SDS-PAGE gels for protein after blotting showed complete transfer of the proteins to the membrane. After incubation for 1 h in blocking buffer (Tris pH 7.8 (Merck), 2 mM CaCl<sub>2</sub> (Merck), 5% (wt/vol.) low fat milk powder (Nutricia, Wageningen, The Netherlands), 0.05% (wt/vol.) Triton X-100 (BDH), and 0.05% (vol./vol.) Antifoam® (Sigma), the blots were incubated overnight at 4°C with one of the primary antibodies (Table 4.1). After rinsing in blocking buffer, the blots were incubated for 2 h in blocking buffer, containing 0.1 µCi/ml <sup>125</sup>I-labeled protein A (Amersham).

After rinsing 3 times in Tris buffer (pH 7.8) the blots were dried and exposed to PhosphorImager plates for 3 days. Each individual protein marker yielded clear and reproducible protein bands at the expected molecular weight as described in the original publications (Table 4.1). Signals were quantified as described above.

#### Statistical analysis

Changes in mRNA and protein expression levels during damage and regeneration were statistically analyzed using the Mann-Whitney U-test. The statistical correlation coefficient ( $\rho$ ) between mRNA and protein expression and between morphological parameters and mRNA/protein expression was analyzed using Spearman's test, based on data from the individual rats. Similarly, correlation coefficients between the various mRNAs/proteins were used to study coordinate gene expression. In all tests,  $p < 0.05$  was considered statistically significant.

## Results

#### The model

Using this animal-model, we have shown previously that we could induce characteristic cytotoxic damage to the intestinal epithelium of rats by a two-day treatment with methotrexate (Verburg et al. 2000). As noted in this previous study, the pattern of damage and regeneration varied slightly between individual animals. As it appeared, data were most clearly presented by pooling the data obtained from animals of 2 consecutive time points to correct for the observed temporal variations. Data are presented from four characteristic windows in the course of damage and regeneration, as described earlier (Verburg et al. 2000).

1 Days 1-2 after the last MTX injection were characterized as a period of inhibited proliferation, severe cell damage in the small intestinal crypt epithelium, and decreased crypt depth. Villus height was slightly decreased, but the villus epithelial cells appeared normal.

2 Days 3-4 were characterized by hyperproliferation, crypt regeneration, and villus atrophy. The villus epithelial cells were depleted and appeared flattened.

3 During days 5-6, villus regeneration occurred, whereas proliferation gradually returned to normal.

4 Regeneration was complete on days 8-10. Basically the response to MTX was similar in each region of the small intestine (Verburg et al. 2000), and results not shown), therefore only representative data of the jejunum are shown here. There were no macroscopical or microscopical lesions in the epithelium at any time during the course of damage and regeneration (not shown). It should be noted therefore that the epithelial barrier was not breached, and there was no apparent denuding of the mucosa during the experiment. This was particular relevant for the changes in the expression patterns of the enterocyte markers, which were basically expressed within the same villus epithelial cells. Thus, the relative changes in quantitative gene expression patterns of the individual markers were measures of specific gene regulation under these circumstances. In addition to this, it is of note that the correlation analyses between quantitative data regarding gene expression were calculated using the data for each marker of the individual animals.

#### Enterocytes

Immunohistochemistry was performed to study the fate of enterocytes during the experiment and to localize enterocyte specific protein expression. Since a very sensitive, yet non-linear, detection method was used to visualize binding of antibodies, staining intensities were not quantitatively interpreted throughout the manuscript. In control rats, CPS protein was expressed in a mosaic pattern and was localized in series of adjacent enterocytes, both in crypt and in villus epithelium (Fig. 4.1a). On days 1-2 most of the crypts were not stained for CPS, but the protein was still present in the villus region (Fig. 4.1b). On days 3-4, CPS-protein expression was less abundant on the villi compared to controls and

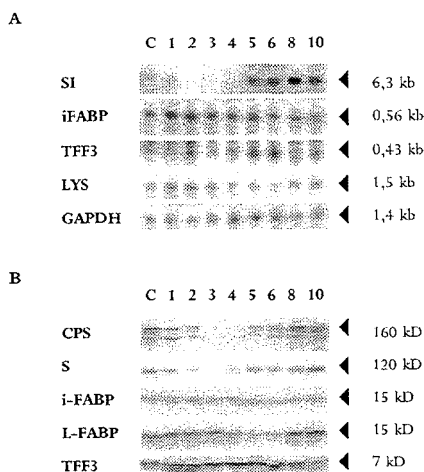


**Figure 4.3**  
Representative Northern-blots (A) and Western-blots (B) demonstrating the expression of selected small intestinal markers. Days after MTX-treatment are indicated above the graphs. C, indicates control. All results are shown for one rat at each time point. To the right the size of the mRNA (in kilobases, panel A) and of the proteins (in kilodalton, panel B) are indicated.

rats of days 1-2. Part of the enterocytes on the villus tips showed CPS-immunoreactivity during this period of severe villus damage, but mostly the crypt and villus enterocytes were CPS-negative (Fig. 4.1 c). On days 5-6, the mosaic pattern of CPS had returned on part of the villi, and the expression pattern was fully restored on days 8-10 (Fig. 4.1 d).

SI was found in the brush border and in the Golgi region of villus enterocytes in control rats (Fig. 4.1 e). The estimated number of SI-positive villus cells decreased according to the length of the villi, and during the phase of damage on days 1-4 the intracellular Golgi staining was absent (Figs 4.1 f and g). Very few SI-positive cells were seen on days 3-4, during maximal villus damage on the tips of the rudimentary villi (Fig. 4.1 g). As the villi increased in length during regeneration, the localization of SI-positive cells returned to normal (Fig. 4.1 h).

Like SI, GLUT5, and SGLT1 proteins were localized in the brush border of villus enterocytes in control tissue (Figs 4.1 i and m). The estimated numbers of GLUT5- as well as SGLT1-positive villus enterocytes decreased gradually towards the tips of the shortening villi during days 1-4, until both markers were undetectable on day 4 (Figs 4.1 k and o). From day 6 onwards, expression patterns of SGLT1 and GLUT5 were similar to those found in controls (Figs 4.1 l and p).

I-FABP and L-FABP expression was localized in the cytoplasm of all villus enterocytes in controls (Figs 4.1 q and u). MTX-induced changes in expression were similar for both FABP proteins. These changes were much less pronounced than for the brush border markers SI, GLUT5 and SGLT1. Despite the increasing villus cell damage up to 4 days after MTX-treatment, I-FABP and L-FABP immunostaining remained present in enterocytes of the remaining villus enterocytes (Figs 4.1 r, s, v, and w). Like in controls, I-FABP and L-FABP were expressed in all villus enterocytes on days 5-10 (Figs 4.1 t and x).



Lactase mRNA levels could be detected as enterocyte marker, but lactase protein could not be localized using the available antibodies, due to its very low expression levels in these adult rats (Rings et al. 1994) and data not shown).

#### Goblet and Paneth cells

The fate of goblet and Paneth cells was studied by immunohistochemistry for secretory products produced specifically by these cells. In contrast to the enterocyte markers, the markers or these cell types appeared to largely persist throughout the course of damage and regeneration. MUC2 was stained in the goblet cells at all time points during the experiment, and MUC2-positive goblet cells were also expressing TFF3 (Fig. 4.2). The estimated number of MUC2- and TFF3-positive cells was decreased compared with controls during days 1-2 along the crypt villus axis during the increasing villus atrophy (Figs 4.2 b and f). This was followed around day 4 by a depletion of MUC2- and TFF3-positive cells in the lower villus region and an accumulation of MUC2- and TFF3-positive cells in the villus tip region (Figs 4.2 c and g). During regeneration, MUC2 and TFF3 expression became comparable with controls (Figs 4.2 d and h).

Paneth cells in the crypts were lysozyme-positive at all days analyzed. A transient induction of lysozyme immunostaining was seen during crypt damage on days 1-2 (Figs 4.2 i and j), which gradually returned to normal staining patterns on days 3-4 and beyond (Figs 4.2 k and l).

Expression of enterocyte-specific mRNAs  
The expression of cell type-specific mRNA was quantified on Northern-blot for each individual rat, as illustrated in Figure 4.3 a. Pooling of quantitative data from 2 consecutive time points was performed to minimize intra-animal variations and to accentuate the differences between markers during the course of damage and regeneration (Fig. 4.4).

The changes in mRNA expression of each enterocyte marker had a characteristic pattern

in time (Fig. 4.4 a). Yet, the level of each enterocyte mRNA returned to levels that were not significantly different from control levels at day 8-10 after MTX-treatment. We performed correlation analysis on changes in the mRNA levels of these markers on the data from each individual animal. Four types of patterns could be distinguished, based on temporal differences in sensitivity to MTX-treatment. Within each type, the expression patterns of the markers were highly correlated, whereas there were no statistically significant correlations with the expression patterns of the markers from any other type. We could distinguish: type 1, CPS and SI; type 2, SGLT1 and lactase; type 3, I-FABP and L-FABP; and type 4, GLUT5 (Fig. 4.4). Of these, CPS and SI mRNAs were most affected at an early stage. During minimal crypt depth on days 1-2, levels of CPS and SI mRNA expression were 82% and 62% decreased respectively, compared with controls (Fig. 4.4 a). During maximal villus damage on days 3-4, CPS and SI were still significantly decreased, but the levels recovered relatively rapid compared to the other markers.

SGLT1 and lactase mRNA levels were the most affected at a later stage, at maximal villus damage on days 3-4 and recovered more slowly compared to CPS and SI (Fig. 4.4 a). The expression of SGLT1 and lactase mRNA was already significantly decreased on days 1-2 compared with control (-50%). This decrease progressed on to days 3-4, when SGLT1 and lactase mRNAs were hardly detectable (-77% and -76%, respectively). In contrast to CPS and SI mRNAs, SGLT1 and lactase mRNAs were still significantly decreased on days 5-6.

I-FABP AND L-FABP mRNA levels were markedly less affected than the previous four markers and were first significantly affected at maximal villus damage, whereas the mRNA levels recovered relatively late and more slowly when compared to CPS, SI, SGLT1, and lactase (Fig. 4.4 a). Expression levels of I-FABP and L-FABP mRNAs decreased significantly on days 3-4 with 52% and 45%, respectively

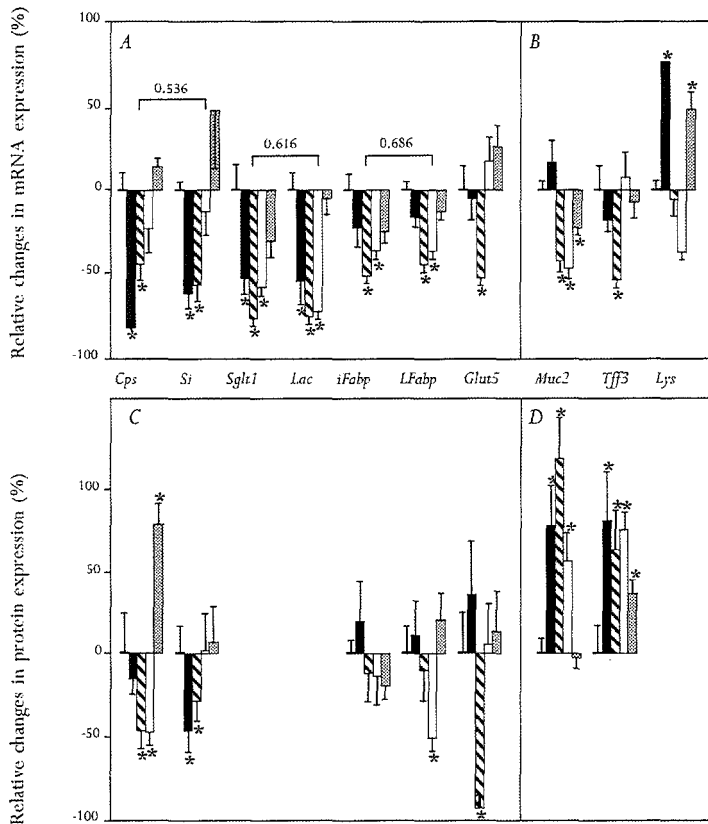


Figure 4.4

Relative changes in epithelial mRNA and protein expression in the jejunum after MTX-treatment. Panels indicate the mRNA levels of enterocyte (A) and of goblet and Paneth cell markers (B) as detected by Northern blotting, and of the protein levels of enterocyte (C) and of goblet and Paneth cell markers (D) as detected through Western blotting. Control levels, defined as 100%, were set at 0 on the horizontal axis. The relative in-/decrease, expressed as percentage of control levels, was analyzed on days 1-2 (black bars), days 3-4 (crosshatched bars), days 5-6 (open bars) and days 8-10 (gray bars). Closely correlated expression patterns could be distinguished in enterocyte-specific mRNAs as indicated by brackets (indicated is the correlation coefficient  $\rho$ , according to Spearman's test): between CPS and SI ( $\rho=0.536$ ,  $p=0.008$ ), between SGLT1 and lactase ( $\rho=0.616$ ,  $p=0.001$ ), and between I-FABP and L-FABP ( $\rho=0.686$ ,  $p<0.0005$ ). LAC; lactase, LYS; lysozyme. Error bars indicate SEM, and asterisks indicate statistically significant differences relative to control levels at  $p<0.05$ .

(Fig. 4.4A). Like for SGLT1 and lactase, regeneration within the tissue was not immediately associated with a normalization of I-FABP and L-FABP mRNA expression, since both markers were still significantly decreased on days 5-6.

In contrast to all other enterocyte markers, the mRNA levels of GLUT5 were only affected significantly during one specific phase of disease: i.e. at maximal villus damage (days 3-4, -53%), and recovered fast during regeneration (Fig. 4.4A).

We analyzed the relations between the level of expression of each marker and the crypt depth and villus atrophy, measured as described previously (Verburg et al., 2000). CPS and SI mRNA expression levels were correlated to changes in crypt depth ( $\rho=0.399$  and  $\rho=0.432$  respectively,  $p<0.05$ ) as well as

villus height ( $\rho=0.377$  and  $\rho=0.483$  respectively,  $p<0.05$ ). The temporal patterns of expression levels of lactase, GLUT5, SGLT1, I-FABP and L-FABP mRNA did not correlate to the variations in crypt depth or villus height.

#### Expression of goblet and Paneth cell-specific mRNAs

The response of each of the markers for the goblet and Paneth cells was very specific and different from any of the changes seen for the enterocyte markers (Figs 4.3 a and 4.4 a). MUC2 mRNA expression was significantly, yet inversely, correlated to crypt depth ( $\rho = -0.610$ ,  $p=0.001$ ). During early damage on days 1-2, MUC2 mRNA levels remained stable. Thereafter, MUC2 mRNA levels were significantly decreased and remained below control levels up to days 8-10 (Fig. 4.4 b). MUC2 and TFF3 protein co-localized to the same cells (Fig. 4.2). Interestingly though, TFF3 mRNA levels were not significantly correlated to MUC2 mRNA levels. TFF3 mRNA levels were decreased only on days 3-4 relative to controls (Fig. 4.4 b).

Lysozyme mRNA levels were significantly increased (+76%) at early stages of damage on days 1-2 (Fig. 4.4 b), in agreement with the immuno-histochemical localization of the protein (Fig. 4.2 j), and were rapidly normalized on days 3-6. There was no significant correlation with any of the morphological parameters. Surprisingly, a second induction of lysozyme mRNA levels occurred on days 8-10 (Fig. 4.4 b), despite the seemingly normal lysozyme protein expression at the immunohistological level (Fig. 4.2 l).

Expression levels of epithelial proteins  
Temporal expression patterns of epithelial proteins were quantified on Western blots, as illustrated in Figure 4.3 b, and compared with expression patterns of the encoding mRNAs. Despite our efforts we were not able to quantify the protein levels of all markers. Thus, we were not able to quantify SGLT1, lactase and lysozyme protein, due to lack of

antibodies that were able to reproducibly detect these antigens on Western blot.

The protein expression level of each enterocyte marker showed a specific pattern in time. Correlation analysis, determined from the data of the individual rats, revealed significant correlations between protein expression levels and the cognate mRNA levels of CPS ( $\rho=0.520$ ,  $p=0.01$ ), SI ( $\rho=0.900$ ,  $p=0.037$ ), I-FABP ( $\rho=0.482$ ,  $p=0.015$ ), and L-FABP ( $\rho=0.591$ ,  $p=0.001$ ), but not of GLUT5.

Two isoforms of the CPS protein were detected using these polyclonal antibodies, as described earlier (Fig. 4.3 b, Gaasbeek Janzen et al. 1984). CPS protein levels were significantly decreased on days 3-6, whereas CPS protein was significantly increased compared with controls on days 8-10, in accordance with the changes in mRNA levels (Figs 4.4 a and c). SI protein levels were 50% decreased during days 1-2, parallel to the decreased mRNA levels, and remained decreased on days 3-4. SI protein was increased to control levels on days 5-10 (Fig. 4.4 c).

I-FABP and L-FABP protein levels tended to decrease compared with controls from day 3 onwards, but only L-FABP protein decreased significantly on days 5-6 (Fig. 4.4 c). On days 8-10, expression of both FABP protein levels was not statistically different from controls. As shown in Fig. 4.4 c, GLUT5 protein levels tended to increase during the early phase of damage on days 1-2, but levels were dramatically decreased on days 3-4 compared with controls. During regeneration GLUT5 protein expression was rapidly increased as it was in the range of control levels on days 5-10, in line with GLUT5 mRNA expression (Figs 4.4 a and c).

In goblet cells, protein levels were not significantly correlated to the levels of the encoding mRNAs. MUC2 as well as TFF3 protein levels were significantly increased during all phases of damage, despite the reduced mRNA levels (Figs 4.4 b and d). In contrast to MUC2,

TFF3 protein remained significantly elevated on days 8-10. Despite the overall similarity in response to MTX, there was no significant correlation between MUC2 and TFF3 protein levels, as based on the analysis of the data from the individual rats.

## Discussion

The loss of small intestinal epithelial cells and the occurrence of villus atrophy through MTX has been well described and was appreciated since the seventies (Altmann 1974; Jeaynes and Altmann 1978). The unexpected diversity in our study regarding temporal expression patterns of ten epithelial gene products in response to MTX indicates the involvement of specific regulation, distinct and independent from extensive cell loss.

There are strong indications from our results and from previously published data (Kralovanszky and Prajda 1985; Taminiau et al. 1980; Tanaka et al. 1998), that glucose absorption is severely impaired during MTX-induced damage, due to the absence of important proteins, thereby contributing to malabsorption symptoms. SI and SGLT1 contribute to the digestion of starch and the absorption of glucose, the primary carbohydrate sources in the diet of the rats in our study. Since both SI and SGLT1 were significantly decreased during damage, these glucose-based energy sources will not be efficiently utilized. The physiological importance of the absence of carbohydrate digestion and absorption is underscored by the loss of body weight that occurs up to day 4 after MTX-treatment (Verburg et al. 2000).

Decreased expression of SGLT1 mRNA during damage is in agreement with previous findings using 5-FU as cytostatic drug (Tanaka et al. 1998). Yet our data additionally demonstrated that SGLT1 mRNA was still significantly decreased during regeneration on days 5-6, when the length of the intestinal villi and the morphology of the epithelial cells appeared normal. At this time the epithelium was still in a higher proliferative state than controls (Verburg et al. 2000). Most likely, decreased

SGLT1 expression was a result of incomplete differentiation of enterocytes. As a consequence, absorption of free glucose and sodium by SGLT1 was very likely impaired during damage as well as during regeneration. Defects in sodium absorption likely contributes to the development of diarrhea, which occurs during days 2-6 after MTX-treatment (Verburg et al. 2000).

Glycohydrolase expression, measured by si and lactase mRNA and si protein, was significantly correlated to villus height. The decreased expression of these brush border proteins during villus damage confirms previous findings (Kralovanszky and Prajda 1985; Taminiau et al. 1980). The significant correlation between si protein and mRNA indicates that si expression was primarily transcriptionally regulated, in agreement with previous work on si gene regulation (Krasinski et al. 1994; Traber et al. 1992).

GLUT5 is responsible for the uptake of fructose. Fructose, which was absent from the diet in the present study, has been shown to induce GLUT5 mRNA and protein expression (Corpe et al. 1998). GLUT5 mRNA and protein expression levels were only significantly decreased during the phase of severe villus damage. If fructose would be added as carbohydrate source to the diet, it could have had stimulatory effects on GLUT5 expression during intestinal damage and regeneration, which could contribute to energy uptake to prevent malnourishment in the MTX-treated rat.

The strong correlation between crypt depth and CPS mRNA expression was in line with the fact that CPS mRNA is expressed exclusively by crypt enterocytes, while the protein is also found in villus enterocytes (Van Beers et al. 1998). The time-lag between the decrease in CPS mRNA and protein levels can also be explained by their different localization pattern along the crypt-villus axis. A role for this mitochondrial protein in the intestinal urea cycle has been demonstrated by Davis and

Wu (Davis and Wu 1998). These authors showed in post-weaning pig-enterocytes, that CPS favors the net synthesis of citrulline from ammonia,  $\text{HCO}_3^-$  and ornithine. So far, a contribution of intestinal CPS to the systemic nitrogen balance by the consumption of ammonia may be underestimated compared to hepatic CPS. Our findings however could explain the reported hyper-ammonaemia of patients treated with cytostatic drugs (Fine et al. 1989; Liaw et al. 1993).

Several functions have been reported for the cytosolic fatty acid binding proteins in epithelial cells, reviewed by Storch and Thumser (Storch and Thumser 2000). Their role in the uptake and transport of fatty acids is important in the regulation of cellular membrane fatty acid levels and intracellular fatty acid concentrations that modulate fatty acid responsive genes. Despite the relative slow recovery during regeneration, the expression of I-FABP and L-FABP mRNAs and proteins was the least affected among the panel of our enterocyte markers during the phase of crypt damage and villus damage. This was underscored using immunohistochemistry. Thus, the FABPs were relatively resistant to damage compared with carbohydrate metabolizing enzymes and transporters, and are probably important for maintaining membrane integrity and fatty acid absorption in villus enterocytes. This indicates that fatty acids are potentially important as energy-source for use during cytostatic drug treatment. The strong correlation between I-FABP and L-FABP gene expression suggests that both genes were coordinately regulated under this physiological state. Furthermore, because of the strong correlations between mRNA and protein levels, expression of both FABP proteins appeared transcriptionally regulated after MTX-treatment.

In general, the presence and functionality of goblet cells and Paneth cells was preserved during the MTX-induced pathology. The expression patterns of MUC2, TFF3 and lysozyme indicated a generally enhanced

secretion of cytoprotective molecules during MTX-induced damage by goblet cells and Paneth cells. Secretion of mucin and trefoil factor molecules is known to contribute to protection of the epithelium via a mucus layer (MUC2), and by promoting epithelial restitution (TFF3) (Dignass et al. 1994). During all phases of damage (days 1-4) the observed changes in goblet cell-specific mRNA expression did not reflect the changes in protein expression, neither for MUC2 nor for TFF3. At early time points (days 1-2), the stable MUC2 and TFF3 mRNA expression was associated with highly increased protein expression. During villus atrophy (days 3-4), the decreased MUC2 and TFF3 mRNA expression was associated with increased protein expression. The reduced mRNA levels and increased protein levels can be explained by the loss of epithelial goblet cells, as we previously described (Verburg et al. 2000), and the involvement of post-transcriptional regulatory mechanisms allowing enhanced secretion of mucin and trefoil factor molecules. Yet, it is in contrast with the observation of Xian and colleagues, who reported no significant changes in TFF3 mRNA expression and significant decreased TFF3 protein expression in the proximal jejunum of MTX-treated rats during damage (Xian et al, 1999). Technically, the study of Xian et al. was performed differently by giving 3 subcutaneous injections of MTX, using different antibodies against TFF3, and using ribonuclease protection assays instead of Northern blots for analysis of mRNA expression. Also, they had selected for another small intestinal region and another rat strain (Sprague-Dawley). They did not detect TFF3 protein during maximal damage, either immunohistochemically or on Western blot, in contrast to our findings. Therefore, it is most likely that the intensity of damage was more severe in the study of Xian et al., leading to a much more decreased goblet cell function than in our study. Despite the overall similarities in MUC2 and TFF3 protein and mRNA levels, no significant correlations were found in their levels of gene expression during MTX-induced damage and

regeneration. This suggests that both genes were not coordinately regulated in goblet cells in response to chemotherapeutic damage, confirming recent work of others (Matsuoka et al. 1999).

The defense provided by Paneth cells is likely to act locally in the crypt micro-environment, e.g. in the area of the stem cells, via the secretion of a variety of crypt defensins and peptides that enhance mucosal innate immunity (Wilson et al. 1999). The MTX-induced increase in lysozyme mRNA expression and lysozyme immuno-staining, seen on days 1-2, confirmed our previous findings (Verburg et al. 2000), and likely represents an adaptive response in Paneth cells to contribute to increased protection, during the vulnerable stages of the crypt epithelium.

In our study, an unexpected diversity in responses to MTX was observed between the ten epithelial gene products. In particular, the remaining villus enterocytes during villus atrophy show a markedly specific response regarding their gene expression. These moribund cells seem to go through a programmed set of events that may be destined to maintain optimal epithelial performance during this stressed situation. Clinically, it may be possible to take advantage of these pre-programmed decisions by the absorptive epithelial cells to maintain optimal nutritional status of patients treated with cytostatic drugs. The central importance of the epithelial barrier function and the ability to regenerate after serious insults is reflected by the response of goblet cells and Paneth cells, in producing mucus, trefoil peptides and bactericidal peptides. The intestine thus reacts very specifically and diversely to severe damage or noxes and it seems very important to understand the different mechanisms involved in order to tailor enteral nutrition for patients treated with cytostatic drugs.

## 5 Protection of the Peyer's patch-associated crypt and villus epithelium against methotrexate-induced damage is based on its distinct regulation of proliferation

The crypt and villus epithelium associated with Peyer's patches (PPs) was largely spared from methotrexate (MTX)-induced damage compared to the epithelium located more distantly from PPs, i.e. the non-patch (NP) epithelium. To assess the mechanism(s) preventing damage to the PP epithelium after MTX treatment, epithelial proliferation, apoptosis and cell functions were studied in a rat-MTX model. Small intestinal segments containing PPs were excised after MTX-treatment. Epithelial proliferation and apoptosis were assessed by detection of incorporated BrdU and cleaved caspase-3, respectively. Epithelial functions were determined by the expression of cell type specific gene-products at mRNA and protein level. Before and after MTX treatment, the number of BrdU-positive cells was higher in PP crypts than in NP crypts. BrdU incorporation was diminished in NP crypts, while in PP crypts incorporation was hardly affected. In PP and NP crypts, similar and increased levels of cleaved caspase-3-positive cells were observed after MTX. The enterocyte markers, sucrase-isomaltase, sodium-glucose cotransporter 1, glucose transporters 2 and -5, and intestinal- and liver fatty acid binding protein were down-regulated after MTX in NP epithelium, but not in PP epithelium. In contrast, expression of the goblet cell markers, MUC2 and trefoil factor 3, and the Paneth cell marker lysozyme was maintained after MTX in both PP and NP epithelium. In conclusion: As MTX-induced apoptosis was similar in PP versus NP crypts, the protection of the PP epithelium seems to be based on differences in regulation of epithelial proliferation. Enterocyte functioning in the PP epithelium was unaffected by MTX treatment. Goblet and Paneth cell functioning was maintained in NP and PP epithelium.

### Acknowledgements

*We thank the following scientists for kindly providing the antibodies or cDNAs used in this study: Dr K.Y. Yeh for anti-rat sucrase-isomaltase antibodies; Dr P.G. Traber for rat sucrase-isomaltase cDNA; Dr B. Hirayama for anti-rabbit SGLT 1 antibodies; Dr C. Burant for rat SGLT 1 cDNA; Dr D.R. Yver for anti-rat GLUT5 antibodies; Prof. Dr J.I. Gordon for anti-rat intestinal FABP and liver FABP antibodies, and rat intestinal FABP and liver FABP cDNAs; Dr D.K. Podolsky for WE9 (anti-human MUC2 antibodies), anti-rat TFF3 antibodies, and rat TFF3 cDNA; Dr J.H. Power for lysozyme cDNA.*

### Published as

Melissa Verburg, Ingrid B. Renes, Danielle J.P.M. van Nispen, Sacha Ferdinandusse, Marieke Jorritsma, Hans A. Büller, Alexandra W.C. Einerhand and Jan Dekker. 'Protection of the Peyer's patch-associated crypt and villus epithelium against methotrexate-induced damage is based on its distinct regulation of proliferation' in *J.Pathology* 2002; 198 (1) 60-68.



## Introduction

The small intestinal epithelium proliferates rapidly and is therefore very sensitive to cytostatic drug treatment. Cytostatic drugs primarily inhibit DNA synthesis thereby deranging epithelial homeostasis leading to impaired intestinal epithelial functions (Pinkerton et al. 1982). Among the cytostatic agents, the effects of methotrexate (MTX) on the small intestinal epithelium of human and rat are well described (Pinkerton et al. 1982; Altmann 1974; Taminiau et al. 1980; Trier 1962). MTX is known to induce loss of crypts, crypt and villus atrophy, and flattening of crypt- and villus cells (Pinkerton et al. 1982; Altmann 1974; Taminiau et al. 1980; Trier 1962; Verburg et al. 2000). This damage occurs as a consequence of the MTX-induced inhibition of epithelial proliferation and induction of epithelial apoptosis. Recently, we demonstrated that MTX also induced a down-regulation of enterocyte-specific gene expression leading to enterocyte malfunctioning with regard to the degradation and absorption of nutrients (Verburg et al. 2000). In contrast, goblet cell- and Paneth cell gene expression were maintained after MTX treatment, suggesting that both goblet cells and Paneth cells were selectively spared. In the small intestinal mucosa lymphoid nodules, also known as Peyer's patches (PP), are located at the anti-mesenteric side of the intestine. The PPs consist of immuno-competent cells covered partly by follicle-associated epithelium and partly by the normal intestinal (crypt/villus) epithelium. Intriguingly, we recently observed that the epithelial morphology up to 2-3 crypt-villus units adjacent to and overlying the PP remained relatively intact after MTX-treatment when compared to the 'non-patch' (NP) epithelium (Renes et al. 2000). Yet, the mechanisms involved in the protection of the PP epithelium were unidentified. In the present study, we aimed to assess the mechanism(s) responsible for the protection of the PP epithelium from morphological damage after MTX treatment. Secondly, as the morphology of the PP epithelium was relatively but

not completely unaffected after MTX treatment, we studied epithelial cell functions of the PP epithelial cells after MTX treatment. Therefore, special attention was paid to epithelial proliferation, apoptosis and cell type-specific gene expression. As enterocytes are specialised in the degradation, uptake and transport of nutrients the following markers were used to analyse enterocyte function: sucrase-isomaltase (SI), sodium glucose transporter 1 (SGLT1), glucose/fructose transporters 2 and -5 (GLUT2 and -5), and liver- and intestinal fatty acid binding protein (I- and L-FABP). Goblet cell function was analysed by the expression of the mucin MUC2, which is the structural component of the protective mucus layer (Van Klinken et al. 1995), and trefoil factor 3 (TFF3), a bioactive peptide that is implied in epithelial protection and repair (Dignass et al. 1994; Mashimo et al. 1996). Paneth cells were analysed by the expression of the anti-bacterial enzyme lysozyme. By studying these parameters in conjunction we aimed to get insight in PP epithelial protection, to be able to develop therapies to prevent intestinal damage occurring as a side effect in cytostatic drug treatment.

## Materials and Methods

### Animals

Eight weeks-old, specified pathogen free, male Wistar rats (Broekman, Utrecht, The Netherlands) were housed individually at constant temperature and humidity on a 12-h light-dark cycle. The rats had free access to a standard pelleted diet (Hope Farms, Woerden, The Netherlands) and water. All the experiments were performed with the approval of the Animal Studies Ethics Committee of our institution.

### Experimental Design

A dosage of 30 mg/kg MTX (Ledertreaxate SP Forte, Cyanamid Benelux, Etten-Leur, The Netherlands) was injected intravenously under light anaesthesia. Control animals were treated with equivalent volumes of 0.9% NaCl solution. To study epithelial proliferation, 50

mg BrdU/kg body weight (Sigma, St. Louis, USA) was injected intraperitoneally 1 h before decapitation. On 6.5 h, days 1, 2, 3, and 4 after MTX four animals per timepoint were sacrificed. One control animal per timepoint was sacrificed at 6.5 h after MTX and on days 1, 2 and 4. Segments of the duodenum, jejunum and ileum containing PPs were dissected, immediately fixed in 4% paraformaldehyde in phosphate buffered saline (PBS) and prepared for light microscopy.

#### Histology

Sections of 5  $\mu\text{m}$  thickness were routinely stained with alcian blue-nuclear fast red (BDH, Brunschwig Chemie, Amsterdam, The Netherlands) to study goblet cells and morphological alterations like crypt- and villus atrophy.

#### Immunohistochemistry

Five  $\mu\text{m}$  thick paraffin sections were cut and deparaffinized through a graded series of xylol-ethanol. To visualize BrdU incorporation, sections were incubated with 2 M HCl for 1.5 h, washed in borate buffer (0.1 M  $\text{Na}_2\text{B}_4\text{O}_7$ , pH 8.5), incubated in 0.1% (w/v) pepsin in 0.01 M HCl for 10 min at 37°C, and rinsed in PBS. Endogenous peroxidase activity was inactivated by 1.5% (v/v) hydrogen peroxide in PBS for 30 min, followed by a 30 min incubation with TENG-T (10 mM Tris-HCl, 5 mM EDTA, 150 mM NaCl, 0.25% (w/v) gelatin, 0.05% (w/v) Tween-20) to reduce non-specific binding. This was followed by overnight incubation with a 1:500 dilution of mouse anti-BrdU (Boehringer Mannheim, Mannheim, Germany). Then, the sections were incubated for 1 h with biotinylated horse anti-mouse IgG (diluted 1:2000, Vector Laboratories, England) followed by 1 h incubation with ABC/PO complex (Vectastain Elite Kit, Vector Laboratories) diluted 1:400. Binding was visualised after incubation in 0.5 mg/ml 3,3'-diaminobenzidine (DAB), 0.02% (v/v)  $\text{H}_2\text{O}_2$  in 30 mM imidazole, 1 mM EDTA (pH 7.0). Finally, sections were counterstained with haematoxylin, dehydrated and mounted. Apoptotic cells and the expression

of the cell type-specific markers were demonstrated according to the above described protocol with omission of the HCl incubation, washing with borate buffer, and pepsin treatment. Anti-cleaved caspase-3 (1:100, Cell Signaling Technologies, Beverly, MA, USA) was used to identify apoptotic cells, anti-rat SI (1:6000, (Yeh et al. 1989)), anti-rabbit SGLT1 (1:1000, (Hirayama et al. 1996)), anti-rat GLUT2 (1:6000, Biodesign, Camprom Scientific, Veenendaal, The Netherlands), anti-rat GLUT5 (1:2500, (Payne et al. 1997)), anti-rat I-FABP (1:4000, (Cohn et al. 1992)), and anti-rat L-FABP (1:6000, (Sweetser et al. 1988)) were used to determine enterocyte-specific protein expression. As marker for goblet-cell specific protein expression a MUC2 specific antibody (WE9: 1:300, (Tytgat et al. 1995a)) and anti-TFF3 (1:6000) were used. Anti-lysozyme (1:25, Dako, Glostrup, Denmark) was used to detect Paneth cell-specific protein expression. To stain SGLT1, GLUT2 and GLUT5, and apoptotic cells, sections were boiled in 0.01 M citrate buffer at pH 6.0 for 10 min prior to incubation with the respective primary antibodies.

To study differences in epithelial proliferation and apoptosis between the PP- and NP epithelium, 6 well-oriented PP- and NP crypts were chosen per intestinal segment per animal. The 6 PP crypts were located adjacent to (3 crypts at each side of the PP) or overlying a PP and the NP crypts were located at the lateral side of the intestine. The number of BrdU-positive cells in the crypts was counted and expressed per crypt, per intestinal segment, per time point. The number of cleaved caspase-3-positive cells was counted and expressed as follows: 0, 0-1 positive cell per 6 crypts; 1, 2-5 positive cells per 6 crypts; 2, >5 positive cells per 6 crypts. This scoring method was used because the variance in the number of caspase-3-positive cells between crypts per time point was relatively large. To determine the number of BrdU- and caspase-3-positive cells in PP- and NP crypts in each intestinal region, sections were judged twice by two independent observers, who were unaware of the experimental conditions.

#### In Situ Hybridisation

Non-radioactive in situ hybridisations were performed according to the method described previously with slight modifications (Linderbergh-Kortleve et al. 1997). Briefly, sections were deparaffinized, hydrated and incubated in the following solutions: 0.2 M HCl, distilled water, 0.1% (w/v) pepsin in 0.01 M HCl, 0.2% (w/v) glycine in PBS, 4% paraformaldehyde in PBS, and finally in 2 x SSC (0.03 M Na<sub>3</sub>-citrate in 0.3 M NaCl). Until hybridisation, sections were stored in a solution of 50% (v/v) formamide in 2 x SSC at 37°C. For hybridisation, cell type-specific probes were diluted in hybridisation solution (50% (v/v) deionized formamide, 10% (w/v) dextran sulfate, 2 x SSC, 1 x Denhardt's solution, 1 µg/ml tRNA, 250 µg/ml herring sperm DNA) to a concentration of 100 ng/ml, incubated at 68°C for 15 min and layered onto the sections. Sections were hybridised overnight at 55°C in a humid chamber. Post-hybridisation washes were performed at 45°C using the following steps: 50% (v/v) formamide in 2 x SSC, 50% (v/v) formamide in 1 x SSC and 0.1 x SSC. A 15 min incubation with RNase T1 (2 U/ml in 1 mM EDTA in 2 x SSC) at 37°C was followed by washes of 0.1 x SSC at 45°C and 2 x SSC at room temperature. The digoxigenin-labeled hybrids were detected by incubation with anti-digoxigenin (Fab, 1:2000) conjugated to alkaline phosphatase for 2.5 h at room temperature. Thereafter, sections were washed in 0.025% (v/v) Tween in Tris-buffered saline pH 7.5. For staining, sections were layered with detection buffer (0.1 M Tris-HCl, 0.1 M NaCl, 0.05 M MgCl<sub>2</sub> pH 9.5) containing 0.33 mg/ml 4-nitroblue tetrazolium chloride, 0.16 mg/ml 5-bromo-4-chloro-3-indolyl-phosphate, 8% (v/v) polyvinylalcohol (Mw 31000-50000, Aldrich Chemical Milwaukee, WI, USA) and 1 mM levamisole (Sigma). The color reaction was performed overnight in the dark and was stopped when the desired intensity of the resulting blue precipitate was reached. Finally, sections were washed in 10 mM Tris-HCl containing 1 mM EDTA, distilled water and mounted with Aquamount improved (Gurr, Brunswick, Amsterdam, The Netherlands).

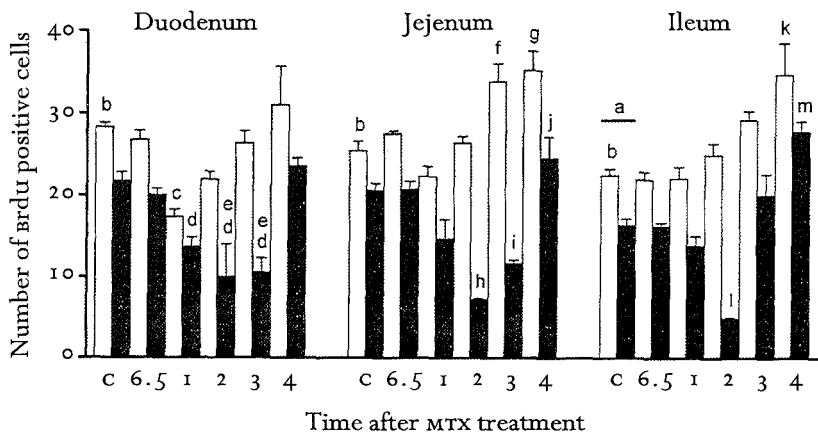


Figure 5.2

Epithelial proliferation in the duodenum, jejunum and ileum of control and MTX-treated rats.

Proliferation was studied by immunohistochemical detection of incorporated BrdU at 6.5 h and days 1, 2, 3, and 4 after MTX. Average numbers of BrdU-positive cells in both the Peyer's patch (PP) crypts (white bars) and 'non-patch' (NP) crypts (black bars) were calculated per intestinal region, per rat.

Subsequently, mean BrdU-positive cell numbers ( $\pm$ SEM) were calculated for PP- and NP crypts. In control ileum proliferation in PP- and NP crypts was significantly lower than in duodenum and jejunum ( $a$ ,  $p < 0.05$ ). In each intestinal region of controls, proliferation in the PP crypts was significantly higher than in the NP crypts ( $b$ ,  $p < 0.015$ ). In the PP crypts of the duodenum proliferation was significantly decreased on day 1 compared to controls and day 4 ( $c$ ,  $p < 0.05$ ). In contrast, in the NP crypts of the duodenum proliferation was decreased on days 1-3 compared to controls and day 4 ( $d$ ,  $p < 0.05$ ) and on days 2 and 3 compared to 6.5 h ( $e$ ,  $p < 0.05$ ). In the jejunum, proliferation in PP crypts was significantly increased on day 3 compared to controls and day 1 ( $f$ ,  $p < 0.05$ ) and on day 4 compared to controls, 6.5 h, and days 1 and 2 ( $g$ ,  $p < 0.05$ ). In the NP crypts of the jejunum a significant decrease in proliferation was seen on day 2 compared to controls, 6.5 h, and days 1 and 4 ( $h$ ,  $p < 0.05$ ), and on day 3 compared to controls and 6.5 h ( $i$ ,  $p < 0.05$ ). On day 4, a significant increase in proliferation in NP crypts was seen compared to days 1-3 ( $j$ ,  $p < 0.01$ ). In the PP crypts of the ileum proliferation was significantly increased on day 4 compared to controls, 6.5 h, and days 1 and 2 ( $k$ ,  $p < 0.05$ ). In the NP crypts of the ileum proliferation was significantly decreased on day 2 compared to controls, 6.5 h, days 1, 3 and 4 ( $l$ ,  $p < 0.05$ ), and significantly increased on day 4 compared to all other groups ( $m$ ,  $p < 0.05$ ).

Probe preparation for in situ hybridisation  
Digoxigenin-11-UTP-labeled RNA probes were prepared according to the manufacturer's prescription (Boehringer Mannheim GmbH, Biochemica, Mannheim, Germany) using T3, T7 or SP6 RNA polymerase. The following enterocyte-specific probes were used: a 827 bp fragment of rat S1 cDNA clone ligated in pBluescript KS (Traber 1990), a 1 kb NcoI fragment based on the 2.4 kb fragment of rat SGLT1 cDNA clone ligated in pBluescript II SK (You et al. 1995), and a 350 bp fragment of rat L-FABP cDNA clone ligated in pBluescript (Simon et al. 1993). As Goblet cell-specific probes a 200 bp EcoRI/NotI fragment based on the 1.1 kb fragment of rat MUC2 as described previously (Verburg et al. 2000), and a 438 bp EcoRI fragment of rat TFF3 ligated in pBluescript KS were used (Suemori et al. 1991). A 990 bp fragment of rat lysozyme cDNA ligated in pBluescript KS+/L8 was used as marker for Paneth cell specific mRNA expression (Yogalingam et al. 1996). Transcripts longer than 450 bp were hydrolysed in 80 mM NaHCO<sub>3</sub> and 120 mM Na<sub>2</sub>C<sub>3</sub>, pH 10.2 to obtain probes of various lengths  $\leq 450$  bp (Cox et al. 1984).

#### Statistical Analysis

To detect significant differences in epithelial proliferation between the PP- and NP epithelium within an intestinal region and

between intestinal regions, analysis of variance was performed followed by an unpaired *t*-test. Differences were considered significant when  $p < 0.05$ . Data were represented as the mean  $\pm$  standard error of the mean (SEM).

## Results

### Histological Evaluation

MTX-induced damage to the 'normal' small intestinal epithelium, i.e. 'non-patch' (NP) epithelium, is characterised by villus atrophy, and flattening of crypt and villus cells (Taminiau et al. 1980, Verburg et al. 2000). In the present study, we observed similar changes in the NP epithelium of the duodenum, jejunum and ileum after MTX treatment (Fig. 5.1c, jejunum). However, focussing on the epithelium near a PP (i.e. 2-3 crypt-villus units adjacent to and lining the PP) in each small intestinal segment, we observed that MTX-induced damage was much less pronounced (Fig. 5.1d, jejunum).

### Epithelial Proliferation

Epithelial proliferation was studied by immunohistochemical detection and quantitation of metabolically incorporated BrdU. In controls, the number of BrdU-positive cells in PP crypts was significantly higher than in NP crypts in each intestinal segment (Fig. 5.2). In addition, the number of BrdU-positive cells in control intestine decreased significantly from duodenum toward the ileum in both the PP- and NP crypts. At 6.5 h after MTX treatment no changes in the number of BrdU-positive cells were observed in any intestinal segment in the NP and PP crypts compared to controls. However, major differences in the number of BrdU-positive cells in each intestinal segment, in both PP and NP crypts, were observed on days 1-4 following MTX treatment. In the duodenum, significantly decreased levels of BrdU-positive cells were seen only on day 1 in the PP crypts, whereas decreased levels were observed on days 1-3 in the NP crypts. In addition, in the PP crypts of the duodenum the number of BrdU-positive cells were comparable with control levels on days 2 and 3,

and were slightly increased on day 4 although not significantly. In the jejunum, no alterations in the number of BrdU-positive cells were seen in the PP crypts on days 1 and 2. However, on days 3 and 4 the levels of BrdU-positive cells were significantly increased in the PP crypts compared to controls. In contrast, in the NP crypts of this segment decreased numbers of BrdU-positive cells were seen on days 2 and 3. On day 4 the number of BrdU-positive cells in the NP crypts was comparable to controls. Similar to the jejunum, the number of BrdU-positive cells in the ileal PP crypts was unaltered on days 1 and 2, and significantly increased on days 3 and 4. On the other hand, in the NP crypts the number of BrdU-positive cells was significantly decreased on day 2, comparable with control levels on day 3, and significantly increased on day 4.

### Epithelial apoptosis

To detect apoptotic cells we used an antibody specific for the cleaved form of caspase-3. Caspase-3 is one of the key executioners of apoptosis (Nicholson et al. 1995). Activation of caspase-3 requires proteolytic cleavage of its inactive zymogen into activated p17 and p12 subunits. The antibody used in this study detects only the large fragment of activated caspase-3, whereas it does not recognise full length caspase-3 or other caspases. At each time point investigated, the scores of cleaved caspase-3-positive cells were similar for the duodenum, jejunum, and ileum. Therefore, only the scores for the duodenum are given in Table 5.1. MTX treatment resulted in an increase in the score of cleaved caspase-3-positive cells at 6.5 h and at day 1 in both NP- and PP crypts (Table 5.1 and Fig. 5.3b). On day 2, the score of cleaved caspase-3-positive cells decreased in NP- and PP crypts compared to 6.5 h and 1 day after MTX treatment, but was still elevated compared to controls (Fig. 5.3c). In both the NP- and PP crypts, the score of cleaved caspase-3-positive cells was comparable with control values on days 3 and 4. No differences in the score or position of cleaved caspase-3-positive cells were seen between the NP- and PP crypts, at each time

Table 5.1

Scoring of caspase-3-positive cells in PP- and NP crypts in the duodenum of control and MTX-treated rats

Time after MTX Treatment	Cleaved caspase-3 positive cell score in the duodenum	
	NP crypts	PP crypts
6.5 h	2	2
1 day	2	2
2 days	1	1
3 days	0	0
4 days	0	0
control	0	0

The numbers of cleaved caspase-3 positive cells were counted in the Peyer's patch (PP) epithelium and the non-patch epithelium (NP) of the duodenum, jejunum, and ileum and expressed as follows: 0, 0-1 positive cell per 6 crypts; 1, 1-5 positive cells per 6 crypts; 2, >5 positive cells per 6 crypts. No differences were observed in the scores between duodenum, jejunum, and ileum. Therefore, only the scores of the duodenum are given.

point investigated. Further, there was no inter-animal variance in the score of caspase-3-positive cells at each time point investigated.

Enterocyte-specific gene expression  
Enterocyte-specific mRNA expression was studied by in situ hybridisation using rat SI-, rat SGLT1-, and rat L-FABP specific probes. SI-, SGLT1-, and L-FABP mRNA was normally expressed in duodenal, jejunal, and ileal villus enterocytes (Fig. 5.4a and c, SGLT1 and L-FABP, respectively). At 6.5 h, and days 1 and 2 after MTX treatment no alterations in the enterocyte-specific mRNA expression patterns were seen in any of the intestinal segments (not shown). However, on days 3 and 4 we observed dramatic alterations in enterocyte-specific mRNA expression patterns between the NP- and PP epithelium. Specifically, SI-, SGLT1-, and L-FABP mRNA expression was decreased on day 3 in the NP villus epithelium in each intestinal segment, but not in the PP villus epithelium (not shown). On day 4 SI- and SGLT1 mRNA expression was even completely absent in the NP villus epithelium, but remained present at high levels in the PP villus epithelium (Fig. 5.4b, SGLT1). Similar to SI- and SGLT1 mRNA, L-FABP mRNA remained present in the PP villus epithelium on day 4 after MTX treatment (Fig. 5.4c, L-FABP). Additionally, many enterocytes of the NP villi were negative for L-FABP mRNA on day 4. Enterocyte-specific protein expression was studied immunohistochemically using antibodies against SI, SGLT1, GLUT2 and -5, and i- and L-FABP. SI-, SGLT1- and GLUT5 protein expression was normally confined to the brush border of villus enterocytes in NP- and PP epithelium of each intestinal segment (Fig. 5.4e, SI). GLUT2 protein was expressed at the basolateral membrane of enterocytes in NP- and PP villi in control duodenum, jejunum and ileum (Fig. 5.4g). In contrast to the membrane-bound expression patterns of the markers described above, i- and L-FABP proteins were normally found in the cytosol of duodenal, jejunal and ileal villus enterocytes (Fig. 5.4 i, L-FABP). Similar to the mRNA expression patterns, no alterations in

enterocyte-specific protein expression patterns were observed on 6.5 h and days 1 and 2 after MTX treatment in the NP epithelium or in the PP epithelium (not shown). On day 3 each of the enterocyte-specific protein markers appeared to be decreased in the NP villus epithelium of each intestinal segment, while the expression seemed to be unaffected in the PP villus epithelium. On day 4, the NP villus enterocytes were even negative for SI -, SGLT1 -, GLUT2 and GLUT5 protein (Fig. 5.4f and h, SI and GLUT2, respectively). Additionally, many NP villus enterocytes were negative for I-FABP protein (Fig. 5.4l) as well as L-FABP protein (Fig. 5.4j and k).

**Goblet cell-specific gene expression**  
Goblet cell-specific gene expression patterns were studied using rat MUC2- and rat TFF3 specific CRNA probes and antibodies. MUC2- and TFF3 mRNA and protein were expressed by goblet cells in crypts and villi of the NP- and PP epithelium in control duodenum, jejunum and ileum (Fig. 5.5a and e, MUC2- and TFF3 protein, respectively). Following MTX treatment, goblet cells in each intestinal segment appeared to maintain MUC2- and TFF3 mRNA expression in the NP epithelium (Fig. 5.5d, MUC2 mRNA) as well as PP epithelium (Fig. 5.5c, MUC2 mRNA). MUC2- and TFF3 protein expression were also maintained in the PP- and NP epithelium at day 4 (Fig. 5.5b and f). Although goblet cells continued to express MUC2 - and TFF3 protein, the distribution pattern of goblet cells along the crypt-villus axis changed after MTX treatment in the NP epithelium, but not in the PP epithelium. Specifically, in the NP epithelium goblet cells were largely absent in crypts on day 2 after MTX treatment (not shown), but accumulated both in crypts and at villus tips on day 4 (Fig. 5.5b, d and f).

**Paneth cell-specific gene expression**  
Lysozyme was used as marker for Paneth cell-specific cell function. In controls lysozyme mRNA and protein was expressed in Paneth cells at the crypt base of NP- and PP epithelium of the duodenum, jejunum and ileum (Fig.

5.6a, mRNA). Additionally, also within immunocompetent cells of the PP lysozyme mRNA and protein expression was observed. No changes in lysozyme mRNA or protein expression patterns by Paneth cells occurred after MTX treatment in the NP- and PP epithelium. However on days 2 and 3, lysozyme mRNA and protein were maintained in the PP crypts and seemed up-regulated in NP crypts (Fig. 5.6b, mRNA). Moreover, within the PP the number of immunocompetent cells expressing lysozyme mRNA and protein was strongly increased.

## Discussion

In the present study we aimed to determine which mechanism(s) underlie the protection of the PP epithelium against MTX-induced damage. Therefore, we investigated if there were differences in epithelial proliferation and apoptosis between the NP- and PP epithelium after MTX administration. Additionally, as the morphology of the PP epithelium was relatively, but not completely unaffected after MTX treatment, we studied epithelial cell functions of the PP epithelial cells after treatment.

Morphological analysis revealed that MTX-induced damage was characterised by villus atrophy and flattening of crypt and villus cells of the NP epithelium. In contrast, the PP epithelium seemed relatively unaffected by MTX treatment. In several studies similar results were reported concerning the MTX-induced morphological damage to the normal small intestinal epithelium (Taminiau et al. 1980; Verburg et al. 2000; Xian et al. 1999). However, in none of these studies the effects of cytostatic drugs on the epithelial morphology of the PP epithelium have been described. It is generally known that the sensitivity of tissues toward cytostatic agents depends primarily on the proliferation rate, i.e. high proliferation rate leads to high sensitivity. As the epithelial proliferation rate in the NP - and PP epithelium decreased from duodenum toward the ileum, one would expect the MTX-induced inhibition of epithelial proliferation

to be most affected in the duodenum. Indeed, we observed that the duration of MTX-induced inhibition of epithelial proliferation in the NP and PP epithelium was the longest in the duodenum, and decreased from duodenum toward the ileum. These data are in line with our previous study in which we demonstrated that the MTX-induced inhibition of epithelial proliferation in the normal small intestine was least affected in the ileum (Verburg et al. 2000). Further, as the proliferation rate in the PP epithelium of each intestinal region was significantly higher than in the NP epithelium, we expected the MTX-induced inhibition of epithelial proliferation to be most pronounced in the PP epithelium. However, the opposite appeared to occur. Namely, the MTX-induced inhibition of proliferation was less pronounced, shorter in duration, or did not occur at all in the PP crypts. Similarly, Moore and Maunda reported that in mice, the mitotic activity in the PP crypts is higher than in the NP crypts (Moore and Maunda 1983; Maunda and Moore 1987). Furthermore, the apparent cell cycle time of epithelial cells in the PP crypts appeared to be insignificantly lower than the cell cycle time in the NP crypts. Interestingly, the latter authors also demonstrated that the PP crypts were less sensitive for radiation and cytostatic drug-induced damage than the NP crypts. It is well known that the response of cells to ionising radiation is influenced by the concentration of oxygen present at the time of radiation (Maunda and Moore 1987). Therefore, asymmetries in the vascular supply in the gut as reported previously (Bhalla et al. 1981), might cause differences in oxygen concentrations between the PP- and NP crypts. Yet, in radiation experiments extra oxygen supply by breathing pure oxygen instead of room air or by using a hypoxic cell sensitizer did not sensitise PP crypts to radiation damage (Moore and Maunda 1983). Oxygen need not be the only blood-borne factor unequally distributed between PP - and NP crypts, since Bhalla et al. observed a direct connection between capillaries draining the PP follicles and the crypt plexus of PP crypts (Bhalla et al. 1981). Subsequently, it was suggested that



humoral factor(s) from the PP might regulate proliferation within the PP crypts resulting in differences in proliferation kinetics between the PP- and NP epithelium. In the present study we demonstrated that the numbers of proliferating cells in the PP crypts differed from those in the NP crypts. Moreover, as the PP epithelium was largely unaffected after MTX treatment compared to the NP epithelium, the possible humoral factor(s) which regulate epithelial proliferation in the PP crypts also very likely protect the PP crypts against MTX-induced damage.

Analysis of MTX-induced damage revealed increased apoptotic cell numbers in each intestinal segment at 6.5 h and on days 1 and 2 after MTX in both NP- and PP crypts. No differences were seen in the number and position of apoptotic cells between the NP- and PP epithelium, at all timepoints investigated. However, because the variance in the number of caspase-3-positive cells between crypts per timepoint was large, we can not exclude that there are small differences between the number of apoptotic cells in NP- and PP crypts. These data suggest that the protection from damage of the PP epithelium after MTX treatment can be accounted to differences in proliferation between the NP- and PP epithelium and not, or to a lesser extend accounted to differences in epithelial apoptosis.

Studying enterocyte-specific cell functions we observed major differences between the NP- and PP epithelium in the duodenum, jejunum and ileum. After MTX administration we observed that each enterocyte-specific marker, i.e. SI, SGLT1, GLUT2 and -5, and i- and L-FABP was down-regulated in the NP epithelium, but not in the PP epithelium. These data demonstrate a negative correlation between enterocyte-specific gene expression and the MTX-induced morphological damage. The down-regulation of enterocyte-specific gene expression in the NP epithelium implies enterocyte malfunctioning within this epithelium with regard to the degradation, absorption and transport of sugars and fatty acids. Furthermore, the retained proliferation

and enterocyte-specific gene expression in the PP epithelium after MTX treatment suggest that maintenance of proliferation is a prerequisite for unperturbed enterocyte functioning after MTX treatment. Regarding the down-regulation of enterocyte-specific gene expression in the NP epithelium after MTX treatment, Tanaka et al. reported similar results for enterocyte-specific SI- and SGLT1 expression in the normal small intestinal epithelium of rats treated with 5-fluorouracil (Tanaka et al. 1998).

In contrast to the enterocyte-specific gene expression, goblet cell-specific gene expression (i.e. MUC2 and TFF3) appeared to be maintained after MTX treatment in the NP- as well as PP epithelium. Maintenance of MUC2 and TFF3 gene expression suggests an important role for goblet cells in the defence and repair of the small intestinal mucosa after MTX. Interestingly, several days after MTX injection goblet cells accumulated at the villus tips of the NP epithelium. These data are in line with our previous study in which we demonstrated that the goblet cells that accumulated at villus tips after MTX were selectively spared from extrusion (Verburg et al. 2000).

Paneth cell-specific gene expression was maintained in the PP epithelium and seemed even up-regulated in the NP epithelium in response to MTX treatment. Moreover, the up-regulation of lysozyme also occurred in immunocompetent cells of the PP.

Quantitation of lysozyme mRNA levels, as described in a recent study by our laboratory, showed a strong up-regulation of lysozyme mRNA during the first two days after MTX treatment (Verburg et al. 2000). In addition, Paneth cell hyperplasia in rat small intestine after sublethal doses of MTX was described previously (Jeynes and Altmann 1978). These data in conjunction suggest that Paneth cells and also immunocompetent cells within the PP actively contribute to the protection of the small intestinal mucosa after MTX treatment. In summary, the PP epithelium is protected from damage induced by MTX treatment. No differences in MTX-induced apoptosis between

the NP- and PP epithelium seemed to occur. In contrast, proliferation was strongly inhibited after MTX treatment in the NP epithelium, whereas in the PP epithelium inhibition of proliferation was less pronounced or did not occur at all. Therefore, the protection of PP epithelium is based, at least partly, upon differences in the regulation of proliferation. MTX treatment induced a down-regulation of enterocyte-specific gene expression in the NP epithelium, but not in the PP epithelium. These data suggest maintenance of enterocyte functions in the PP epithelium after MTX treatment with regard to the degradation, absorption and transport of sugars and fatty acids. Maintenance of MUC2 and lysozyme expression after MTX in both the NP- and PP epithelium suggest an important role for goblet cells, Paneth cells and immuno-competent cells of the PP in the mucosal defence after MTX administration. Additionally the maintained expression of TFF3 in the NP- and PP epithelium indicates that the mucosal repair capacity may not be affected after MTX treatment. Collectively these data indicate that maintenance of epithelial defence mechanisms and most importantly epithelial proliferation near PPs after MTX preserve enterocyte-specific functions such as nutrient degradation, absorption and transport. Therefore, identification of the factor(s) which control epithelial proliferation in the PP epithelium before and after MTX might be of relevance to develop clinical therapies to protect cancer patients from intestinal damage induced by chemotherapy.

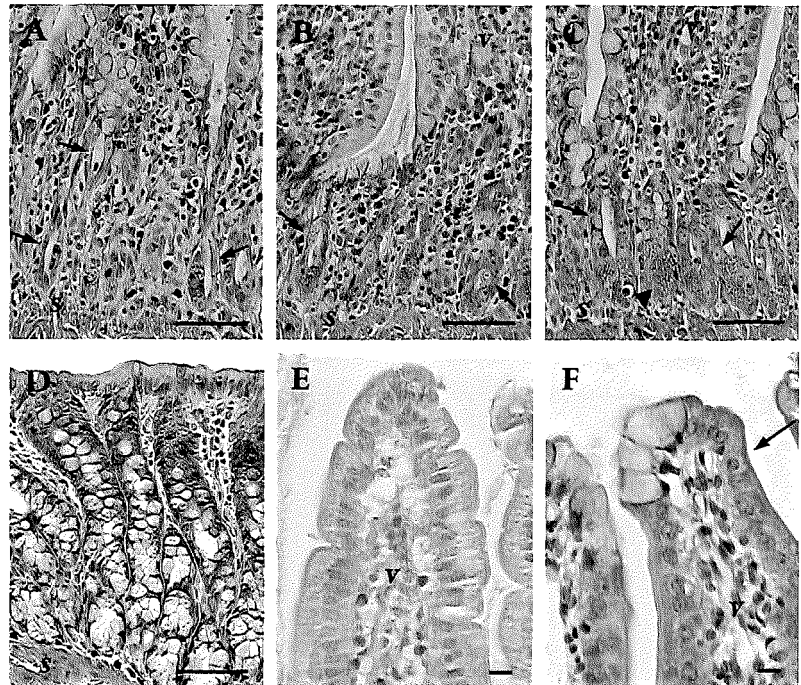


Figure 3.4

HE-stained sections showing MTX-induced changes in epithelial morphology along the small intestine and colon. Crypt damage was seen in the small intestine and characterized by loss of crypt cells and flattening of remaining epithelium (arrows). Crypt damage was most severe on day 2 in the duodenum (A). Less severe damage was seen in the jejunum (B) and the ileum (C). No epithelial abnormalities were seen in the colon on day 2 (D). During villus atrophy on days 2-4 in all small intestinal regions, high numbers of epithelial cells were lost and the remaining cells appeared flattened, as shown in the jejunum on day 4 (E), when compared to controls (F). v: villus, s: serosal side. Bars represent 50  $\mu$ m (A-D) or 10  $\mu$ m (E-F).

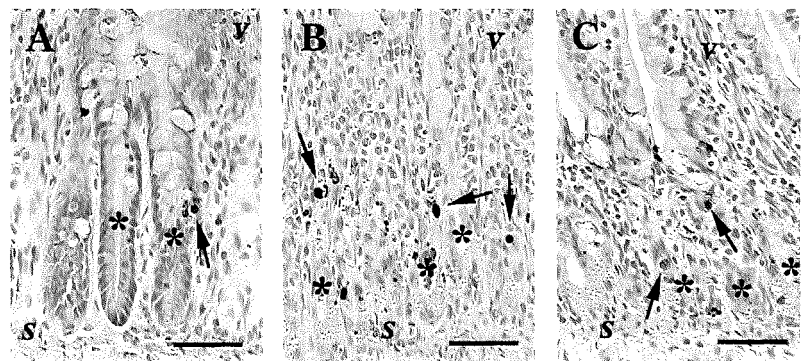


Figure 3.5

MTX-induced apoptosis in the small intestine of MTX-treated rats. Increased numbers of TUNEL-positive cells (arrows) were seen in the crypts of the jejunum at day 1 (B) and day 2 (C) when compared to controls (A). S: serosal side, V: villus, \*: crypts. Sections were counterstained with hematoxylin. Bars represent 50  $\mu$ m.

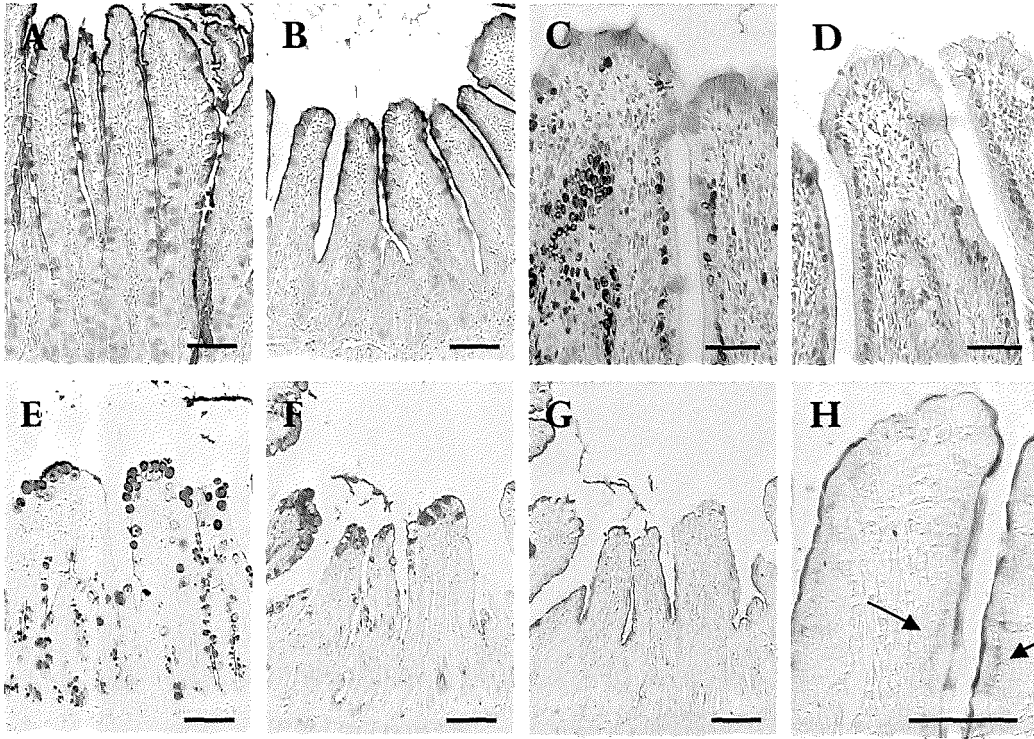


Figure 3.6

Effects of MTX-treatment on the (immuno-) histochemical detection of intestinal epithelial differentiation markers in rat jejunum and colon. A-B: AP activity and alcian blue double staining in the jejunum of control (A) and MTX-treated (B) rats. AP activity remained detectable in the brush border of jejunal enterocytes during villus atrophy on day 4 after MTX-treatment as in controls, despite severe cell loss; C, D: alcian blue and rd double staining of a jejunal section on day 4 after MTX-treatment (C) and a serial section stained for PCNA (D). During MTX-induced villus atrophy, goblet cells (in blue) accumulated at villus tips along the small intestine surrounded by BrdU- or PCNA-positive cells (in brown); E, F: Goblet cell-specific expression of MUC2 (E) and TFF3 (F) at villus tips during -induced villus atrophy on day 4 after MTX. G-H: SI expression in rat jejunum on day 4 after MTX-treatment. During MTX-induced villus atrophy, SI was decreased (G) when compared to controls (not shown). The intracellular staining of SI-precursor detected high up the villus (arrows) indicates the late moment of enterocyte differentiation (H). I-J: lysozyme immunostaining in Paneth cells of control jejunum (I) and at day 2 after MTX (J). Lysozyme expression was increased during crypt damage on days 1 and 2 after MTX-treatment, when compared to controls. Bars represent 50  $\mu\text{m}$  (C-D, H-J), 100  $\mu\text{m}$  (A-B, E-G).

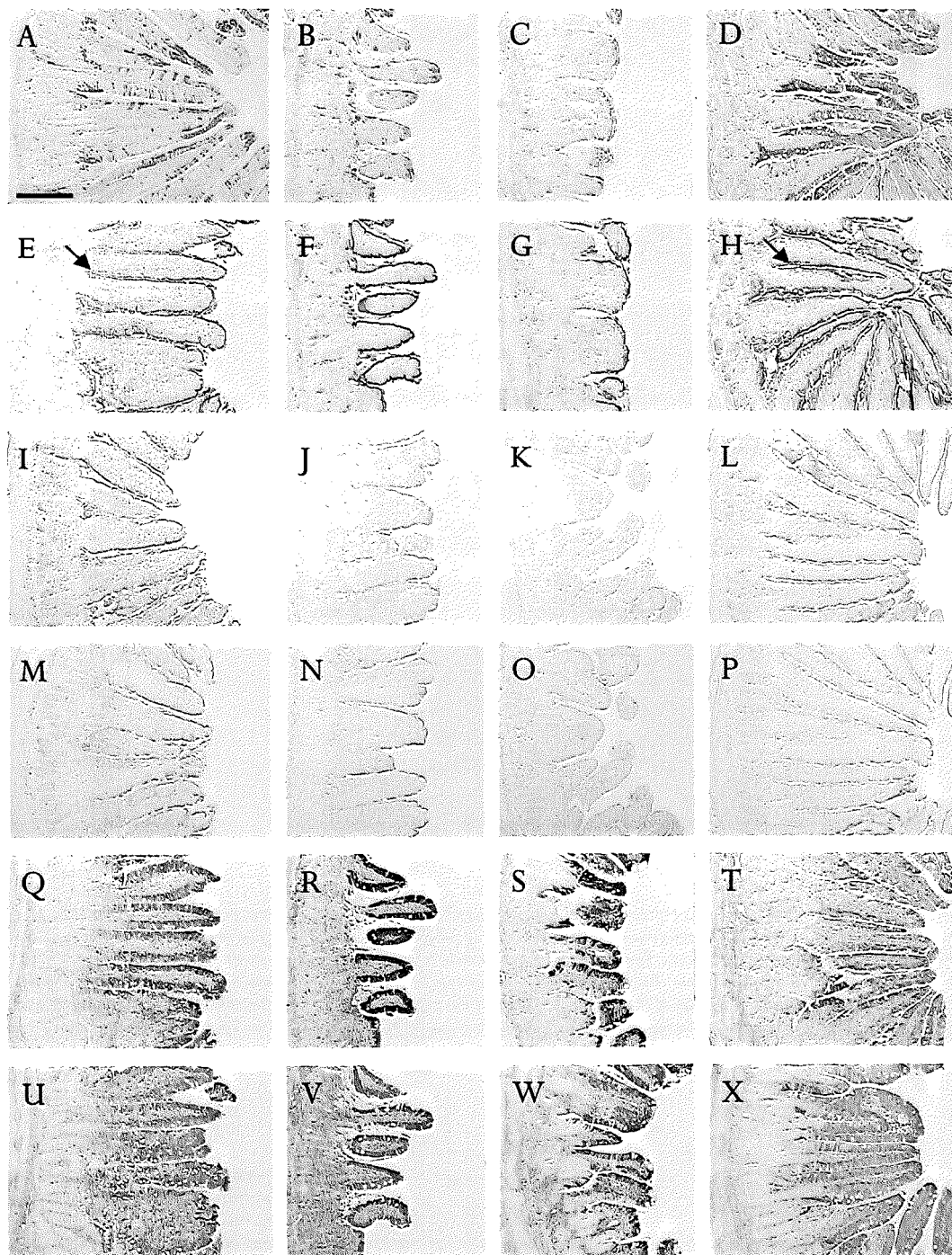


Figure 4.1

Immunohistochemical detection of proteins expressed in jejenum enterocytes during different phases of MTX-induced damage and regeneration. The following enterocyte-specific proteins were detected; CPS (A-D), SI (E-H), GLUT 5 (I-L), SGLT 1 (M-P), I-FABP (Q-T), and L-FABP (U-X). Panels A, E, I, M, Q, and U, show control sections. Panels B, F, J, N, R, and V, show sections at 2 day after MTX-treatment. Panels C, G, K, O, S, and W show sections at 4 days after MTX-treatment. Panels D, H, L, P, T, and X show tissue 8 days after MTX-treatment. The arrows in panels E and H indicate staining of the Golgi complex by the anti-SI antibodies. All micrographs have the same magnification, the representative bar in panel A represents 200  $\mu\text{m}$ .

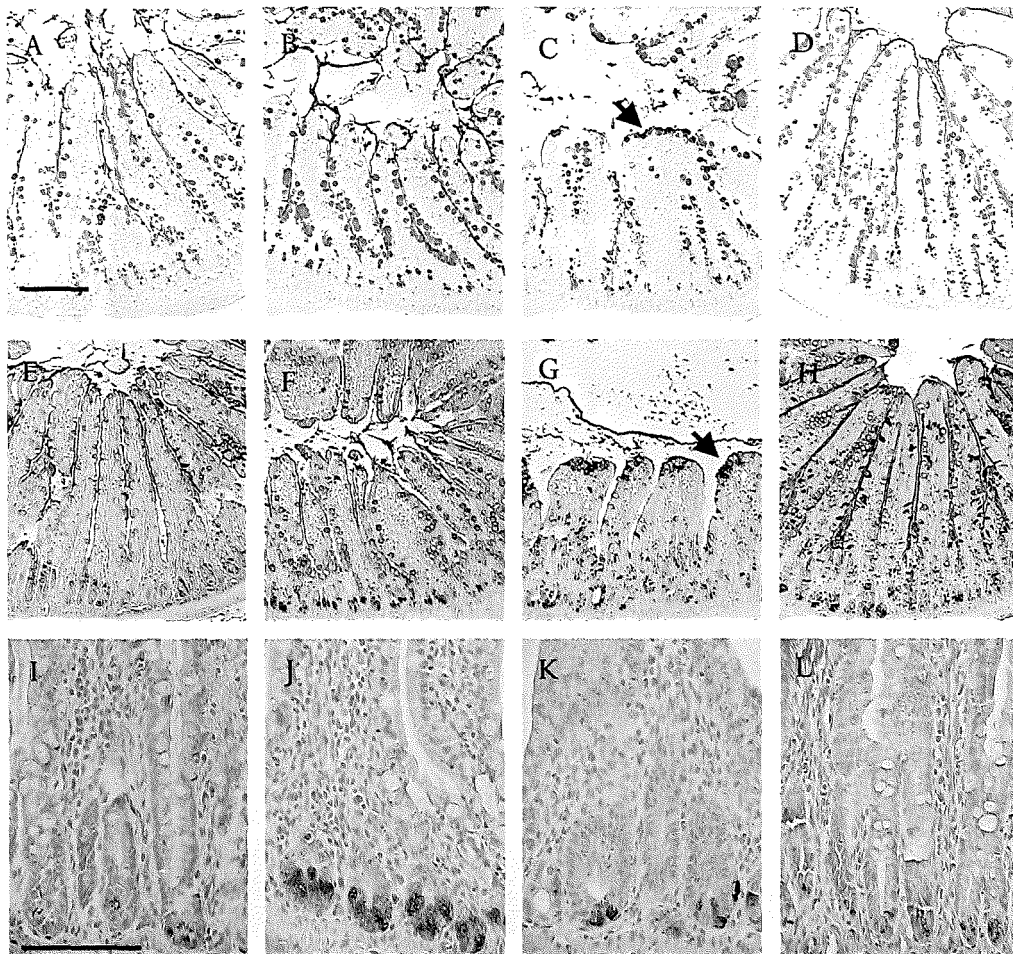


Figure 4.2

Immunohistochemical detection of proteins expressed in jejunum goblet or Paneth cells during different phases of MTX-induced damage and regeneration. MUC2 (A-D) and TFF3 (E-H) were detected in goblet cells, whereas lysozyme (I-L) was detected in Paneth cells. Panels A, E, and I show control sections. Panels B, F, and J show sections at 2 day after MTX-treatment. Panels C, G, and K show sections at 4 days after MTX-treatment. Panels D, H, and L show tissue 8 days after MTX-treatment. Arrows in panels C and G indicate goblet cells accumulated at the tips of the rudimentary villi, 4 days after MTX-treatment. Sections displayed in panels E-L were briefly stained with hematoxylin. Micrographs A-H have the same magnification (Panel A, bar = 200  $\mu$ m). Panels I-L also have the same magnification (Panel I, bar = 100  $\mu$ m).

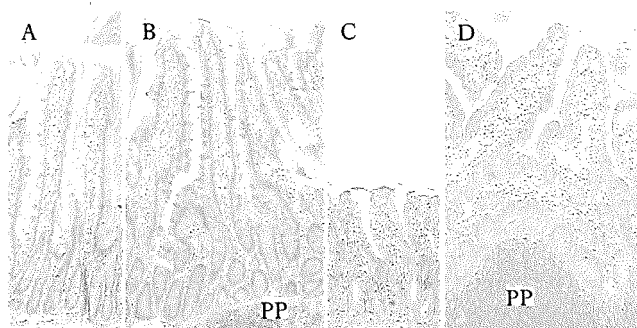


Fig. 5.1

Morphology of the normal jejunal epithelium (i.e. 'non-patch' (NP) epithelium) and the jejunal epithelium near and lining Peyer's patches (PP) (i.e. PP epithelium) before and after MTX-treatment. Alcian Blue-Nuclear Fast Red staining. A and B: jejunum of control rat; C and D: jejunum 4 days after MTX treatment. Villus atrophy and flattening of crypt and villus epithelial cells were observed in the normal intestinal epithelium, i.e. 'non-patch' (NP) epithelium on day 4 (C). The epithelium up to 2-3 crypt-villus units next to and lining Peyer's patches (PPs), i.e. the PP epithelium appeared to be spared from damaged (D).



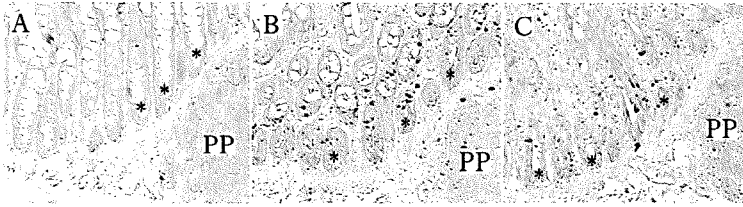


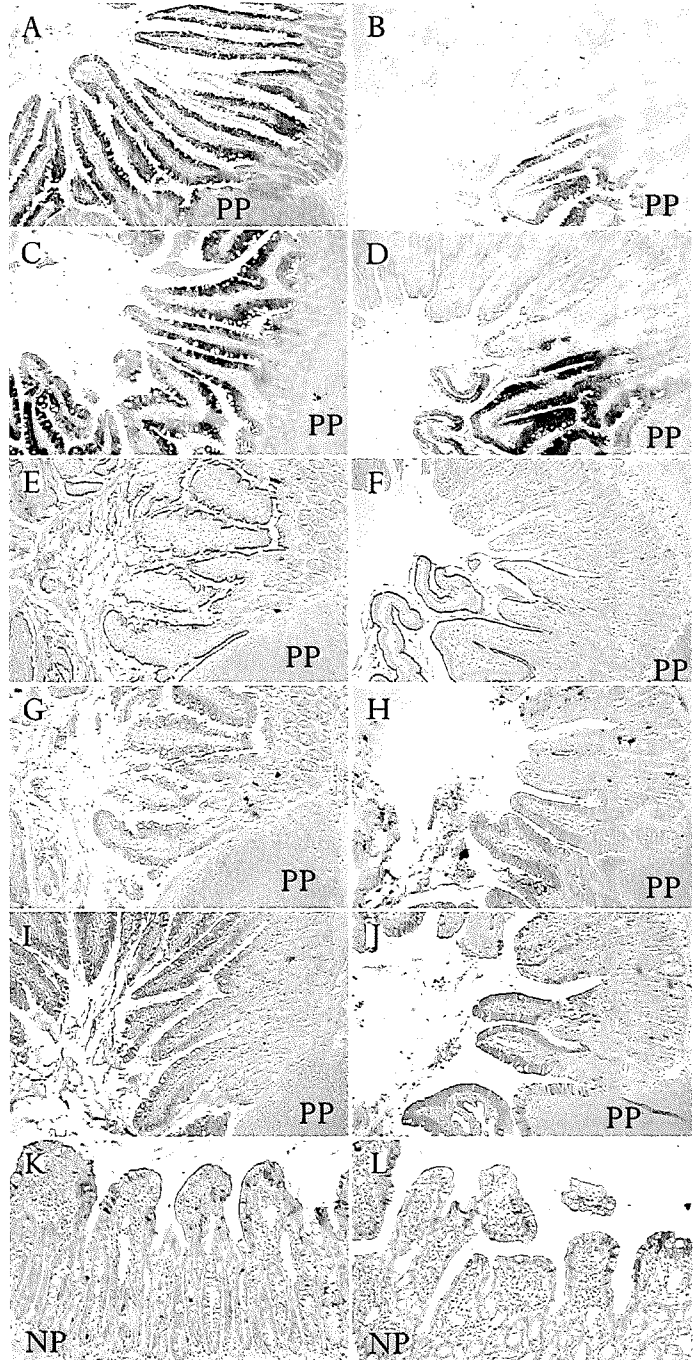
Figure 5.3

MTX-induced apoptosis in the normal intestinal epithelium (i.e. 'non-patch' (NP) epithelium) and the epithelium near and lining Peyer's patches (PP) (i.e. PP epithelium).

A: jejunum of control rat; B: jejunum 6.5 hrs after MTX; jejunum 2 days after MTX. Caspase-3-positive cells are present 6.5 hrs and 2 days after MTX in the NP- and PP epithelium. Some crypts are indicated with asterisks.

Figure 5.4

Effects of MTX on enterocyte-specific gene expression in the normal intestinal epithelium (i.e. 'non-patch' (NP) epithelium) and the epithelium near and lining Peyer's patches (PP) (i.e. PP epithelium). A, C, E, G, I: jejunum of controls; B, D, F, H, J, K, L: jejunum on day 4 after MTX. SGLT1 mRNA (A), L-FABP mRNA (C), SI protein (E), GLUT2 protein (G), and L-FABP protein (I) were expressed in the NP- and PP epithelium in controls. Four days after MTX, SGLT1 mRNA (B), L-FABP mRNA (D), SI protein (F), GLUT2 protein (H) and L-FABP protein (J) were expressed at high levels in the PP epithelium, but were not expressed or less expressed in the NP epithelium. L-FABP protein (K) and I-FABP protein (L) were expressed in the PP epithelium and in some cells of the NP epithelium at day 4.



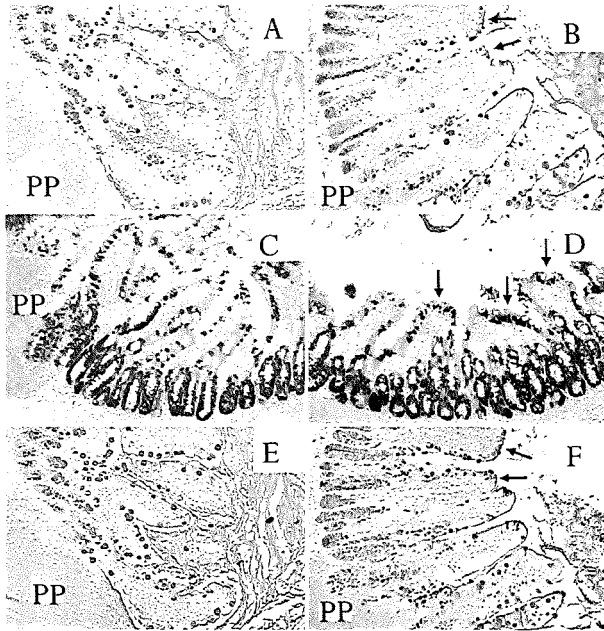


Figure 5.5

Effects of MTX treatment on goblet cell-specific gene expression in the 'non-patch' (NP) epithelium and the epithelium near and lining Peyer's patches (PP). A and E: rat control jejunum; B, C, D, and F, rat jejunum 4 days after MTX treatment. MUC2 protein (A) and TFF3 protein (E) were normally expressed by goblet cells in both the PP- and NP epithelium. Four days after MTX treatment, goblet cell-specific MUC2 mRNA was maintained both in the PP epithelium (C) and NP epithelium (D). MUC2 protein (B) and TFF3 protein (F) expression were also maintained in the PP- and NP epithelium at day 4. Note that in the NP epithelium goblet cells seemed to accumulate at the villus tips (arrows).

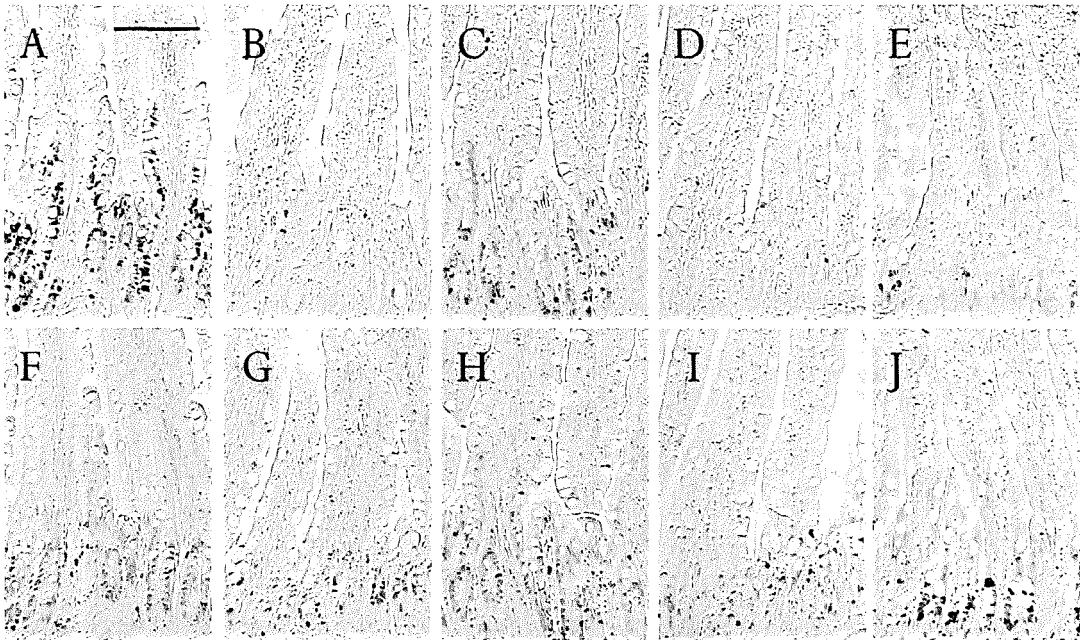


Figure 6.1

Intestinal epithelial proliferation in MTX-treated rats. BrdU-incorporation (A-E) and PCNA-expression (F-J) were localized immunohistochemically in the jejunum of saline-injected rats (A, F) and 48 h after the first MTX injection in single-dose or double-dose treatments. In saline-injected rats, BrdU-positive cells were abundantly present in the crypt region and had migrated partially up the villus in the 24 h following the administration of BrdU (A). In serial sections, epithelial PCNA-expression was confined to the crypts (F). After 30 mg MTX/kg in rats subjected to isolation, BrdU-staining was virtually absent (B) and PCNA-expression was strongly decreased (G), in contrast to group housed rats that received a single dose of 30 mg MTX/kg (C, H). A single dose of 60 mg MTX/kg (D, I) and a fractionated dose of 20 plus 10 mg MTX/kg (E, J) each decreased both BrdU-incorporation and PCNA expression in group housed rats. Bar represents 100  $\mu$ m (A-J).



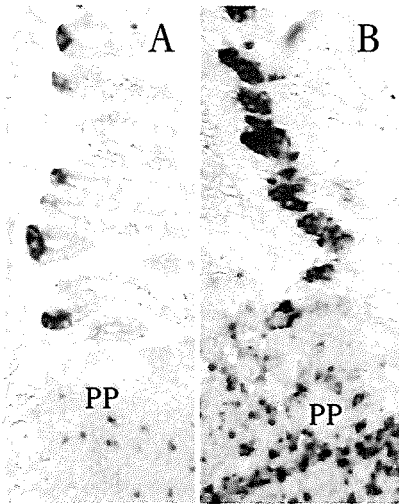


Figure 5.6

Effects of MTX on Paneth cell-specific gene expression in the 'non-patch' (NP) epithelium and the epithelium near and lining Peyer's patches (PP). Lysozyme mRNA was expressed by Paneth cells in the NP- and PP epithelium, and by immunocompetent cells within the PP (A). Two days after MTX treatment lysozyme mRNA seemed to be up-regulated in the NP- and PP epithelium and in immunocompetent cells within the PP.

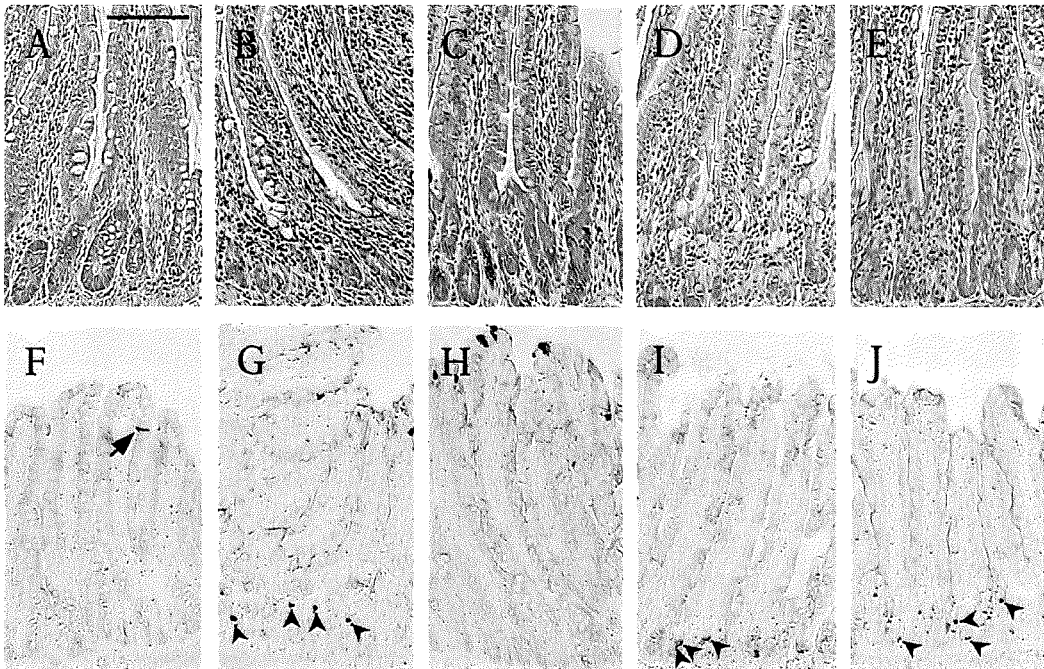
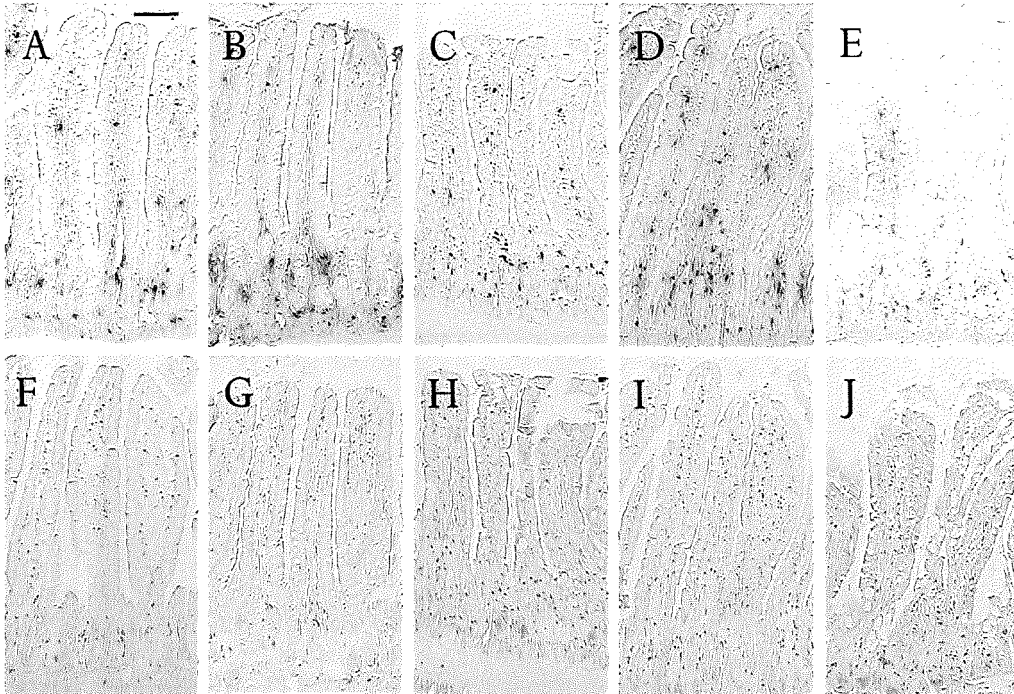


Figure 6.2

Intestinal epithelial morphology and apoptosis in MTX-treated rats. Hematoxylin and eosin staining (A-E) and cleaved caspase-3 expression (F-J) in the jejunum of saline injected rats (A, F) and 48 h after the first MTX-injection in single-dose or double-dose treatments. Crypt damage, characterized by flattened epithelial cells and loss of crypts, was apparent after a single-dose of 30 mg MTX/kg in isolated rats (B), but not in group housed rats (C). A single dose of 60 mg MTX/kg (D) as well as a fractionated dose of 20 mg MTX/kg plus 10 mg MTX/kg (E) each resulted in crypt damage in group housed rats. Cleaved caspase-3 was hardly detected immunohistochemically in the crypts of saline-injected controls (F). In isolated rats, 30 mg MTX/kg resulted in an increase in cleaved caspase-3-staining in the crypt epithelium (G), in contrast to group housed rats (H). Cleaved caspase-3-staining increased in the crypts after a single dose of 60 mg/kg MTX (I) as well as after a fractionated dose of 20 mg MTX/kg plus 10 mg MTX/kg (J) in group housed rats. Bar represents 100  $\mu$ m (A-E), Bar represents 50  $\mu$ m (F-J).



**Figure 6.4**

*Localization of mucosal mast cells in MTX-treated rats. Mucosal mast cells were localized immunohistochemically (A-E) and histochemically (F-J) in serial sections of rat jejunum in saline-injected controls (A, B, F, J) and at 48 h after the MTX-treatment (C-E, H-J). RMCP11-positive mucosal mast cells were localized in the lamina propria of crypts and villi of saline-injected group housed rats (A). Slightly more mucosal mast cells were identified in the villus region using toluidine blue (F). Isolation stress had no effect on the staining patterns of RMCP11 and toluidine blue in saline-injected rats (B, G). There were no changes in the staining patterns of mucosal mast cells after 30 mg MTX/kg in isolated rats (C, H) or group-housed rats (D, I). No changes in mucosal mast cell staining were observed after a fractionated dose of 20 plus 10 mg MTX/kg in group housed rats (E, J). Bar represents 100  $\mu$ m (A-J).*

Table 6.1

Summary of all semi-quantitative results of 6 separate experiments. In experiment 1 isolation-stress was induced in rats by solitary caging, whereas in all other experiments the rats were housed in groups of three animals. In total 14 different events, i.e. characteristic parameters for damage imposed on the intestinal epithelium by MTX were measured as delineated in Materials and Methods. Each parameter of MTX-induced damage was studied in non-Peyer's Patch-associated epithelium (NP) as well as in Peyer's Patch-associated epithelium (PP). The latter was defined as three crypt-villus units of the intestinal epithelium that were immediately adjacent to the Peyer's Patch. Days on which the events occurred are indicated from the start of the MTX-treatment. N.D., not determined; Y, event occurred; N, event did not occur; N.A., not applicable. A, protein was undetectable; B, rats were killed at day 4 after MTX-treatment; C, events occurred at day 2 after MTX-treatment.

Experiment	Stress	MTX (mg/kg)	Number of animals	Reduction proliferation in crypts		Increased cleaved caspase-3		Increased lysozyme experssion		Flattening crypt cells		Reduction crypt length		Depletion Muc2 in crypts		Loss of Golgi-SI	
				1-2		1-2		1-2		1-2		1-2		1-2		1-4	
				NP	PP	NP	PP	NP	PP	NP	PP	NP	PP	NP	PP	NP	PP
Day on which event was observed				NP	PP	NP	PP	NP	PP	NP	PP	NP	PP	NP	PP	NP	PP
1	Yes	30	30	y	n	y	y	y	n	y	n	y	n	y	n	y	n
2	Yes	—	6	n	n	n	n	n	n	n	n	n	n	n	n	n	n
3	No	30+15	12	y	n	y	y	n,A	n	y	n	y	n	y	n	y	n
4	No	30	70	y	n	n	n	n	n	n	n	n	n	n	n	n	n
5	No	45	6	y	n	y	y	y	n	n	n	n	n	n	n	n	n
6	No	60	6	y	n	y	y	y	n	y	n	n	n	n	n	n	n
7	No	20+10	45	y	n	y	y	y	n	y	n	y	n	y	n	y	n

Experiment	Stress	MTX (mg/kg)	Number of animals	Loss of SGLT1 from brush border		Accumulation of Goblet cells on villus tips		Villus shortening		Flattening villus cells		Proliferation on villus		Crypt lengthening		Recovery	
				3-4		3-4		3-4		3-4		5-6		5-6		8-10	
				NP	PP	NP	PP	NP	PP	NP	PP	NP	PP	NP	PP	NP	PP
Day on which event was observed				NP	PP	NP	PP	NP	PP	NP	PP	NP	PP	NP	PP	NP	PP
1	Yes	30	30	y	n	y	n	y	n	y	n	y	n	y	n	y	NA
2	Yes	—	6	n	n	n	n	n	n	n	n	n	n	n	n	NA	NA
3	No	30+15	12	y	n	y	n	y	n	y	n	ND,B		ND,B		ND,B	
4	No	30	70	n	n	n	n	n	n	n	n	y,C	n	n	n	y	NA
5	No	45	6	n	n	n	n	n	n	n	n	y,C	n	n	n	y	NA
6	No	60	6	n	n	n	n	n	n	n	n	y,C	n	n	n	y	NA
7	No	20+10	45	y	n	y	n	y	n	y	n	y	n	y	n	y	NA

## 6 Isolation-stress increases small intestinal sensitivity to chemotherapy in rats

**Background & Aims:** Severe gastrointestinal damage often complicates the use of chemotherapeutic agents such as methotrexate for anti-cancer treatment. Psychological stress is known to be detrimental to normal intestinal physiology. We set out to determine if psychological stress adds to the intestinal damage provoked by chemotherapy.

**Methods:** Rats were treated with various doses of methotrexate and housed either solitary, which induces mental stress, or maintained in groups of three animals. Treatment was evaluated by (immuno)histological parameters

**Results:** Epithelial crypt damage, increased lysozyme expression, decreased sucrase-isomaltase and sodium/glucose transporter 1 expression and pathological changes in mucin and trefoil factor protein expression, could be prevented by avoiding isolation. Enhanced cytotoxicity of methotrexate through isolation was about 2-fold and involved an augmented inhibition of proliferation, increased epithelial apoptosis, increased villus damage and delayed recovery. We could not identify a role for mucosal mast cells in the increased epithelial damage under isolated conditions.

**Conclusions:** The clear beneficial effects of avoiding mental stress on the protection of the intestinal epithelium during cytostatic drug-treatment may be an important element for the treatment of cancer patients.

Published as

Melissa Verburg, Ingrid B. Renes, Hans A. Büller, Alexandra W.C. Einerhand and Jan Dekker.

'Isolation-stress increases small intestinal sensitivity to chemotherapy in rats' in *Gastroenterology* 2003; 124 (3):660-71

### Acknowledgements

We gratefully acknowledge our colleagues for their indispensable contribution in donating antibodies: Dr C. Wilson (St Louis MA, USA) for the matrilysin antibodies, Dr K.Y. Yeh (Shreveport, USA) for the sucrase-isomaltase antibodies, Dr B. Hirayama (Los Angeles, USA) for the SGLT 1 antibodies and Dr D.K. Podolsky (Boston, USA) for the MUC2 as well as the TFF3 antibodies.

## Introduction

The intestinal epithelium forms an active and selective barrier between the intestinal lumen and the body's interior. Any condition that disrupts this protective barrier would allow introduction of potentially life-threatening antigens, microorganisms, and toxins into the systemic circulation. Compromised intestinal functioning may arise in cancer patients treated by chemotherapy, as indicated by symptoms like diarrhea, malabsorption and sepsis (Daniele et al. 2001; Fata et al. 1999; Kohout et al. 1999; Lewis et al. 1982). Studies in rodents showed that the use of cytostatic drugs or irradiation therapy give rise to an inhibition of proliferation in the intestinal epithelium and an increase in intestinal permeability (Devik and Hagen 1973; Nakamaru et al. 1998; Verburg et al. 2000). Furthermore, chemotherapy results in intestinal epithelial damage within 2 days via increased apoptosis in the crypts and continuing cell loss from the villus tips (Verburg et al. 2000). In response to this type of damage, epithelial cells contribute to the preservation of the epithelial barrier via restitution (Lotz et al. 2000), i.e. flattening and migration of cells filling the gaps left behind by dying cells, and through increased secretion of protective mucins, trefoil factors and bactericidal peptides (Verburg et al. 2000). The severity of small intestinal damage by irradiation and cytostatic drugs and the ability of the epithelium to regenerate were shown to be dose-dependent (Ramadan et al. 1988; Taminiau et al. 1980). Our hypothesis, explored in this study, is that environmental factors such as mental stress aggravate the negative effects of cytostatic drugs on intestinal epithelial functions.

In general, any form of stress either physical or mental has pleiotrophic effects on gut morphology and function in humans (Peura 1987). Restraint stress has shown to increase intestinal permeability in epithelial cells, and induce erosive injuries in rat small intestine (Kiliaan et al. 1998; Meddings and Swain 2000; Saunders et al. 1994; Greand et al. 1988; Ren

et al. 2000). There is also evidence from studies in rats that chronic stress impairs the intestinal epithelial barrier function and leads to growth retardation (Santos et al. 2000). In other studies, mental stress evoked by high human activity in the animal facility has led to pathological changes in the epithelial-endothelial barrier in the rat intestinal mucosa (Wilson and Baldwin 1999). An important transducer in stress-related functional disorders of the bowel is formed by the mucosal mast cells. These cells are localized in close proximity to nerve-endings in the lamina propria of the intestine, just beneath the epithelial layer (Stead et al. 1989). Following stimulation, mucosal mast cells secrete a range of biogenic amines and proteases such as histamine and mast cell protease (RMCPH) that were shown to increase both epithelial and endothelial permeability in rat (Wilson and Baldwin 1999; Scudamore et al. 1998; Wilson and Baldwin 1998; Yu and Perdue 2001).

We have previously described the relatively fast induction of Paneth cell-specific lysozyme expression that occurred simultaneously with the anti-proliferative and pro-apoptotic effects of cytostatic drug treatment in the crypt region of the rat small intestine (Verburg et al. 2000). This defensive reaction to chemotherapy-induced damage was followed by an accumulation of goblet cells at the tips of the remnant villi, actively expressing mucin and trefoil factor molecules (Verburg et al. 2000). At the same time, a dramatic and damage-related decrease in gene expression was seen in enterocytes for sodium glucose transporter-1, sucrase-isomaltase, and other important intestinal proteins (Verburg et al. 2002). However, the finding that solitary housed rats were more prone to the cytotoxic actions of methotrexate than their group-housed littermates prompted us to investigate this phenomenon systematically, assuming that the isolation stress was a key trigger that aggravated the damaging actions of cytostatic drugs on the intestine. With the use of (immuno)histochemical methods, we compared single and double MTX-treatments of

various doses in the presence or in the absence of isolation stress, and analyzed the intensity and duration of their effects on epithelial proliferation, cell death, morphology, and expression of specific proteins in the small intestine. The possible contribution of intestinal mucosal mast cells to epithelial damage was investigated.

## Materials and methods

### Animals

A total of 200 male Wistar and WAG/Rij rats (Broekman, Utrecht, The Netherlands), aged 6-8 weeks, were kept in a specific pathogen free environment with free access to water and chow (Hope farms, Woerden, The Netherlands). The animals were randomly assigned to one of the treatment groups in which a single-dose or a double-dose of methotrexate was given, in combination with either group- or solitary housing. The methotrexate (MTX, Ledertrexate SP forte, Cyanamid Benelux, etten-Leur, The Netherlands), dissolved in 0.9% (wt/vol.) NaCl, was injected intravenously under light anesthesia at 9 AM (Day 0). For the double-dose, MTX was injected at two consecutive mornings at 9 AM (Day -1 and Day 0). Control rats received equivalent volumes of 0.9% (wt/vol.) NaCl. Stress was introduced after an acclimatization period of one week by isolation of the group-housed rats into individual cages, immediately following the first MTX- or NaCl injection. The rats remained isolated until they were killed by decapitation at sequential days, until the tenth day after the MTX-treatment. Treatment of group-housed rats was identical in all aspects. During and after the acclimatization period these rats were housed in the same room in small groups, of three colony mates each, and were all three killed at the same time point during the experiment. The following dosages of MTX were used (in mg MTX per kg body weight): three single-doses were used: 1 x 30 mg/kg, 1 x 45 mg/kg, and 1 x 60 mg/kg, and two double-doses were used: 1 x 20 mg/kg followed by 1 x 10 mg/kg, and 1 x 30 mg/kg followed by 1 x 15 mg/kg. To allow analysis

of epithelial cell proliferation, the rats were injected i.p. with 50 mg BrdU /kg body weight (Sigma, St. Louis MO, USA) dissolved in PBS, 24 h prior to decapitation. Segments (5.0 mm) of the jejunum from the anatomical middle of the small intestine as well as jejunal segments containing a Peyer's Patch distal from the middle of the small intestine were excized, fixed in 4% (wt/vol.) paraformaldehyde (Merck, Darmstadt, Germany) dissolved in PBS, and processed for immunohistochemistry according to standard procedures (Verburg et al. 2000). The results obtained in Wistar and WAG/Rij (a Wistar inbred strain) rats were identical. Therefore, we did not further discriminate between the results for these two strains in this article.

**Immunohistochemistry**  
Epithelial proliferation and protein expression were analyzed on paraformaldehyde-fixed tissue sections using standard immunohistochemical methods, as described (Verburg et al. 2000). To assess morphological changes jejunal tissue sections of each rat were routinely stained with hematoxylin and eosin (HE). Proliferation was analyzed on days 1, 2, 3, and 4 after the onset of MTX-treatment by the detection of incorporated BrdU and expression of proliferating cell nuclear antigen (PCNA) on serial sections using the mouse monoclonals anti-BrdU (1:100, Boehringer Mannheim, Mannheim, Germany) and anti-human PCNA (1:1500, Boehringer Mannheim) antibodies, respectively. Apoptosis was analyzed by detection of cleaved caspase-3 (Grossmann et al. 1998), using rabbit polyclonal anti-cleaved caspase-3 antibodies (1:500, Cell Signaling Technology, New England Biolabs, Beverly MA, USA). To detect cleaved caspase-3, antigen unmasking was performed by heating the sections for 10 min at 100°C in 1 mM EDTA, pH 8. As marker of crypt damage, Paneth cell-specific lysozyme expression was localized on day 2 and 3 after the onset of MTX-treatment, using rabbit polyclonal anti-human lysozyme (1:50, DAKO, Glostrup, Denmark).

The role of mucosal mast cells in the development or progression of epithelial damage was investigated on day 2 and 3 after onset of MTX-treatment via localization of rat mast cell protease-II (Scudamore et al. 1998) (RMCP-II) using rabbit polyclonal anti-RMCP-II antibodies (1:1000, Moredun Scientific Limited, Edinburgh, UK). Epithelial damage, characterized by changes in epithelial protein expression, was analyzed on day 4 and 5 after the onset of MTX-treatment, when damage to the small intestinal villi was most prominent (Verburg et al. 2000). The enterocyte-specific expression of sucrase-isomaltase (SI) and sodium glucose transporter-1 (SGLT1) was detected using rabbit polyclonal anti-rat SI (Yeh et al. 1989) (1:6000) and mouse monoclonal anti-rabbit SGLT1 (Hirayama et al. 1991) (1:1000) antibodies, respectively. For goblet cell-specific expression of mucin (Muc2) and trefoil factor 3 (TFF3) we used mouse monoclonal anti-human MUC2 (Podolsky et al. 1986) (1:100) and rabbit polyclonal anti-rat TFF3 (Suemori et al. 1991) (1:6000) antibodies, respectively. As negative controls, parallel sections were incubated with normal rabbit serum instead of the primary antibody. Negative controls were consistently negative.

**Scoring of epithelial damage**  
As markers of crypt epithelial damage we chose 6 parameters of which we showed earlier that these were characteristic of MTX-induced damage in the small intestinal crypt epithelium (Verburg et al. 2000; Verburg et al. 2002; Renes et al. 2002). Each parameter was analyzed semi-quantitatively on (immuno)histochemically stained tissue sections. We used intestinal tissues of days 1 and 2 of the MTX-treated animals and of saline-injected controls. For each marker, tissue sections were stained and 10 crypt/villus units were analyzed per animal. The occurrence of damage in the jejunum of each animal within each experimental group was very uniform and never focal. Attention was paid to the normal intestinal epithelium and the crypt-villus epithelium in close proximity to Peyer's

Patches (PP). In the latter, the three crypt-villus unit were studied, immediately adjacent to the Peyer's Patch, which was defined as Peyer's Patch-associated epithelium in a previous paper (Renes et al. 2002).

1 BrdU-incorporation was considered to be decreased relative to controls, if 3 or less BrdU-positive cells were present per crypt (Renes et al. 2002).

2 A reduction in crypt length of at least 25% relative to the length of the crypts in control animals (normal crypt length, 1.25 mm) was considered as shortened (Verburg et al. 2000). Crypt length was judged using a micrometer on well-oriented crypts.

3 Cell height was judged by eye and the epithelial cells were defined as flattened if the width of the cells was equal to or larger than the height of the cells (Veburg et al. 2000; Renes et al. 2002).

4 Cleaved caspase-3 staining, detected immunohistochemically, was virtually absent in intestinal crypts of saline-injected controls. It was considered increased if more than 5 positive cells were present in each tissue section (Renes et al. 2002).

5 Muc2 depletion was characterized by the complete loss of intracellular staining from crypt goblet cells, as determined by immunohistochemical staining for Muc2 (Verburg et al. 2002; Renes et al. 2002).

6 Lysozyme immuno-detection was considered to be increased if the granular area of the Paneth cells was enlarged relative to controls, and the immunohistochemical staining for lysozyme clearly covered the entire crypt base (Verburg et al. 2000).

Damage to epithelial villus cells was characterized by 5 parameters which were previously identified as characteristic for MTX-induced villus damage (Verburg et al. 2000; Verburg et al. 2002; Renes et al. 2002). Each parameter was analyzed semi-quantitatively on intestinal tissue sections (10 crypt villus units per animal) of days 3 and 4 of the different MTX-treated groups and in saline-injected controls using the following methods.



1 Flattening of epithelial villus cells was determined by criteria as described above for crypt cells.

2 Decreased villus length. The villi were defined as shortened if the villi were at least 25% shorter than villi of control animals (normal villus length, 450  $\mu$ m).

3 Loss of  $\alpha$ 1 immuno-staining in the Golgi region of the villus enterocytes. Typically  $\alpha$ 1 is demonstrated in the Golgi region of villus enterocytes, which is lost upon MTX-treatment (Verburg et al. 2002).

4 Loss of SGLT1 immuno-staining in the brush border of villus enterocytes, whereas SGLT1 is normally abundantly expressed on the brush border of normal enterocytes (Verburg et al. 2002).

5 Accumulation of MUC2-positive and TFF3-positive goblet cells at villus tips (Verburg et al. 2000), as determined by immunohistochemistry for both proteins. Goblet cell accumulation was seen if the goblet cell area was larger than the enterocyte area on villus tips, as judged by comparing  $\alpha$ 1- with MUC2- and TFF3 immuno-staining on adjacent tissue sections.

Regeneration of small intestinal tissue after MTX-treatment was studied through analysis of proliferation and crypt-elongation on days 5 and 6 after MTX-treatment (Verburg et al. 2000). Crypt-elongation was indicated if crypts were at least 25% longer than crypts in controls. The proliferative zone was considered to be enlarged, relative to controls, if PCNA-expression was present within villus enterocytes.

Recovery of the small intestinal epithelium was analyzed on days 8 and 10 in the different MTX-treated animals. Recovery was complete if all the above mentioned characteristics were not different from saline-injected controls. Among the animals within each experimental group the results were uniform using the described criteria. There was no inter-animal variation when considering these criteria and therefore a single score of 'yes' (i.e. characteristic change occurred in each animal of the

group) or 'no' (i.e. characteristic change did not occur in any of the animals of within the group) could be given for the entire group.

#### Mast cell staining

Mucosal mast cells were identified histochemically on tissue sections using a toluidine blue staining method (Stead et al. 1987). Briefly, following treatment with 0.1 M HCl, deparaffinized sections were incubated for 10 days at 37°C in 2% (wt/vol.) toluidine blue (Mochrome, London, UK) dissolved in 0.1 M HCl. After rinsing in 0.1 M HCl sections were dehydrated and mounted in Entellan, (Merck). Toluidine blue-positive mast cells were compared with the immunohistochemical localization of RMCPII on serial sections.

## Results

Isolation of rats increased MTX-induced inhibition of epithelial proliferation

The anti-proliferative effect of MTX in the small intestine was analyzed immunohistochemically through detection of incorporated BrdU and expression of PCNA (Table 6.1). In combination with isolation, a single dose of 30 mg MTX/kg was able to inhibit epithelial proliferation, indicated by the absence of incorporated BrdU (Fig. 6.1 b) and strongly decreased expression of PCNA (Fig. 6.1 g) in the crypt epithelium at days 1 and 2 after MTX, compared with saline-injected controls (Figs 6.1 a and f). In contrast, in group housed rats a single dose of 30 mg MTX/kg did not lead to changes in BrdU-incorporation (Fig. 6.1 c) or PCNA expression (Fig. 6.1 h). When the dosage of MTX was raised to 60 mg MTX/kg in group housed rats, the effects on proliferation were comparable to treatment with a single dose of 30 mg MTX/kg in isolated rats. Likewise, hardly any epithelial cell was BrdU-positive (Fig. 6.1 d), and the number of PCNA-positive cells was strongly reduced (Fig. 6.1 i). A single dose of 45 mg MTX/kg in group housed rats resulted in proliferative changes that were intermediate to doses of 30 mg/kg and 60 mg/kg and were only observed at day 1 after MTX administration (Table 6.1).

Interestingly, when the exposure time of the intestinal mucosa to MTX was increased in group housed rats, using a fractionated administration of 20 mg MTX/kg followed by 10 mg MTX/kg given at two consecutive days, the inhibition of BrdU-incorporation (Fig. 6.1 e) and the decrease in PCNA expression (Fig. 6.1 j) was comparable to single-dose treatments with 30 mg/kg in isolated rats (Figs 6.1 b and g), and single-dose treatments with 60 mg/kg in group housed rats (Figs 6.1 d and i). A further augmented administration of MTX in group housed rats given in pilot studies, using 30 mg MTX/kg plus 15 mg MTX/kg on two consecutive days, appeared highly toxic (Table 6.1). Due to severe malaise, the remaining rats of this group had to be killed at day 4 after the MTX administration.

The duration of inhibited proliferation (in h after the start of the treatment) was dependent on the number of MTX injections and the presence of isolation stress (Table 6.1). In group housed rats, epithelial proliferation resumed at day 3 after single-dose treatments with 30 mg MTX/kg (72 h) and at day 3 after double-dose treatments with 20 plus 10 mg MTX/kg (96 h). In isolated rats, epithelial proliferation resumed at day 4 after single-dose treatments with 30 mg MTX/kg (96 h). Thus, isolation stress delayed the re-occurrence of epithelial proliferation with a period of 24 h, compared to group housed rats. The resumption of epithelial proliferation was always characterized by hyperproliferation, with an enlarged BrdU-positive zone within the epithelium and more extensive PCNA-staining compared to saline-injected rats (Table 6.1). Interestingly, hyperproliferation was apparent even after a single-dose of 30 mg MTX/kg in group housed rats, which did not show initial adverse effects of MTX-treatment, although in this case hyperproliferation was observed at an earlier time point, namely at day 2 (Table 6.1).

Isolation of rats increased

MTX-induced crypt damage

Crypt morphology was analyzed semi-quantitatively on HE-stained tissue sections

(Fig. 6.2). The phase of inhibited proliferation in rats subjected to isolation stress and injected with a single dose of 30 mg MTX/kg was associated with flat appearing crypt epithelial cells and crypt loss (Fig. 6.2 b), compared with saline-injected controls (Fig. 6.2 a). In contrast, in group housed rats there were no signs of damage in terms of cell flattening or crypt atrophy using a single dose of 30 mg/kg MTX (Figs 6.2 c). Increasing the single dose to 60 mg MTX/kg (Figs 6.2 d) or applying a double-dose of 20 plus 10 mg MTX/kg in group housed rats (Figs 6.2 e) both induced crypt epithelial flattening. Double-dose treatments in group housed rats, which appeared highly toxic (30 mg/kg plus 15 mg/kg MTX), resulted in an extensively damaged epithelium, as reflected by the presence of crypt abscesses and erosions (not shown).

The toxicity of MTX, leading to apoptosis in the proliferative zone of the crypt epithelium<sup>7</sup>, was analyzed semi-quantitatively through detection of cleaved caspase-3 immunostaining (Fig 6.2 f-j, Table 6.1). Crypt staining of cleaved caspase-3 appeared dependent on both the dosage of MTX and the treatment schedule (Table 6.1). Although an occasional cleaved caspase-3-positive cell was seen at villus tips, no staining occurred in the crypt epithelium of saline-injected controls (Fig. 6.2 f), irrespective of isolation stress. This reflects the relative low frequency of apoptosis in the crypt epithelium of saline-injected rats. After a single-dose of 30 mg MTX/kg, cleaved caspase-3 was localized in the crypt epithelium in isolated rats (Fig. 6.2 g), but not in group housed rats (Fig. 6.2 h). The numbers of cells positive for cleaved caspase-3, dose-dependently increased in the crypt epithelium of group housed rats, as they appeared more prominent after a single dose of 45 mg MTX/kg (not shown) and 60 mg MTX/kg (Fig. 6.2 i), compared to a 30 mg MTX/kg-dose (Fig. 6.2 h). After a fractionated dose of 20 mg MTX/kg plus 10 mg MTX/kg in group housed rats (Fig. 6.2 j), the detection-level of cleaved caspase-3 was comparable to isolated rats after a single

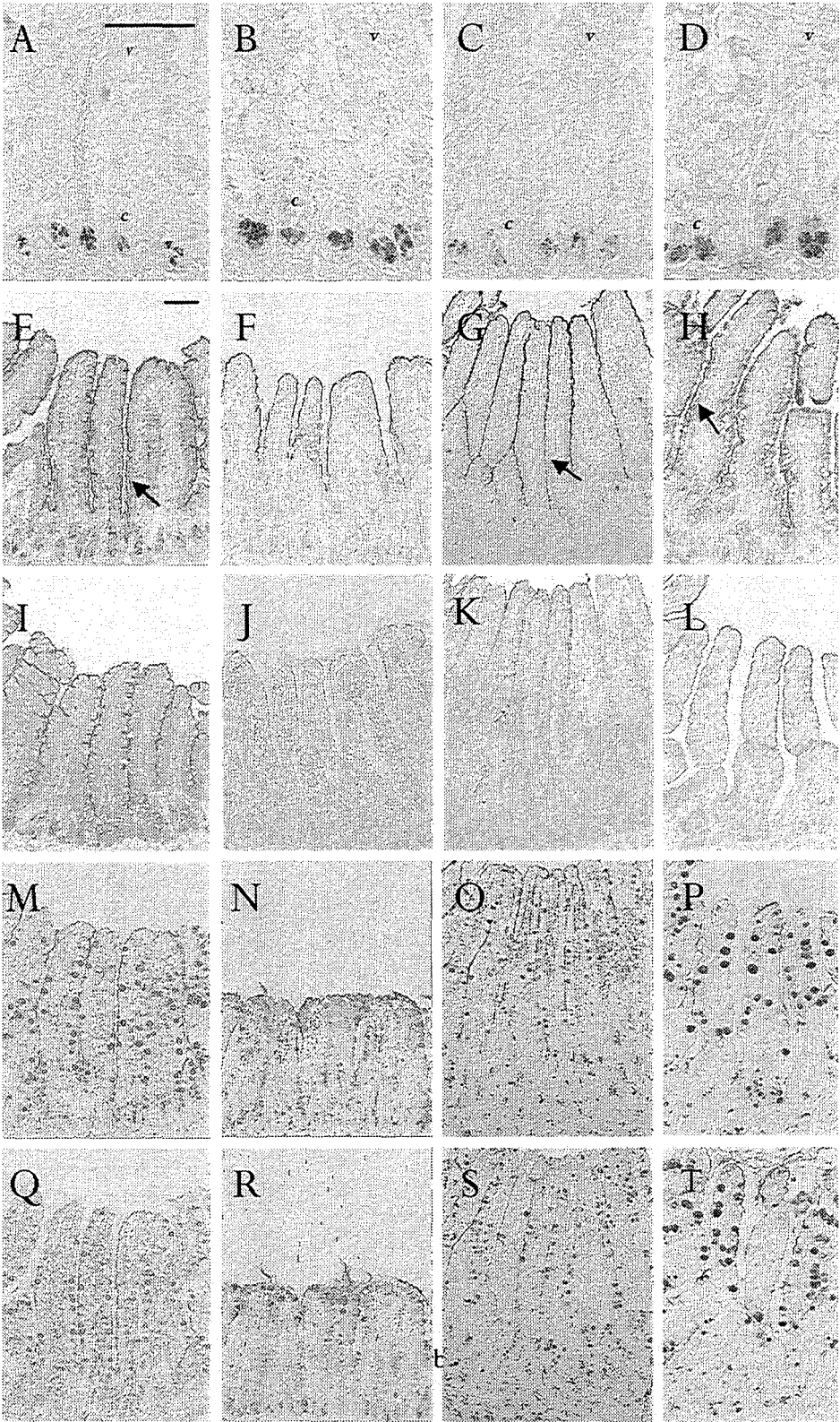
dose of 30 mg MTX/kg (Fig. 6.2 g).

Fractionated doses of MTX which appeared highly toxic (30 plus 15 mg MTX/kg) further increased the amount of caspase-3-immunostaining in the crypt epithelium in group-housed rats (Table 6.1 and data not shown).

Changes in epithelial protein expression are dose and stress dependent

A relative early response of the intestinal epithelium towards MTX-induced crypt damage is a marked up-regulation of lysozyme expression in Paneth cells (Verburg et al. 2000). This induction of lysozyme was analyzed semi-quantitatively at days 1 and 2 in the MTX-treated groups (Table 6.1). In combination with isolation stress, intense lysozyme immunostaining was seen after injection of a single dose of 30 mg MTX/kg (Fig. 6.3 b), compared with saline-injected controls (Fig. 6.3 a). In contrast, no changes in immunostaining for lysozyme were observed in group housed rats treated with a single dose of 30 mg MTX/kg (Fig. 6.3 c). When 60 mg MTX/kg was given in a single dose (Fig. 6.3 d), or when 20 mg MTX/kg plus 10 mg MTX/kg was given on two consecutive days (not shown) an up-regulation of lysozyme expression was equally apparent in group housed rats. When MTX-induced damage appeared highly toxic, such as after a fractionated dose of 30 plus 15 mg MTX/kg in grouped rats, Paneth cell-specific lysozyme expression was no longer detected (not shown).

Consequences of the anti-proliferative effects of MTX for the expression of epithelial proteins along the villi were analyzed at day 3 and 4 after the MTX (Table 6.1). In saline-injected controls, the presence of isolation stress alone did not lead to differences in enterocyte- or goblet cell-specific protein expression (Table 6.1). Epithelial damage to the villus appeared after a single dose of 30 mg MTX/kg in isolated rats, but not after an identical treatment with MTX in group housed rats. For example, si immunostaining in the Golgi region of villus enterocytes, and SGLT1 immunostaining in the brush border of villus enterocytes were both



absent in isolated rats (Fig. 6.3 f, j), but not in group housed rats (Fig. 6.3 g, k). Concomitant with these changes in villus enterocytes, MUC2- and TFF3-positive goblet cells accumulated at villus tips on days 3 and 4 in rats kept in isolation (Fig. 6.3 n, r), but not in group-housed rats (Fig. 6.3 o, s). Despite the inhibited proliferation on days 1 and 2, observed in group housed rats treated with a single dose of 45 or 60 mg MTX/kg (Table 6.1), very little changes were seen on days 3 and 4 in expression of either SI (Fig. 6.3 h) or SGLT1 (Fig. 6.3 l) along the villi. The absence of damage under these regimes was also evident from the near normal distribution of MUC2-positive goblet cells (Fig. 6.3 p) and TFF3-positive goblet cells (Fig. 6.3 t) along the crypt-villus axis in these rats, compared with saline injected controls. Using a fractionated dose of 20 mg/kg plus 10 mg/kg MTX in group housed rats resulted in changes in lysozyme, SI, SGLT1, MUC2 and TFF3 protein expression that were comparable to a single dose of 30 mg MTX/kg in isolated rats (Table 6.1 and data not

shown). A dosage of MTX which was highly toxic (30 mg/kg plus 15 mg MTX/kg in grouped rats) resulted in a virtually complete loss of immuno-reactive proteins from the remaining Paneth cells, enterocytes and goblet cells (not shown).

#### Mucosal mast cells

To identify a possible role for mucosal mast cells in the aggravation of damage in rats submitted to isolation, we localized these cells at 24-72 h after MTX-treatment, during the time window when epithelial damage appeared to either persist or reverse its course. The acid granules of activated or recruited mucosal mast cells in the lamina propria of the small intestine were visualized using toluidine blue (Stead et al. 1987). In addition, a mucosal mast cell specific antibody detecting RMCPII was used on serial sections. Both staining methods recognized similar cells in saline injected controls, irrespective of stress. These mucosal mast cells were present in small groups in the upper crypt region, and as isolated cells along the villus (Fig. 6.4 a, b, f, and g). We did not find differences in the small intestinal localization pattern of mucosal mast cells in MTX-treated versus non-treated rats, irrespective of dose and treatment schedule (Fig. 6.4 c-e and h-j). Representative data are shown in figure 4 for rats at 48 h after the onset of MTX-treatment, however the numbers and staining characteristics of these cells were highly similar when recorded 24 h or 72 h after start of treatment (not shown).

#### Discussion

In this study we used morphological and physiological parameters of the small intestinal epithelium in rats to demonstrate a contribution of psychological factors to the development of intestinal damage evoked by MTX. We showed that a dose of MTX, which is well tolerated by the small intestinal epithelium under specific circumstances (30 mg MTX/kg, group-housing), can lead to severe cell damage when applied in combination isolation. The characteristics of cell damage in the small

**Figure 6.3**  
*Intestinal epithelial protein expression in MTX-treated rats. Lysozyme (A-D), SI (E-H), SGLT1 (I-L), MUC2 (M-P) and TFF3 (Q-T) expression were localized immuno-histochemically in the jejunum of saline-injected rats (A, E, I, M, Q) and at 48 h (B-D) or 96 h (F-H, J-L, N-P, R-T) after the MTX-treatment. Relative to saline-injected rats (A), lysozyme expression was markedly induced after a single-dose of 30 mg MTX/kg in isolated rats (B), but not in group housed rats (C). In group housed rats, increased lysozyme expression was seen after a single dose of 60 mg MTX/kg (D). In saline-injected rats, SI (E) and SGLT1 (I) were localized in the brush border of villus enterocytes. SI was additionally detected in the Golgi region (E, arrow). Serial sections showed expression of MUC2 (M) and TFF3 (Q) by all goblet cells. In combination with isolation stress, a single dose of 30 mg MTX/kg resulted in loss of SI-expression in the Golgi apparatus (F) and loss of SGLT1 from the villus brush border (J). MUC2 (N) and TFF3 expression (R) remained detectable in the goblet cells, but were localized predominantly at villus tips and in the crypts. In group housed rats, a single dose of neither 30 mg MTX/kg (G, K, O, S), nor 60 mg MTX/kg (H, L, P, T) did lead to changes in the expression patterns of SI, SGLT1, MUC2 or TFF3, compared with saline-injected rats. Bar represents 100  $\mu$ m (A-J). C, indicates crypts; V, indicates villus.*

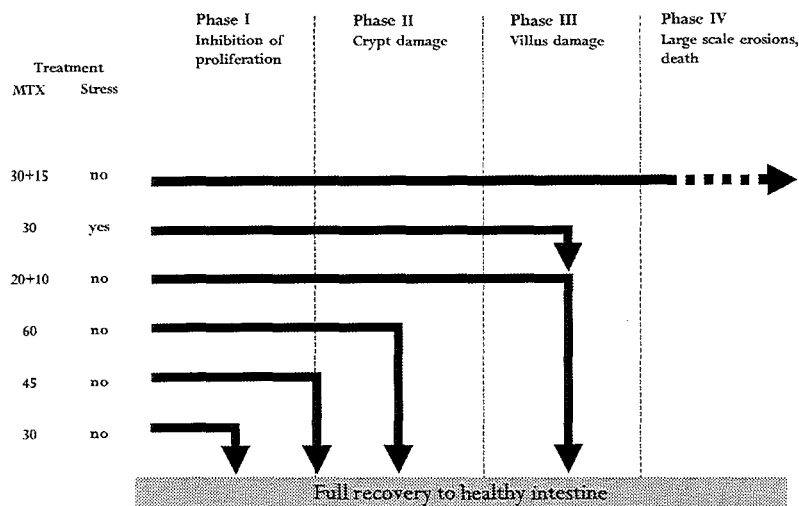


**Figure 6.5**  
Schematic representation of the contribution of isolation stress to the development of chemotherapeutic damage in rat small intestinal epithelium. Single-dose or double-dose MTX injections (indicated as mg/kg) give dose-dependently rise to crypt and subsequent villus damage. Four phases of increasing damage were defined as described in *Materials and Methods and Results*: indicated here as phase I-IV. Dashed arrow indicates the probable death of the animals under study; i.e. animals were killed as result of their bad condition. Two-days MTX treatments were significantly more toxic compared to one-day treatments. Isolation stress increased MTX-toxicity at least two-fold, as deduced from tolerance differences in one-day MTX treatments (30 versus 60 mg/kg) and from tolerance differences in exposure times using total doses of 30 mg MTX/kg (one-day versus two-day treatments).

intestinal epithelium, using this dose, were in agreement with our previous results (Verburg et al. 2000; Verburg et al. 2002; Renes et al. 2002) and involved decreased proliferation and increased apoptosis, as well as changes in the localization of protein expression within enterocytes, goblet cells and Paneth cells.

The contribution of isolation stress to the development of damage in the small intestine can be deduced from differences that were observed in the extent and duration of inhibited proliferation, crypt damage, and villus damage between the different MTX-treatment groups. The sequential effects of damage due to the different MTX treatment protocols have been schematically summarized in Figure 6.5. We showed that a single dose of 30 mg MTX/kg in isolated rats and a single dose of 60 mg MTX/kg in group housed rats had similar effects on epithelial proliferation and crypt damage. Likewise, when the same dosage of MTX (30 mg/kg) was given, the exposure time of MTX to the epithelium could be doubled in group-housed rats compared to isolated rats, before inducing similar changes in epithelial proliferation, apoptosis, morphology and protein expression. Therefore, we conclude that the mental stress as induced by isolation, increased the chemotherapeutic damage about two-fold in rat small intestinal epithelium.

The mechanism through which isolation stress aggravates intestinal epithelial damage remains unknown. There are indications that the development of intestinal epithelial damage is a result of local factors, since the epithelium surrounding Peyer's Patches (PP) appeared protected against MTX-induced damage, in contrast to non-Peyer's Patch (NP) epithelium (Renes et al. 2002). Assuming a similar blood supply to both these areas of the epithelium, it is unlikely that the regional variation in MTX-sensitivity was the result of systemic factors. Therefore, it seems reasonable to assume that also stress-dependent differences in sensitivity towards MTX are the result of local factors.

The mechanisms involved during isolation stress are probably not comparable with physical types of stress, which were demonstrated to have a direct effect on cell proliferation in the intestine (Tutton and Helme 1973). For instance, it has been shown through <sup>3</sup>H-thymidine incorporation that a 12 h period of immobilization stress significantly inhibited cell proliferation in rat small intestine (Greant et al. 1988). Already in the seventies, the consequences of psychologically stressful situations on gastrointestinal morphology and physiology were investigated. The observation by Allen that the formation of a new colony, consisting of wild male and female rats, resulted in the death of 20% of the males within days was striking (Allen 1972). No physical violence had occurred among these animals and death was solely attributed to the massive intestinal ulcerations that had appeared in response to psychological stress. This phenomenon supports our findings, in which an opposite situation, i.e. isolation from the colony, also increased the vulnerability of the intestinal epithelium, compared with animals not suffering the loss of their social environment.

We found in the group-housed rats that increasing the dosage from 30 mg MTX/kg to 60 mg MTX/kg did not result in changes in epithelial protein expression, apart from a

specific rise in lysozyme at the latter dose. However, increasing the exposure time using two treatments instead of one without increasing the total amount of drug (i.e. 30 mg/kg versus 20 plus 10 mg/kg), did affect epithelial protein expression (Fig. 6.5). This is in line with previous results in mice in which a prolonged treatment increased the toxicity of MTX towards the small intestine (Devik and Hagen 1973). Apparently, the period of inhibited proliferation, independently of stress, is one of the major determinants for the development of damage and most probably malfunctioning in the intestinal epithelium. From the observed increase in apoptosis, it seems likely that a prolonged inhibition of epithelial proliferation is associated with increasing loss of stem cells and clonogenic daughter cells, as suggested by others in irradiated mice (Potten et al. 1997). Furthermore, we have observed a specific up-regulation of the mRNA encoding lysozyme during damage in group-housed rats subjected to a two-days (20 plus 10 mg MTX/kg) MTX treatment (Verburg et al. 2002). Thus, it seems highly unlikely that the decreased epithelial protein expression, which develops after prolonged inhibition of epithelial proliferation, results from general inhibitory effects of MTX on *de novo* RNA synthesis.

The observed differences between isolated versus group-housed rats in the development of epithelial damage after single-dose MTX-treatments, could mean that the half-life of the drug may be longer under stressed conditions. However, a perhaps more plausible explanation for this difference could be based on damaging effects of both factors on endothelial cells. In rats, mental stress has been shown to increase the permeability of the microvasculature underneath the epithelium (Wilson and Baldwin 1999). In this study, the reported changes in vascular permeability resulted from an activation of mucosal mast cells. Furthermore, it has recently been shown that irradiation-damage to intestinal stem cells can indirectly evolve from damage of the underlying endothelial cells (Paris et al. 2001).

Thus, in addition to an inhibition of proliferation, chemotherapy in combination with mental stress may aggravate epithelial damage via endothelial malfunctioning.

Despite our efforts, we could not identify a neuronal effect of stress via increased numbers of (activated) mucosal mast cells, at least in our 24 h window at which tissue was analyzed. We used the secretory protease RMCPII to detect all the mucosal mast cells within the mucosa (Kimura et al. 1998), and a marker for the acidic mast cell granules, toluidine blue (Stead et al. 1987). Activated mucosal mast cells that release their contents can be identified at a light microscopical level by their staining with toluidine blue and the presence of large empty vacuoles (Wilson and Baldwin 1999). Also the secreted granules can be visualized using this method (Alexacos et al. 1999). Irrespective of the treatment by MTX, the numbers and appearance of RMCPII- or toluidine-stained mast cells were similar in the small intestinal mucosa. This indicates firstly that there was no influx of mucosal mast cells, and secondly that these cells were not degranulated. It is still possible though that mast cell degranulation may have occurred during the first 24 h of the experiment, and that these degranulated mucosal mast cells had recovered at 24 h after start of treatment. Yet, mast cell degranulation does not seem to play a role at the critical time-window during the experiments, i.e. 48-72 h after the first injection, at which the tissue is apparently damaged beyond repair or is still able to recuperate from the insult.

In conclusion, the impact of psychological factors on intestinal epithelial sensitivity for MTX in the rat may also have implications for the treatment of patients. We have used dosages of MTX that are representative and meaningful to the clinical application of this drug. The enormous variability in side effects of chemotherapy as seen in cancer patients may partially arise from variations in mental status during treatment. It seems therefore important to make an effort to apply the



obtained results in rats to the situation in humans. It is obvious that chemotherapy in daily clinical practice affects the intestinal epithelium. If mental stress may influence the reactions of the intestine to chemotherapeutic drugs, we should use this information to our advantage in the treatment of cancer patients.

Table 7.1

Detailed summary of the effects of Methotrexate on the small intestinal epithelium.

Event	D 0	D 1	D 2	D 3	D 4	D 5	D 6	D 8	D 10
<b>Effects on Proliferation:</b>									
Inhibition of proliferation (absence of PCNA and BrdU)									
Hyper-proliferation (PCNA and BrdU)									
<b>Crypt-located events:</b>									
Crypt apoptosis (TUNEL, cleaved caspase 3)									
Crypt cell loss (number of cells)									
Crypt shortening (crypt length)									
Crypt loss (number of crypts)									
Crypt cell restitution ( cell height < cell width)									
Paneth cell maintenance (number of cells)									
Paneth cell activation (lysozyme increased)									
Crypt goblet cell depletion (Alcian Blue)									
Crypt regeneration (crypt length >100% controls)									
<b>Villus-located events:</b>									
Villus enterocytes cell loss (number of cells)									
Villus shortening (<80% control length)									
Enterocyte restitution (cell height < cell width)									
Enterocyte carbohydrate absorption collapse <sup>1A</sup>									
Enterocyte fatty acid absorption spared <sup>1B</sup>									
Goblet cell sparing (at villus tips)									
Increased goblet cell functions (Muc2 and TFF3)									
Villus regeneration (length > 100% controls)									

Events following MTX administration have been indicated in three categories: 1. general effects on proliferation in the epithelium, 2. crypt-located events, and 3. villus-located events. D1, indicates the effects measured at 24 h after MTX administration, D2 after 48 h after MTX administration, etc. Behind each event, the key observation or key marker(s) is indicated. The original data supporting the events as mentioned in this Table can be found in Chapters 2 and 3. Abbreviations: TUNEL, is terminal transferase deoxyuridine nick-end labeling; PCNA, is proliferating cell nuclear antigen; BrdU, is bromo-deoxyuridine.

<sup>1A</sup>, Measured by the decreased expression of SGLT1, SI, GLUT5, lactase

<sup>1B</sup>, Measured by the relative sparing of enterocyte-located iFABP, LFABP

## 7 Summarizing discussion

In this thesis, we described the specific characteristics of the different epithelial cell types and in the various regions of the small intestine in response to chemotherapy with the use of the rat as a model. In understanding the changes that occur in epithelial functioning during the course of epithelial damage and regeneration, we were able to discriminate two consecutive phases of damage and two consecutive phases of regeneration. Due to the general direction of migration of epithelial cells along the crypt/villus axis, the events that characterize these phases differ in their localization along this axis. That is, damage to crypts occurs first, followed by damage to the villi. Then regeneration occurs in the same order.

The effects of damage and regeneration of the intestinal epithelial functions and the moment at which these were observed are shown in Table 7.1. As long as the epithelial proliferation was inhibited, i.e. during the earliest phase of damage, damage was prominent in the crypts and was characterized by apoptosis of proliferating crypt cells. This loss of epithelial crypt cells resulted in crypt shortening, restitution of the remaining crypt cells, and loss of entire crypts. This 2-days period of crypt damage subsequently gave rise to epithelial damage at the small intestinal villi, most likely due to continued cell death at the villus tips in the absence of replacement of these cells by crypt cells. These villi became blunted, the number of villus enterocytes was severely reduced, whereas goblet cells accumulated at the villus tips. This phase of villus damage coincided with the phase of early regeneration in the crypts, where proliferation resumed. During subsequent late regeneration, the villus epithelium regenerated completely. The regeneration in both crypts and villi were both characterized by a mild hypertrophy of these structures. Crypts as well as villi appeared significantly longer during about 2 days after the regeneration of these respective structures had resumed, and then returned to their control lengths. This hypertrophy was most likely due to the hyperproliferation occurring during early crypt regeneration.

A major determinant for the development of intestinal epithelial damage was the length of time during which the proliferation was inhibited. In adult rat the turnover of the cells of the small intestinal epithelium is 3 days. In our rat model, inhibition of epithelial proliferation for a period of 2 days induced the above described crypt and villus abnormalities, which both disappeared during regeneration (Table 7.1). Shorter periods of inhibited proliferation induced only mild crypt abnormalities which resolved quickly, and without measurable effects on villus structure and functions. Much to our surprise the inhibition of intestinal epithelial proliferation appeared to be under the control of local factors in the intestinal mucosa, in addition to MTX concentrations and treatment regime (see 'Local regulation of intestinal epithelial differentiation'). Also, a mild form of stress, induced by social isolation of the animals, appeared to drastically affect the MTX-induced inhibition of intestinal epithelial proliferation (see 'Intestinal damage and stress').

Epithelial cytoprotection has priority over digestive functions

Of the epithelial cell types, the enterocyte as most abundant cell type appeared to be the most sensitive to chemotherapeutic damage. This cell type is particularly designed for the digestion and absorption of nutrients, which we were able to measure through a selection of the proteins involved in these important functions (Chapter 3 and 4). We have shown that the massive loss of epithelial cells during early damage (day 1-2 after MTX-administration), as well as the changes in enterocyte-specific gene expression during later damage (day 3-4 after MTX-administration), gave rise to a progressively reduced capacity of the small intestinal epithelium to digest and absorb nutrients (Chapter 3-4). On the other hand, in response to these clinically relevant doses of MTX, the cytoprotective properties of Paneth cells and goblet cells remained intact during all phases of damage and regeneration (Chapters 3-4). Importantly, markers for the protective functions of these cell types (i.e. lysozyme,

MUC2 and TFF3) were expressed in significantly higher amounts during severe damage to the epithelium. This adaptation in small intestinal epithelial functioning is very clearly illustrated by our results demonstrated in Chapter 3, where we have shown that goblet cells dominate the small intestinal villi of MTX-treated rats during late phases of damage (Table 7.1). One of our main conclusions from these studies is that the cytoprotection, as exerted by the intestinal epithelium, has a higher priority over the nutrient uptake during severe damage. Apparently, protective functions are of more importance for the survival of the individual rat than nutrient uptake, during this life-threatening event. With respect to possible therapy to alleviate these side effects of chemotherapy, a further stimulation of the cytoprotective properties of the intestinal epithelial cells by administration of exogenous factors during chemotherapy may help to prevent gastrointestinal toxicity from becoming a life-threatening problem (see 'Possible interventions').

Local regulation of intestinal epithelial proliferation and differentiation

The length of the period during which the proliferation was inhibited in the intestinal epithelium appeared to be a major determinant in the further development of intestinal epithelial damage. Strikingly there was one notable exception to this rule, and this was related to the position of the crypt/villus epithelium in the intestine. We demonstrated that the MTX-induced inhibition of intestinal epithelial proliferation was less pronounced in the epithelial crypts in close proximity to the small intestinal Peyer's patches, when compared to the epithelium at more distance from the patch (Chapter 5). Although this zone of protection against MTX-induced damage reached for only 3 crypt/villus units around the Peyer's patch, this protective effect was very distinctive. Apparently, the anti-proliferative effects of MTX can be modified locally in the intestinal epithelium by factors thus far unknown. The local nature of this MTX-resistance, since it was extinct at a distance of 3 crypts

from these lymphoid patches, suggests the involvement of an endogenous diffusible factor, originating from this lymphoid tissue. There is considerable therapeutic potential in identifying the particular factor(s) that mediate this intestinal epithelial protection Peyer's patch-associated epithelium. It should be possible to define in our or other models one or more Peyer's patch-derived cytokines or growth factors that could be used for possible improvement of the existing anti-cancer treatments in patients. The availability of specific knockout mice that lack specific cytokines or growth factors, like the  $IL-10^{-/-}$  mice, offers the possibility of studying this phenomenon in more detail. In these animal it could be determined if the protection near to the Peyer's patches either occurs or not, and thereby one could identify if the knocked out cytokine is involved in this particular form of cytoprotection from MTX.

Presently there are several clues that point towards the involvement of candidate cytokines or growth factors in the cytoprotection near Peyer's patches. Peyer's patches are known to contain low levels of  $IL-12$  in rodents. Therefore, the T cells are strongly biased toward Th2 responses and produce correspondingly immunosuppressive cytokines, such as  $IL-4$ ,  $IL-10$  and TGF-beta (MacDonald and Monteleone 2001). In particular, there are indications that TGF-beta plays a role in epithelial defense against chemotherapeutic damage. In irradiation studies, using the mouse as a model, intraperitoneal injection of commercially available TGF-beta-3 was shown to protect the intestinal epithelium and to enhance survival of the irradiated mice by reducing intestinal stem cell proliferation (Booth et al. 2000). If one or more of the immunosuppressive cytokines plays a role in intestinal epithelial cytoprotection in Peyer's patch-associated rat intestinal epithelium, this MTX-resistance near Peyer's patches might not be observed in humans. In contrast to rodents, human Peyer's patches contain high levels of  $IL-12$  that normally drive a pro-inflammatory Th 1

responses (MacDonald and Monteleone 2001). Nevertheless, it may be worthwhile to investigate if the Peyer's patch-associated epithelium is protected from cytostatic actions of MTX. Be this as it may, the factors that further experiments in rodents might identify could very well have therapeutic use in human cancer patients.

#### Intestinal damage and stress

The variations we observed between groups of differently treated animal, with respect to their housing, in their reaction towards MTX has pointed to a role of the Central Nervous System (CNS) in regulating the proliferation and differentiation of intestinal epithelial cells in response to chemotherapy. This contribution of the CNS, activated by psychological factors (isolation stress), appeared to increase the sensitivity of the intestinal epithelium towards damage when exposed to MTX, via an augmented inhibition of the epithelial proliferation (Chapter 6). The implications of the enhanced intestinal toxicity of MTX in response to environmental stress for cancer patients are that a well-informed treatment with maximal care might considerably help to reduce intestinal damage during chemotherapy.

Information on the mechanism through which stress alone may induce intestinal damage comes mainly from studies that focus on long-term effects of chronic psychological stress, such as the stress induced by water deprivation for repetitive periods of time. This kind of stress leads to mucus depletion, increased bacterial adherence, and increased permeability of the small intestinal epithelium. In mast cell-deficient (Ws/Ws) rats it was shown that mucosal mast cells play a crucial role in the deterioration of these epithelial barrier functions in response to stress. It has become clear in recent years that the role of mucosal mast cells in the gastrointestinal mucosa is not only to react to antigens, but also to actively regulate the barrier and transport properties of the intestinal epithelium.

Mucosal mast cells thus play a role in 'chronic' stress-related mucosal injury. The stress that was induced in rats by exposure to a high human activity in the animal facility room for 3-4 weeks gave rise to significantly higher numbers of degranulated mucosal mast cells and activated goblet cells in the intestinal mucosa (Wilson and Baldwin 1999). Degranulation of mast cells will lead to a reduced barrier function of the epithelium via an increased permeability (Scudamore et al. 1998). Studies in models of hypersensitivity and stress have provided evidence that changes in mucosal function are due to either direct action of mediators released by mast cells on epithelial receptors and/or indirect action via nerves/neurotransmitters (Yu and Perdue 2001). Interestingly, mucosal mast cells seem to have cytoprotective properties in response to chemotherapy. With the use of histochemical methods it was demonstrated that the intestinal epithelium of mast cell deficient (Ws/Ws) rats was significantly more sensitive to irradiation injury, compared to their wild type littermates (Zheng et al. 2000a). Epithelial protection provided by mucosal mast cells could explain why we were unable to identify mucosal mast cell protease activation in our model following acute stress, that is the isolation stress (Chapter 6). It seems likely that mucosal mast cells have deteriorating effects on intestinal function while exposed to chronic stress, whereas mucosal mast cells might actually be protective during exposure to acute stress, like in our experiments. The increased sensitivity of the intestinal epithelium to MTX under stressed conditions is a likely consequence of neuronal signals, coming from the brain, thus directly affecting the intestinal epithelial barrier/proliferation.

#### Possible Interventions

In the recent years, various growth factors, immune mediators, and regulatory peptides have been identified, each of which to some extent seems to contribute to preservation of the intestinal epithelial barrier (e.g. EGF, IGF, TGF-beta, KGF, IL-11, TFF3 and GLP-2). Some of these have shown useful in the preserving

intestinal epithelial integrity during chemotherapeutic damage. The cytoprotective properties of TGF-beta and its receptor were demonstrated in a variety of animal models (Booth et al. 2000; Zheng et al. 2000b; Van't Land et al. 2002). In these studies, different subtypes of TGF-beta protected the small intestinal epithelium of mice against irradiation injury by reducing apoptosis and accelerating healing.

The epithelium-specific growth and differentiation factor keratinocyte growth factor (KGF) is a member of the fibroblast growth factor family, which was shown to specifically enhance goblet cell differentiation in vivo (Bjerknes and Cheng 2001). KGF was recently shown to be effective in chemotherapy-treated mice (Farrell et al. 2002). In these mice, oral administration of KGF resulted in improved crypt survival and preserved villus height. Also, it resulted in an induction in the expression of genes that play a role in mucosal protection such as TFF3. The protective effects of KGF for intestinal epithelial barrier function might imply a similar protection in human patients receiving chemotherapy, indicating that KGF is potentially a therapeutic agent in reducing chemotherapeutic damage.

Interleukin-11 (IL-11) is a pleiotropic cytokine secreted at low levels by mesenchymal cells in the bone marrow microenvironment. The mechanism of the anti-inflammatory activity of rhIL-11 has been extensively studied (Schwertschlag et al. 1999). In vitro, rhIL-11 reduces CD4+ T cell production of Th1 cytokines, such as IFN gamma, while enhancing Th2 and Th3 cytokine production. Thus, the action of IL-11 is immunosuppressive rather than pro-inflammatory. In vitro studies with rat intestinal epithelial cell lines showed that recombinant human IL-11 (rhIL-11) can directly affect intestinal epithelial cells by delaying the entry of cells into the S-phase of the cell cycle, which leads to growth retardation (Peterson et al. 1996). In an in vivo follow up study, mice treated with rhIL-11 showed reduced apoptosis and increased mi-

toses in the small intestine (Orazi et al. 1996). In other studies, rhIL-11 has the potential to prevent intestinal epithelial apoptosis and to enhance survival from 5-FU or radiation-induced damage in mice (Orazi et al. 1996; Potten 1996). Thus, in vivo rhIL-11 may block the proliferation of normal undamaged epithelial cells and thereby protect these cells from cytotoxic damage, while enhancing proliferation following injury. Possibly, IL-11 could be important for improvement of the anti-cancer therapies for human patients.

Another very interesting peptide with respect to possible therapeutic use in chemotherapy is glucagon-like peptide 2 (GLP-2). GLP-2 is an intestinal hormonal peptide expressed by entero-endocrine cells of the intestinal epithelium in response to nutrient ingestion (Drucker 2002a). GLP-2 promotes nutrient absorption via the expansion of the mucosal epithelium by stimulation of crypt cell proliferation and inhibition of apoptosis in the small intestine. The mechanism through which GLP-2 inhibits apoptosis involves reduced caspase activation, as was shown in transfected fibroblasts (Yusta et al. 2000a). GLP-2 also reduces intestinal epithelial permeability.

GLP-2 is enzymatically inactivated by dipeptidyl peptidase IV, hence the native peptide has a  $T_{1/2}$  of minutes in vivo. Experiments with the DPP-IV-resistant analogue H{GLY2}-GLP-2 in rodents have demonstrated its therapeutic potential (Drucker 2002b). For instance, subcutaneous injections of recombinant H{GLY2}-GLP-2 prevented apoptosis and increased crypt proliferation in the small bowel of mice treated with non-steroidal anti-inflammatory drugs (Boushey et al. 1999). Subcutaneous injections of H{GLY2}-GLP-2 have also been shown to enhance recovery in 5-fluorouracil-treated rats (Tavakkolizadeh et al. 2000). In tumor-bearing mice it was further shown that the intestinal epithelial protection of GLP-2 did not impair 5-fluorouracil-mediated tumor regression (Boushey et al. 2001). Thus, GLP-2 specifically protects the intestinal epithelium against chemotherapeutic

damage and is therefore a very interesting peptide. Although clinical experience with GLP-2 is limited, the results obtained in patients with short bowel syndrome who received two injections of human GLP-2 for 35 days are promising (Jeppesen et al. 2001). Whether GLP-2 may be useful for the prevention of chemotherapy induced mucositis in humans will require further study.

The actions of GLP-2 are mediated by a distinct GLP-2 receptor (GLP-2R), which is expressed in a tissue-specific manner in the gastro-intestinal tract (Munroe et al. 1999). In situ hybridization experiments have localized murine GLP-2R to enteric neurons in the gastro-intestinal tract (Bjerknes and Cheng 2001). These authors demonstrated that the nervous system is a key component in mice of a feedback loop regulating epithelial growth and repair by GLP-2. It is possible that this GLP-2R played a role in the enhanced intestinal toxicity of MTX in the intestinal epithelium under stressed conditions, as observed in our study. For instance, the expression and activity of receptors, specific for GLP-2, may have been altered in response to psychological stress. This could lead to reduced sensitivity towards GLP-2 in the intestinal epithelium, which in turn was shown to specifically disturb enterocyte differentiation in vivo (Bjerknes and Cheng 2001). The involvement of GLP-2 or its receptor in MTX-induced damage would thus be independent of mast cells.

#### Concluding remarks

The intestinal toxicity of anti-cancer drug such as MTX remains a serious problem in the treatment of cancer patients. All together, we have identified roles for local, cell type dependent, and psychological factors in the toxicity of MTX for the small intestinal epithelium. The concerted regulation of intestinal epithelial functions via interactions of mucosal neurons, immunomodulatory factors and epithelial factors offers new perspectives in the prevention of damage through chemotherapeutic drugs. The results of our studies may help to improve clinical therapies in the treatment of cancer patients.

## 8 Nederlandse samenvatting

Schade aan het darmepitheel is een bijwerking van chemotherapie ter bestrijding van kanker in patiënten. In dit proefschrift is de reactie van het darmepitheel op chemotherapie beschreven met gebruikmaking van de rat als in vivo model. Chemotherapie wordt toegepast bij patiënten met kanker en is erop gericht om met name de deling van de sneldelende kankercellen te remmen. Een belangrijk nadeel van deze behandelingen is dat er gezonde weefsels bij beschadigd raken die ook een snelle celdeling kennen. In het bijzonder de darm heeft van nature een zeer snelle celdeling en wordt bij chemotherapie snel beschadigd, dat leidt tot ernstige aantasting van het darmepitheel. Hierbij gaan enerzijds functies verloren die essentieel zijn bij de afbraak en opname van voedingsstoffen, maar anderzijds wordt ook de natuurlijke barrièrefunctie van de darm aangetast, dat kan leiden tot het binnendringen van gevaarlijk stoffen en micro-organismen in het lichaam. Wij zijn nagegaan hoe de relatie is tussen de chemotherapie en de ontstane schade en de daarmee gepaard gaande veranderingen in de functies van de darm.

Naast onze belangstelling voor deze ongewenste bijwerking van chemotherapie op het darmepitheel, en het bestuderen van de effecten daarvan op het functioneren van het darmepitheel, leveren deze studies ook inzicht op in de fundamentele mechanisme die een rol spelen bij de instandhouding en het herstel van het epitheel. Door het darmepitheel bloot te stellen aan een situatie waarbij het epitheel bijna verloren gaat is goed waar te nemen welke prioriteiten het epitheel stelt bij het behouden van essentiële functionaliteiten. De beide groepen van darmfuncties, bescherming enerzijds versus afbraak/opname anderzijds, komen in een dergelijk situatie onder druk te staan. Voor beide groepen van functie hebben wij meerdere uitleesparameters in onze studies bestudeerd, zodat goed is vast te stellen of en hoe deze functie optimaal worden uitgevoerd in een dergelijke situatie.

We hebben geëxperimenteerd met verschillende concentraties en behandelingsprotocollen van de cytostatische drug methotrexaat (MTX), een in patiënten veelgebruikt cytostaticum. De totale dosis MTX varieerde van 30



tot 60 mg/kg lichaamsgewicht van de ratten, overeenkomend met doses die ook aan patiënten wordt gegeven. Deze werd als enkele of als gesplitste dosis intraveneus toegediend. Twee van de gebruikte toedieningsprotocollen resulteerde in ernstige en reproduceerbare schade aan het darmepitheel, zoals beschreven in de hoofdstukken 3-6. In deze gevallen bleek het darmepitheel na zeer ernstige schade weer te regenereren tot een volledig functioneel darmepitheel, zoals dat ook in het algemeen in met cytostatica behandelde kankerpatiënten optreedt. Gedurende deze volledige cyclus van ernstige schade tot en met volledige regeneratie, die 6 tot 8 dagen in beslag neemt, ontstaat zo een goed patroon van veranderende beelden, waarbij alle aspecten van functies en herstelmechanismen kunnen worden bestudeerd.

In hoofdstuk 3 richten we de aandacht op de verschillende regio's van de dunne darm, te weten het duodenum, jejunum en ileum. Deze delen van de dunne darm hebben verschillende functies, en het was niet beschreven of deze regio's in gelijke mate gevoelig zijn voor schade door chemotherapie. Daarnaast hebben wij ook de effecten van MTX op de dikke darm bestudeerd, namelijk het proximale colon. Het colon heeft andere functies dan de dunne darm en het is belangrijk om vast te stellen of deze functies in gelijke mate worden aangetast als de dunne darm functies. We toonden metbehulp van (immuno)histochemische technieken aan, dat de celdeling in het dunne darm epitheel na een enkele dosis MTX vrijwel geheel geremd wordt en dat deze na 2 dagen als eerste in het ileum terugkeert en daarna pas in het jejunum en duodenum. We hebben metingen verricht aan de cryptlengte en villushoogten in deze 3 regio's van de dunne darm. We laten zien op basis van deze gegevens en andere kenmerken vastgelegd in coupes van de dunne darm, dat er 4 fases van schade en regeneratie onderscheiden kunnen worden in het dunne darm epitheel.

Achtereenvolgens treden op:

- 1 schade aan de crypten,
- 2 schade aan de villi,
- 3 regeneratie van de crypten en
- 4 regeneratie van de villi.

Deze fases hebben een lokalisatie en een tijdsafhankelijk verloop die zich verplaatst volgens de migratie richting van de epitheelcellen, te weten van de crypt naar de top van de villus. Daarbij was er overlap in de fase van late schade (aan de villus) met die van vroege regeneratie (in de crypt). Verder tonen we kwalitatief (door het immunohistochemisch kleuren van een aantal epitheel functies) en kwantitatief (door het meten van een aantal morfologische kenmerken) aan, dat het gehele dunne darm epitheel binnen een periode van 6-8 dagen hersteld is van de remming in proliferatie door MTX.

De schade die optrad in het cryptepitheel tijdens remming van de celdeling, zoals beschreven in hoofdstuk 3, werd gekenmerkt door een sterk verhoogde apoptose, waarmee beschadigde cellen verwijderd werden. We laten zien, onder anderen door gebruikmaking van immunohistochemische kleuringen met antilichamen tegen het enzym carbamoyl fosfaat synthase op coupes, dat vooral veel enterocyten hierbij verloren gaan. Als reactie op het verlies van epitheelcellen in de crypten trad restitutie op, dat wil zeggen dat de overgebleven cellen door migratie, maar zonder celdeling, de ruimte van de afgestorven cellen innemen. Dit bleek uit het afplatten van resterende crypt epitheelcellen die hiermee helpen voorkomen dat binnendringen van ongewenste stoffen en organismen door het epitheel kan optreden. Ook laten we in dit hoofdstuk 3 zien dat de Paneth cellen, die gelokaliseerd zijn in de basis van de crypten onder de stamcellen, aanwezig blijven na MTX-behandeling. Dit celtype bleek resistent te zijn tegen de schade die MTX aanbrengt en dragen zeer waarschijnlijk bij aan bescherming van de kwetsbare crypten, omdat deze cellen vooral antibacteriële peptiden en enzymen secreteren in het cryptlumen.

Het colon bleek resistent te zijn tegen de gevolgen van MTX toediening (hoofdstuk 3). Weliswaar werd de celdeling in vrijwel gelijke mate geremd als in de dunne darm, maar de gevolgen, in de vorm van verlies aan epitheel cellen en van de functies van deze cellen zoals in de dunne darm, werden niet waargenomen. Dit komt zeer waarschijnlijk omdat de dikke

darm een lager delingstempo kent ten opzichte van de dunne darm. Dit lagere tempo geeft de dikke darm waarschijnlijk langer de gelegenheid om zich te herstellen en weer een geregelde celdeling op gang te brengen, voordat dit consequenties gaat hebben voor de rest van het epitheel.

Ook tonen we in hoofdstuk 3 aan dat naast de Paneth cellen ook de goblet cellen die zich in het crypt en vullis epitheel bevinden relatief resistent zijn tegen epitheliale schade door MTX, in vergelijking tot enterocyten. Dit celtype bleek zich op te hopen op de steeds korter wordende villi, en lijkt zo gespaard te worden bij de algemeen optredende celsterfte waar de enterocyten wel het slachtoffer van worden. Ook de functie van gobletcellen bleef gehandhaafd tijdens epitheliale schade, zoals kon worden afgelezen uit de expressie van de beschermende moleculen MUC2 en TFF3 door deze goblet cellen tijdens fasen van ernstige schade.

In hoofdstuk 4 presenteren we een uitgebreide analyse van de veranderingen die optreden in de celtype-specifieke genexpressie gedurende de 4 fases van schade en regeneratie in het dunne darm epitheel. We hebben hierbij de histologische veranderingen, zoals aangetoond op coupes van het jejunum, vergeleken met kwantitatieve metingen van eiwit en mRNA gehaltes van specifieke markergenen in totaal homogenaten van de verschillende darmsegmenten. Door gebruik te maken van 10 verschillende markergenen hebben we laten zien dat er naast het verlies van epitheelcellen ook veranderingen optreden in de expressie van celtypen-specifieke genen die de functies van deze cellen kenmerken. Daarbij hebben we gebruik gemaakt van statistische methoden om meer inzicht te krijgen in de specificiteit van de gemeten veranderingen. Zo bleek uit de veranderingen in expressie van lactase, sucrase-isomaltase, SGLT1, en GLUT5, dat de resterende enterocyten tijdens vroege en late schade in toenemende mate het vermogen verloren om koolhydraten af te breken en op te nemen. Daarentegen bleven intracellulaire transportfuncties voor transport van vetten, gekenmerkt door door I- en L-FABP expressie in de resterende enterocyten, relatief op peil.

Verder hebben we laten zien dat de expressie van MUC2 en TFF3 in gobletcellen op peil bleef, en zelfs toenam tijdens de fase van ernstige schade aan crypten en villi, zoals beschreven in hoofdstuk 3. Hierbij viel het op dat deze genen, hoewel MUC2 en TFF3 verhoogd tot expressie komen tijdens schade, in goblet cellen onafhankelijk van elkaar gereguleerd werden. Ook de expressie van lysozym, een antibacterieel enzym geproduceerd in Paneth cellen, nam toe tijdens deze fasen van ernstige schade, waarmee de bevindingen uit hoofdstuk 3 bevestigd werden.

Concluderend kunnen we zeggen dat de celtypen en de moleculen die in het dunne darm epitheel aanwezig zijn, die primair gericht lijken te zijn op de verdediging van het epitheel, tijdens schade gehandhaafd blijven (hoofdstukken 3 en 4). Daarnaast zijn met name de enterocyten en de eiwitten die deze cellen tot expressie brengen het sterkst aangetast door de schade door MTX. Wel blijkt dat de eiwitten gericht op de opname van vetten specifiek in veel hogere mate tot expressie komen dan de eiwitten betrokken bij suiker afbraak en opname. Eén en ander geeft aan dat tijdens en na behandeling met cytostatica het mogelijk de voorkeur verdient om juist vetten als energiebron aan de voeding van MTX - behandelde patiënten toe te voegen, in plaats van koolhydraten, die mogelijk veel minder goed zullen worden geabsorbeerd.

Vlak onder het darmepitheel liggen op een aantal plaatsen verspreid in de dunne darm, de zogenaamde Peyerse platen. Dit zijn lymf-follikels en maken deel uit van het darmgeassocieerde immuunsysteem en bevatten grote hoeveelheden cellen van het immuunsysteem. In het door ons gebruikte MTX-model in de rat bleek het epitheel in de nabijheid van Peyerse platen relatief ongevoelig voor schade ten gevolge van MTX, in tegenstelling tot het epitheel op grotere afstand van Peyerse platen. De resultaten hierover worden gepresenteerd in hoofdstuk 5. Met (immuno)histochemische technieken en in situ hybridisatie tonen we daarin aan dat de proliferatie in de crypten nabij Peyerse platen minder geremd werd door MTX dan in het overige darmepitheel. Wel bleek er door bestudering van weefsel-

coupes in de crypten naast de Peyerse platen een gelijke inductie van apoptose op te treden als in de crypten op grotere afstand. We laten zien dat er, ondanks deze effecten van MTX op celdeling en apoptose in de crypten in de nabijheid van de Peyerse platen, geen veranderingen optraden in de morfologie van het epitheel en in de lokalisatie van enterocyte-, goblet- en Paneth celspecifieke mRNAs en eiwitten nabij Peyerse platen.

Het epitheel grenzend aan de Peyerse platen wordt blijkbaar beschermd tegen de schadelijke gevolgen van MTX, ondank het feit dat epitheel enkele honderden micrometers verder van de Peyerse plaat gelegen, wel een cyclus van ernstige schade en regeneratie doormaakt, vergelijkbaar met de schade zoals beschreven in hoofdstukken 3 en 4. Zeer waarschijnlijk is er een factor aanwezig rond de Peyerse platen die beschermend werkt. Door de aard van de cellen in deze structuren lijkt het waarschijnlijk dat het hierbij gaat om een door lymfocyten geproduceerd cytokine. Het vinden van dit nog een dergelijk cytokine zou verstrekkende gevolgen kunnen hebben voor de therapeutische bescherming van darmepitheel tijdens behandeling van patiënten met cytostatica.

In hoofdstuk 6 is beschreven hoe de invloed van psychologische factoren (stress) de schade verergert die MTX aan het darmweefsel kan aanrichten. MTX werd hierbij in verschillende hoeveelheden toegediend aan ratten in klinisch relevante doses. Deze doses werden ofwel eenmalig gegeven of werden gefractioneerd gegeven gedurende twee achtereenvolgende dagen. Vervolgens werden deze ratten aan een zeer milde vorm van omgeving stress blootgesteld. Controle ratten werden na toediening van MTX terug geplaatst in hun oorspronkelijke kooi, samen met de twee ratten waar zij ook oorspronkelijk, voor toediening, de kooi mee deelden. Andere ratten werden na toediening van MTX in een nieuwe kooi gezet, waarbij ze solitair werden gehuisvest. (Immuno)histochemisch gekleurde dunne darmcoupes, afkomstig van de verschillende diergroepen, zijn met elkaar vergeleken, waarbij de parameters werden gebruikt zoals genoemd in voorgaande hoofdstukken 3-5. Het bleek dat

stress de duur van de remming van epitheliale proliferatie verlengde. Ook de daaropvolgende schade aan de epitheelcellen bleek veel ernstiger onder invloed van stress, waaronder het verlies van enterocyten, het afplatten van epitheelcellen, het verkorten van crypten en villi, en de afname in expressie van koolhydraat-afbrekende enzymen en transporter eiwitten. Het bleek dat een dosis van 30 mg/kg lichaamsgewicht zonder stress leidde tot een remming van de proliferatie en een inductie van apoptose in de crypten. Echter, alle andere vormen van schade bleven uit. Dit in tegenstelling tot dieren die de zelfde dosis ontvingen, maar vervolgens solitair werden gehuisvest. Deze laatsten ontwikkelde alle in hoofdstukken 3-5 vermelde vormen van epitheel schade en functieverlies van het epitheel. Deze bevindingen vestigen de aandacht op omgeving stress als mogelijke factor in de behandeling van kankerpatiënten met cytostatica. Mogelijk kan het beperken van stress de darm van deze patiënten in zekere mate beschermen tegen de schade door cytostatica. Samenvattend kunnen een aantal dingen worden aangewezen die van invloed zijn op de schade die MTX aanricht aan het darmepitheel. Allereerst is het duidelijk zo dat de remming van celdeling door MTX niet persé leidt tot schade aan het darmepitheel. Blijkbaar spelen andere locale factoren in de darm of de darmwand daarbij een rol, die kan leiden tot tijdig herstel of tot het 'doorschieten' in de beschreven cyclus van schade en regeneratie. Er zijn twee aanwijzingen in welke richting dit soort stoffen kunnen worden gezocht. De eerste mogelijkheid wijst op een factor uit het immuunsysteem, omdat de Peyerse platen grote resistentie vertonen tegen MTX-geïnduceerde schade. Daarnaast zijn ook factoren die worden geïnduceerd door de activatie van de darm neuronen mogelijke kandidaten voor een mediërende rol in de dit proces. Mogelijk dat één of enkele van onze observaties leidt tot een klinische toepassing, waarbij ofwel de cytostatica beter verdragen kan worden door beperking van de darmschade, ofwel het herstel na ontstane schade kan worden bevorderd.

- Abumrad N, Coburn C, Ibrahim A (1999) Membrane proteins implicated in long-chain fatty acid uptake by mammalian cells: CD36, FATP and FABPM. *Biochim Biophys Acta* 1441:4-13
- Abumrad NA, Sfeir Z, Connelly MA, Coburn C (2000) Lipid transporters: membrane transport systems for cholesterol and fatty acids. *Curr Opin Clin Nutr Metab Care* 3:255-262
- Al-Dewachi HS, Wright NA, Appleton DR, Watson AJ (1980) The effect of a single injection of cytosine arabinoside on cell population kinetics in the mouse jejunal crypt. *Virchows Arch B Cell Pathol Incl Mol Pathol* 34:299-309
- Al-Dewachi HS, Wright NA, Appleton DR, Watson AJ (1977) The effect of a single injection of hydroxyurea on cell population kinetics in the small bowel mucosa of the rat. *Cell Tissue Kinet* 10:203-213
- Alexacos N, Pang X, Boucher W, Cochrane DE, Sant GR, Theoharides TC (1999) Neurotensin mediates rat bladder mast cell degranulation triggered by acute psychological stress. *Urology* 53:1035-1040
- Allen HM (1972) Gastrointestinal erosions in wild rats subjected to 'social stress'. *Life Sci* 11:351-356
- Al-Nafussi AI, Wright NA (1982) The effect of epidermal growth factor (EGF) on cell proliferation of the gastrointestinal mucosa in rodents. *Virchows Arch B Cell Pathol Incl Mol Pathol* 40:63-69
- Alpers DH, Strauss AW, Ockner RK, Bass NM, Gordon JI (1984) Cloning of a cDNA encoding rat intestinal fatty acid binding protein. *Proc Natl Acad Sci U S A* 81:313-317
- Altmann GG (1974) Changes in the mucosa of the small intestine following methotrexate administration or abdominal x-irradiation. *Am J Anat* 140:263-279
- Bach SP, Renahan AG, Potten CS (2000) Stem cells: the intestinal stem cell as a paradigm. *Carcinogenesis* 21:469-476
- Bhalla DK, Murakami T, Owen RL (1981) Microcirculation of intestinal lymphoid follicles in rat Peyer's patches. *Gastroenterology* 81:481-491
- Bjerknes M, Cheng H (2001) Modulation of specific intestinal epithelial progenitors by enteric neurons. *Proc Natl Acad Sci U S A* 98:12497-12502
- Blanchard DK, Budde JM, Hatch GF, 3rd, Wertheimer-Hatch L, Hatch KF, Davis GB, Foster RS, Jr., Skandalakis JE (2000) Tumors of the small intestine. *World J Surg* 24:421-429
- Booth D, Haley JD, Bruskin AM, Potten CS (2000) Transforming growth factor-B<sub>3</sub> protects murine small intestinal crypt stem cells and animal survival after irradiation, possibly by reducing stem-cell cycling. *Int J Cancer* 86:53-59
- Booth D, Potten CS (2001) Protection against mucosal injury by growth factors and cytokines. *J Natl Cancer Inst Monogr* 29:16-20
- Boushey RP, Yusta B, Drucker DJ (2001) Glucagon-like peptide (GLP)-2 reduces chemotherapy-associated mortality and enhances cell survival in cells expressing a transfected GLP-2 receptor. *Cancer Res* 61:687-693
- Boushey RP, Yusta B, Drucker DJ (1999) Glucagon-like peptide 2 decreases mortality and reduces the severity of indomethacin-induced murine enteritis. *Am J Physiol* 277:E937-947
- Bravo R, Macdonald-Bravo H (1987) Existence of two populations of cyclin/proliferating cell nuclear antigen during the cell cycle: association with DNA replication sites. *J Cell Biol* 105:1549-1554
- Brennan PC, Carr KE, Seed T, McCullough JS (1998) Acute and protracted radiation effects on small intestinal morphological parameters. *Int J Radiat Biol* 73:691-698
- Bry L, Falk PG, Midtvedt T, Gordon JI (1996) A model of host-microbial interactions in an open mammalian ecosystem. *Science* 273:1380-1383
- Burant CF, Flink S, DePaoli AM, Chen J, Lee WS, Hediger MA, Buse JB, Chang EB (1994) Small intestine hexose transport in experimental diabetes. Increased transporter mRNA and protein expression in enterocytes. *J Clin Invest* 93:578-585
- Cairnie AB, Lamerton LF, Steel GG (1965) Cell proliferation studies in the intestinal epithelium of the rat. 1. Determination of the kinetic parameters. *Exp Cell Res* 39:528-538
- Castagliuolo I, Lamont JT, Qiu B, Fleming SM, Bhaskar KR, Nikulasson ST, Kornetsky C, Pothoulakis C (1996) Acute stress causes mucin release from rat colon: role of corticotropin releasing factor and mast cells. *Am J Physiol* 271 (5 Pt 1) G884-G892
- Cheng H (1974) Origin, differentiation and renewal of the four main epithelial cell types in the mouse small intestine. IV. Paneth cells. *Am J Anat* 141:521-535
- Cheng H, Leblond CP (1974a) Origin, differentiation and renewal of the four main epithelial cell types in the mouse small intestine. V. Unitarian Theory of the origin of the four epithelial cell types. *Am J Anat* 141:537-561
- Cheng H, Leblond CP (1974b) Origin, differentiation and renewal of the four main epithelial cell types in the mouse small intestine. III. Entero-endocrine cells. *Am J Anat* 141:503-519
- Cohn SM, Roth KA, Birkenmeier EH, Gordon JI (1991) Temporal and spatial patterns of transgene expression in aging adult mice provide insights about the origins, organization, and differentiation of the intestinal epithelium. *Proc Natl Acad Sci U S A* 88:1034-1038
- Cohn SM, Simon TC, Roth KA, Birkenmeier EH, Gordon JI (1992) Use of transgenic mice to map cis-acting elements in the intestinal fatty acid binding protein gene (Fabpi) that control its cell lineage-specific and regional patterns of expression along the duodenal-colonic and crypt-villus axes of the gut epithelium. *J Cell Biol* 119:27-44
- Corpe CP, Boveland FJ, Hoekstra JH, Burant CF (1998) The small intestinal fructose transporters: site of dietary perception and evidence for diurnal and fructose sensitive control elements. *Biochim Biophys Acta* 1402:229-238
- Cox KH, DeLeon DV, Angerer LM, Angerer RC (1984) Detection of mRNAs in sea urchin embryos by in situ hybridization using asymmetric RNA probes. *Dev Biol* 101:485-502
- Daniele B, Secondulfo M, De Vivo R, Pignata S, De Magistris L, Delrio P, Palaia R, Barletta E, Tambaro R, Carratu R (2001) Effect of chemotherapy with 5-fluorouracil on intestinal permeability and absorption in patients with advanced colorectal cancer. *J Clin Gastroenterol* 32:228-230
- Davis PK, Wu G (1998) Compartmentation and kinetics

- of urea cycle enzymes in porcine enterocytes. *Comp Biochem Physiol B Biochem Mol Biol* 119:527-537
- Dekker J, Einerhand A, Büller H (2002a) Carbohydrate malabsorption. In CH L, ed. *Pediatric gastroenterology and nutrition in clinical practice*. New York, USA, Marcel Dekker Inc, 339-374
- Dekker J, Rossen JW, Büller HA, Einerhand AW (2002b) The muc family: an obituary. *Trends Biochem Sci* 27:126-131
- Dekker J, Van Klinken J-W, Tytgat KAMJ, Van den Brink GR, Van de Bovenkamp JHB, Verburg M, Renes IB, Buller HA, Einerhand AWC (1999) regulation of mucin expression in the gastrointestinal tract. In J. Bara YC, M.T. Droy-Lefaix, ed. *Digestive mucus: from research to clinical implications*. Irvin Editions
- Devik F, Hagen S (1973) Effects of X-rays and cytotoxic agents on the cell population of the crypts of the small intestine in mice. Cell proliferation kinetics after single administrations and effects of variations in multiple dose schedules. *Virchows Arch B Cell Pathol* 12:223-237
- Dignass A, Lynch-Devaney K, Kindon H, Thim L, Podolsky DK (1994) Trefoil peptides promote epithelial migration through a transforming growth factor beta-independent pathway. *J Clin Invest* 94:376-383
- Drucker DJ (2002a) Biological actions and therapeutic potential of the glucagon-like peptides. *Gastroenterology* 122:531-544
- Drucker DJ (2002b) Gut adaptation and the glucagon-like peptides. *Gut* 50:428-435
- Drucker DJ, Erlich P, Asa SL, Brubaker PL (1996) Induction of intestinal epithelial proliferation by glucagon-like peptide 2. *Proc Natl Acad Sci USA* 93:7911-7916
- Dudley MA, Hachey DL, Quaroni A, Hutchens TW, Nichols BL, Rosenberger J, Perkinson JS, Cook G, Reeds PJ (1993) In vivo sucrase-isomaltase and lactase-phlorizin hydrolase turnover in the fed adult rat. *J Biol Chem* 268 (18) 13609-13616
- Dutta-Roy AK (2000) Cellular uptake of long-chain fatty acids: role of membrane-associated fatty-acid-binding/transport proteins. *Cell Mol Life Sci* 571:360-372
- Efstathiou JA, Noda M, Rowan A, Dixon C, Chinery R, Jawhari A, Hattori T, Wright NA, Bodmer WF, Pignatelli M (1998) Intestinal trefoil factor controls the expression of the adenomatous polyposis coli-catenin and the E-cadherin-catenin complexes in human colon carcinoma cells. *Proc Natl Acad Sci USA* 95:3122-3127
- Farrell CL, Bready JV, Rex KL, Chen JN, DiPalma CR, Whitcomb KL, Yin S, Hill DC, Wiemann B, Starnes CO, Havill AM, Lu ZN, Aukerman SL, Pierce GF, Thomason A, Potten CS, Ulich TR, Lacey DL (1998) Keratinocyte growth factor protects mice from chemotherapy and radiation-induced gastrointestinal injury and mortality. *Cancer Res* 58:933-939
- Farrell CL, Rex KL, Chen JN, Bready JV, DiPalma CR, Kaufman SA, Rattan A, Scully S, Lacey DL (2002) The effects of keratinocyte growth factor in preclinical models of mucositis. *Cell Prolif* 35 Suppl 1:78-85
- Fata F, Ron IG, Kemeny N, O'Reilly E, Klimstra D, Kelsen DP (1999) 5-fluorouracil-induced small bowel toxicity in patients with colorectal carcinoma. *Cancer* 86:1129-1134
- Fine P, Adler K, Gerstenfeld D (1989) Idiopathic hyperammonemia after high-dose chemotherapy. *Am J Med* 86:629
- Fontaine RN, Gossett RE, Schroeder F, O'Toole BA, Doetschman T, Kier AB (1996) Liver and intestinal fatty acid binding proteins in control and TGF beta 1 gene targeted deficient mice. *Mol Cell Biochem* 159:149-153
- Gaasbeek Janzen JW, Lamers WH, Moorman AF, de Graaf A, Los JA, Charles R (1984) Immunohistochemical localization of carbamoyl-phosphate synthetase (ammonia) in adult rat liver; evidence for a heterogeneous distribution. *J Histochem Cytochem* 32:557-564
- Gill SS, Heuman DM, Mihos AA (2001) Small intestinal neoplasms. *J Clin Gastroenterol* 33:267-282
- Goldman ID, Matherly LH (1985) The cellular pharmacology of methotrexate. *Pharmacol Ther* 28:77-102
- Gordon JI (1993) Understanding gastrointestinal epithelial cell biology: lessons from mice with help from worms and flies. *Gastroenterology* 105:315-324
- Gordon JI (1989) Intestinal epithelial differentiation: new insights from chimeric and transgenic mice. *J Cell Biol* 108:1187-1194
- Gordon JI, Alpers DH, Ockner RK, Strauss AW (1983) The nucleotide sequence of rat liver fatty acid binding protein mRNA. *J Biol Chem* 258:3356-3363
- Greant P, Delvaux G, Willems G (1988) Influence of stress on epithelial cell proliferation in the gut mucosa of rats. *Digestion* 40:212-218
- Grossmann J, Mohr S, Lapentina EG, Fiocchi C, Levine AD (1998) Sequential and rapid activation of select caspases during apoptosis of normal intestinal epithelial cells. *Am J Physiol* 274:G117-124
- Hall C, Youngs D, Keighley MR (1992) Crypt cell production rates at various sites around the colon in Wistar rats and humans. *Gut* 33:1528-1531
- Hall PA, Coates PJ, Ansari B, Hopwood D (1994) Regulation of cell number in the mammalian gastrointestinal tract: the importance of apoptosis. *J Cell Sci* 107:3569-3577
- Hall PA, Levison DA, Woods AL, Yu CC, Kellock DB, Watkins JA, Barnes DM, Gillett CE, Camplejohn R, Dover R, et al. (1990) Proliferating cell nuclear antigen (PCNA) immunolocalization in paraffin sections: an index of cell proliferation with evidence of deregulated expression in some neoplasms. *J Pathol* 162:285-294
- Hendry JH, Potten CS, Ghafoor A, Moore JV, Roberts SA, Williams PC (1989) The response of murine intestinal crypts to short-range promethium-147 beta irradiation: deductions concerning clonogenic cell numbers and positions. *Radiat Res* 118:364-374
- Hirano M, Iwakiri R, Fujimoto K, Sakata H, Ohshima T, Sakai T, Joh T, Itoh M (1995) Epidermal growth factor enhances repair of rat intestinal mucosa damaged by oral administration of methotrexate. *J Gastroenterol* 30:169-176
- Hirayama BA, Lostao MP, Panayotova-Heiermann M, Loo DD, Turk E, Wright EM (1996) Kinetic and specificity differences between rat, human, and rabbit Na<sup>+</sup>/glucose cotransporters (SGLT-1). *Am J Physiol* 270:G919-926
- Hirayama BA, Wong HC, Smith CD, Hagenbuch BA, Hediger MA, Wright EM (1991) Intestinal and renal Na<sup>+</sup>/glucose cotransporters share common structures. *Am J Physiol* 261:C296-304
- Howarth GS, Cool JC, Bourne AJ, Ballard FJ, Read LC (1998) Insulin-like growth factor-1 (IGF-1) stimulates regrowth of the damaged intestine in rats, when administered following, but not concurrent with, methotrexate.

- Growth Factors* 15:279-292
- Howarth GS, Francis GL, Cool JC, Xu X, Byard RW, Read LC (1996) Milk growth factors enriched from cheese whey ameliorate intestinal damage by methotrexate when administered orally to rats. *J Nutr* 126:2519-2530
- Hutchins RR, Bani Hani A, Kojodojo P, Ho R, Snooks SJ (2001) Adenocarcinoma of the small bowel. *ANZ J Surg* 71:428-437
- Hwang ES, Hirayama BA, Wright EM (1991) Distribution of the SGLT1 Na<sup>+</sup>/glucose cotransporter and mRNA along the crypt-villus axis of rabbit small intestine. *Biochem Biophys Res Commun* 181:1208-1217
- Jeppesen PB, Hartmann B, Thulesen J, Graff J, Lohmann J, Hansen BS, Tofte F, Poulsen SS, Madsen JL, Holst JJ, Mortensen PB (2001) Glucagon-like peptide 2 improves nutrient absorption and nutritional status in short-bowel patients with no colon. *Gastroenterology* 120:806-815
- Jeynes BJ, Altmann GG (1978) Light and scanning electron microscopic observations of the effects of sublethal doses of methotrexate on the rat small intestine. *Anat Rec* 191:1-17
- Kanauchi O, Mitsuyama K, Saiki T, Agata K, Nakamura T, Iwanaga T (1998) Preventive effects of germinated barley foodstuff on methotrexate-induced enteritis in rats. *Int J Mol Med* 1:961-966
- Keefe DM, Brealey J, Goland GJ, Cummins AG (2000) Chemotherapy for cancer causes apoptosis that precedes hypoplasia in crypts of the small intestine in humans. *Gut* 47:632-637
- Kiliaan AJ, Saunders PR, Bijlsma PB, Berin MC, Taminiau JA, Groot JA, Perdue MH (1998) Stress stimulates transepithelial macromolecular uptake in rat jejunum. *Am J Physiol* 275:G1037-1044
- Kimura T, Andoh A, Fujiyama Y, Saotome T, Bamba T (1998) A blockade of complement activation prevents rapid intestinal ischaemia-reperfusion injury by modulating mucosal mast cell degranulation in rats. *Clin Exp Immunol* 111:484-490
- Kohout P, Cerman J, Bratova M, Zadak Z (1999) Small bowel permeability in patients with cytostatic therapy. *Nutrition* 15:546-549
- Kralovanszky J, Prajda N (1985) Biochemical changes of intestinal epithelial cells induced by cytostatic agents in rats. *Arch Toxicol Suppl* 8:94-103
- Kraneveld AD, Muis T, Koster AS, Nijkamp FP (1998) Role of mucosal mast cells in early vascular permeability changes of intestinal DTH reaction in the rat. *Am J Physiol* 274 (5 Pt 1):G832-G839
- Krasinski SD, Estrada G, Yeh KY, Yeh M, Traber PG, Rings EH, Buller HA, Verhave M, Montgomery RK, Grand RJ (1994) Transcriptional regulation of intestinal hydrolase biosynthesis during postnatal development in rats. *Am J Physiol* 267:G584-G594
- Lewis IJ, Mainwaring D, Martin J (1982) Enteropathy complicating maintenance therapy in acute lymphoblastic leukaemia. *Arch Dis Child* 57:663-667
- Liaw CC, Liaw SJ, Wang CH, Chiu MC, Huang JS (1993) Transient hyperammonemia related to chemotherapy with continuous infusion of high-dose 5-fluorouracil. *Anticancer Drugs* 4:311-315
- Lindenbergh-Kortleve DJ, Rosato RR, van Neck JW, Nauta J, van Kleffens M, Groffen C, Zwarthoff EC, Drop SL (1997) Gene expression of the insulin-like growth factor system during mouse kidney development. *Mol Cell Endocrinol* 132:81-91
- Loeffler M, Bratke T, Paulus U, Li YQ, Potten CS (1997) Clonality and life cycles of intestinal crypts explained by a state dependent stochastic model of epithelial stem cell organization. *J Theor Biol* 186:41-54
- Logvinova AV, Foehr MW, Pemberton PA, Khazalpour KM, Funk-Archuleta MA, Bathurst IC, Tomei LD (1999) Soy-derived antiapoptotic fractions protect gastrointestinal epithelium from damage caused by methotrexate treatment in the rat. *Nutr Cancer* 33:33-39
- Lopez-Boado YS, Wilson CL, Hooper LV, Gordon JI, Hultgren SJ, Parks WC (2000) Bacterial exposure induces and activates matrilysin in mucosal epithelial cells. *J Cell Biol* 148:1305-1315
- Lotz MM, Rabinovitz I, Mercurio AM (2000) Intestinal restitution: progression of actin cytoskeleton rearrangements and integrin function in a model of epithelial wound healing. *Am J Pathol* 156:985-996
- MacDonald TT, Monteleone G (2001) IL-12 and Th1 immune responses in human Peyer's patches. *Trends Immunol* 22:244-247
- Marshman E, Ottewill PD, Potten CS, Watson AJ (2001) Caspase activation during spontaneous and radiation-induced apoptosis in the murine intestine. *J Pathol* 195:285-292
- Mashimo H, Wu DC, Podolsky DK, Fishman MC (1996) Impaired defense of intestinal mucosa in mice lacking intestinal trefoil factor. *Science* 274:262-265
- Mathews MB, Bernstein RM, Franza BR, Jr., Garrels JI (1984) Identity of the proliferating cell nuclear antigen and cyclin. *Nature* 309:374-376
- Matsuoka Y, Pascall JC, Brown KD (1999) Quantitative analysis reveals differential expression of mucin (MUC2) and intestinal trefoil factor mRNAs along the longitudinal axis of rat intestine. *Biochim Biophys Acta* 1489:336-344
- Maunda KK, Moore JV (1987) Radiobiology and stathmokinetics of intestinal crypts associated with patches of Peyer. *Int J Radiat Biol Relat Stud Phys Chem Med* 51:255-264
- McDermott FT, Roudnew B (1977) Ileal epithelial cell migration after 40% small-bowel resection. Autoradiographic studies in the rat. *Am J Dig Dis* 22:637-640
- Meddings JB, Swain MG (2000) Environmental stress-induced gastrointestinal permeability is mediated by endogenous glucocorticoids in the rat. *Gastroenterology* 119:1019-1028
- Merritt AJ, Potten CS, Kemp CJ, Hickman JA, Balmain A, Lane DP, Hall PA (1994) The role of p53 in spontaneous and radiation-induced apoptosis in the gastrointestinal tract of normal and p53-deficient mice. *Cancer Res* 54:614-617
- Merritt AJ, Allen TD, Potten CS, Hickman JA (1997) Apoptosis in small intestinal epithelial from p53-null mice: evidence for a delayed, p53-independent G2/M-associated cell death after gamma-irradiation. *Oncogene* 14:2759-2766
- Moore JV, Maunda KK (1983) Topographic variations in the clonogenic response of intestinal crypts to cytotoxic treatments. *Br J Radiol* 56:193-199
- Moss SF, Attia L, Scholes JV, Walters JR, Holt PR (1996) Increased small intestinal apoptosis in coeliac disease. *Gut* 39:811-817

- Munroe DG, Gupta AK, Kooshesh F, Vyas TB, Rizkalla G, Wang H, Demchysyn L, Yang ZJ, Kamboj RK, Chen H, McCallum K, Sumner-Smith M, Drucker DJ, Crivici A (1999) Prototypic G protein-coupled receptor for the intestinotrophic factor glucagon-like peptide 2. *Proc Natl Acad Sci U S A* 96:1569-1573
- Nagai Y, Horie T, Awazu S (1993) Vitamin A, a useful biochemical modulator capable of preventing intestinal damage during methotrexate treatment. *Pharmacol Toxicol* 73:69-74
- Nakamaru M, Masubuchi Y, Narimatsu S, Awazu S, Horie T (1998) Evaluation of damaged small intestine of mouse following methotrexate administration. *Cancer Chemother Pharmacol* 41:98-102
- Nicholson DW, Ali A, Thornberry NA, Vaillancourt JP, Ding CK, Gallant M, Gareau Y, Griffin PR, Labelle M, Lazebnik YA, et al. (1995) Identification and inhibition of the ICE/CED-3 protease necessary for mammalian apoptosis. *Nature* 376:37-43
- Nusrat A, Parkos CA, Verkade P, Foley CS, Liang TW, Innis-Whitehouse W, Eastburn KK, Madara JL (2000) Tight junctions are membrane microdomains. *J Cell Sci* 113:1771-1781
- Nyunoya H, Broglie KE, Widgren EE, Lusty CJ (1985) Characterization and derivation of the gene coding for mitochondrial carbamyl phosphate synthetase 1 of rat. *J Biol Chem* 260:9346-9356
- Orazi A, Du X, Yang Z, Kashai M, Williams DA (1996) Interleukin-11 prevents apoptosis and accelerates recovery of small intestinal mucosa in mice treated with combined chemotherapy and radiation. *Lab Invest* 75:33-42
- Ouellette AJ (1999) IV. Paneth cell antimicrobial peptides and the biology of the mucosal barrier. *Am J Physiol* 277:G257-261
- Ouellette AJ (1997) Paneth cells and innate immunity in the crypt microenvironment. *Gastroenterology* 113:1779-1784
- Paris F, Fuks Z, Kang A, Capodiceci P, Juan G, Ehleiter D, Haimovitz-Friedman A, Cordon-Cardo C, Kolesnick R (2001) Endothelial apoptosis as the primary lesion initiating intestinal radiation damage in mice. *Science* 293:293-297
- Payne J, Maher F, Simpson I, Mattice L, Davies P (1997) Glucose transporter Glut 5 expression in microglial cells. *Glia* 21:327-331
- Peterson RL, Bozza MM, Dorner AJ (1996) Interleukin-11 induces intestinal epithelial cell growth arrest through effects on retinoblastoma protein phosphorylation. *Am J Pathol* 149:895-902
- Petschow BW, Carter DL, Hutton GD (1993) Influence of orally administered epidermal growth factor on normal and damaged intestinal mucosa in rats. *J Pediatr Gastroenterol Nutr* 17:49-58
- Peura DA (1987) Stress-related mucosal damage: an overview. *Am J Med* 83:3-7
- Pinkerton CR, Cameron CH, Sloan JM, Glasgow JF, Gwevava NJ (1982) Jejunal crypt cell abnormalities associated with methotrexate treatment in children with acute lymphoblastic leukaemia. *J Clin Pathol* 35:1272-1277
- Podolsky DK, Fournier DA, Lynch KE (1986) Development of anti-human colonic mucin monoclonal antibodies. Characterization of multiple colonic mucin species. *J Clin Invest* 77:1251-1262
- Poelstra K, Bakker WW, Klok PA, Kamps JA, Hardonk MJ, Meijer DK (1997) Dephosphorylation of endotoxin by alkaline phosphatase in vivo. *Am J Pathol* 151:1163-1169
- Poirier H, Degrace P, Niot I, Bernard A, Besnard P (1996) Localization and regulation of the putative membrane fatty-acid transporter (FAT) in the small intestine. Comparison with fatty acid-binding proteins (FABP). *Eur J Biochem* 238:368-373
- Poligeorgis G, Agnantis N, Kottaridis S (1993) Regional intraarterial infusion of methotrexate with leucovorin rescue in a rat tumor model. *Anticancer Res* 13:2193-2199
- Potten CS (1996) Protection of the small intestinal clonogenic stem cells from radiation-induced damage by pretreatment with interleukin 11 also increases murine survival time. *Stem Cells* 14:452-459
- Potten CS, Booth C, Pritchard DM (1997a) The intestinal epithelial stem cell: the mucosal governor. *Int J Exp Pathol* 78:219-243
- Potten CS, Hendry JH (1995) Clonal regeneration studies. In *Radiation and Gut*. Elsevier, 45-59
- Potten CS, Loeffler M (1990) Stem cells: attributes, cycles, spirals, pitfalls and uncertainties. Lessons for and from the crypt. *Development* 110:1001-1020
- Potten CS, Owen G, Hewitt D, Chadwick CA, Hendry H, Lord BI, Woolford LB (1995) Stimulation and inhibition of proliferation in the small intestinal crypts of the mouse after in vivo administration of growth factors. *Gut* 36:864-873
- Potten CS, Owen G, Roberts SA (1990) The temporal and spatial changes in cell proliferation within the irradiated crypts of the murine small intestine. *Int J Radiat Biol* 57:185-199
- Potten CS, Wilson JW, Booth C (1997b) Regulation and significance of apoptosis in the stem cells of the gastrointestinal epithelium. *Stem Cells* 15:82-93
- Powell DW (1981) Barrier function of epithelia. *Am J Physiol* 241:G275-288
- Quaroni A, Isselbacher KJ (1985) Study of intestinal cell differentiation with monoclonal antibodies to intestinal cell surface components. *Dev Biol* 111:267-279
- Ramadan AA, Badr WY, Ali AM (1988) The effect of methotrexate (MTX) on the small intestine of the mouse. 1. A macroscopic study. *Folia Morphol* 36:68-78
- Rand EB, Depaoli AM, Davidson NO, Bell GI, Burant CF (1993) Sequence, tissue distribution, and functional characterization of the rat fructose transporter GLUT5. *Am J Physiol* 264:G1169-1176
- Ren J, Gao J, Ojeas H, Lightfoot SA, Kida M, Brewer K, Harty RF (2000) Involvement of capsaicin-sensitive sensory neurons in stress-induced gastroduodenal mucosal injury in rats. *Dig Dis Sci* 45:830-836
- Renes IB, Verburg M, Bulsing NP, Ferdinandusse S, Buller HA, Dekker J, Einerhand AW (2002) Protection of the Peyer's patch-associated crypt and villus epithelium against methotrexate-induced damage is based on its distinct regulation of proliferation. *J Pathol* 198:60-68
- Rings EH, Krasinski SD, van Beers EH, Moorman AF, Dekker J, Montgomery RK, Grand RJ, Buller HA (1994) Restriction of lactase gene expression along the proximal-to-distal axis of rat small intestine occurs during postnatal development. *Gastroenterology* 106:1223-1232



- Roberts SA, Hendry JH, Potten CS (1995) Deduction of the clonogen content of intestinal crypts: a direct comparison of two-dose and multiple-dose methodologies. *Radiat Res* 141:303-308
- Rubin DC, Ong DE, Gordon JI (1989) Cellular differentiation in the emerging fetal rat small intestinal epithelium: mosaic patterns of gene expression. *Proc Natl Acad Sci USA* 86:1278-1282
- Santos J, Benjamin M, Yang PC, Prior T, Perdue MH (2000) Chronic stress impairs rat growth and jejunal epithelial barrier function: role of mast cells. *Am J Physiol Gastrointest Liver Physiol* 278:G847-854
- Saunders PR, Kosecka U, McKay DM, Perdue MH (1994) Acute stressors stimulate ion secretion and increase epithelial permeability in rat intestine. *Am J Physiol* 267:G794-799
- Schwertschlag US, Trepicchio WL, Dykstra KH, Keith JC, Turner KJ, Dorner AJ (1999) Hematopoietic, immunomodulatory and epithelial effects of interleukin-11. *Leukemia* 13:1307-1315
- Scudamore CL, Jepson MA, Hirst BH, Miller HR (1998) The rat mucosal mast cell chymase, RMCP-II, alters epithelial cell monolayer permeability in association with altered distribution of the tight junction proteins ZO-1 and occludin. *Eur J Cell Biol* 75:321-330
- Shiau YF (1990) Mechanism of intestinal fatty acid uptake in the rat: the role of an acidic microclimate. *J Physiol (Lond)* 421:463-474
- Shields HM, Bates ML, Bass NM, Best CJ, Alpers DH, Ockner RK (1986) Light microscopic immunocytochemical localization of hepatic and intestinal types of fatty acid-binding proteins in rat small intestine. *J Lipid Res* 27:549-557
- Simon TC, Roth KA, Gordon JI (1993) Use of transgenic mice to map cis-acting elements in the liver fatty acid-binding protein gene (Fabpl) that regulate its cell lineage-specific, differentiation-dependent, and spatial patterns of expression in the gut epithelium and in the liver acinus. *J Biol Chem* 268:18345-18358
- Stahl A, Hirsch DJ, Gimeno RE, Punreddy S, Ge P, Watson N, Patel S, Kotler M, Raimondi A, Tartaglia LA, Lodish HF (1999) Identification of the major intestinal fatty acid transport protein. *Mol Cell* 4:299-308
- Stead RH, Dixon MF, Bramwell NH, Riddell RH, Bienenstock J (1989) Mast cells are closely apposed to nerves in the human gastrointestinal mucosa. *Gastroenterology* 97:575-585
- Stead RH, Tomioka M, Quinonez G, Simon GT, Felten SY, Bienenstock J (1987) Intestinal mucosal mast cells in normal and nematode-infected rat intestines are in intimate contact with peptidergic nerves. *Proc Natl Acad Sci USA* 84:2975-2979
- Storch J (1990) A comparison of heart and liver fatty acid-binding proteins: interactions with fatty acids and possible functional differences studied with fluorescent fatty acid analogues. *Mol Cell Biochem* 98:141-147
- Storch J, Thumser AE (2000) The fatty acid transport function of fatty acid-binding proteins. *Biochim Biophys Acta* 1486:28-44
- Suemori S, Lynch-Devaney K, Podolsky DK (1991) Identification and characterization of rat intestinal trefoil factor: tissue- and cell-specific member of the trefoil protein family. *Proc Natl Acad Sci USA* 88:11017-11021
- Sulikowska A, Lewicki Z (1990) Studies on the regeneration of rat intestinal epithelium after exposure to cyclophosphamide. *Mater Med Pol* 22:73-78
- Sweetser DA, Hauft SM, Hoppe PC, Birkenmeier EH, Gordon JI (1988) Transgenic mice containing intestinal fatty acid-binding protein-human growth hormone fusion genes exhibit correct regional and cell-specific expression of the reporter gene in their small intestine. *Proc Natl Acad Sci USA* 85:9611-9615
- Taminiau JA, Gall DG, Hamilton JR (1980) Response of the rat small-intestine epithelium to methotrexate. *Gut* 21:486-492
- Tanaka H, Miyamoto KI, Morita K, Haga H, Segawa H, Shiraga T, Fujioka A, Kouda T, Takedani Y, Hisano S, Fukui Y, Kitagawa K, Takeda E (1998) Regulation of the PepT1 peptide transporter in the rat small intestine in response to 5-fluorouracil-induced injury. *Gastroenterology* 114:714-723
- Tavakkolizadeh A, Shen R, Abraham P, Kormi N, Seifert P, Edelman ER, Jacobs DO, Zinner MJ, Ashley SW, Whang EE (2000) Glucagon-like Peptide 2: A New Treatment for Chemotherapy-Induced Enteritis. *J Surg Res* 91:77-82
- Traber PG (1990) Regulation of sucrase-isomaltase gene expression along the crypt-villus axis of rat small intestine. *Biochem Biophys Res Commun* 173:765-773
- Traber PG, Yu L, Wu GD, Judge TA (1992) Sucrase-isomaltase gene expression along crypt-villus axis of human small intestine is regulated at level of mRNA abundance. *Am J Physiol* 262:G123-130
- Traber PG (1994) Differentiation of intestinal epithelial cells: lessons from the study of intestine-specific gene expression. *J Lab Clin Med* 123:467-477
- Trier JS (1962) Morphological alterations induced by methotrexate in the mucosa of human proximal intestine. *Gastroenterology* 29:5-305
- Tutton PJ, Helme RD (1973) Stress induced inhibition of jejunal crypt cell proliferation. *Virchows Arch B Cell Pathol* 15:23-34
- Tutton PJ, Helme RD (1973) Stress induced inhibition of jejunal crypt cell proliferation. *Virchows Arch B Cell Pathol* 15 (1) 23-34
- Tutton PJ, Helme RD (1974) The influence of adreno-receptor activity on crypt cell proliferation in the rat jejunum. *Cell Tissue Kinet* 7 (2) 125-136
- Tutton PJ (1975a) The influence of cholinergic activity on the mitotic rate in the crypts of Lieberkuhn in rat jejunum. *Clin Exp Pharmacol Physiol* 2 (3) 269-276
- Tutton PJ (1975b) Neural stimulation of mitotic activity in the crypts of Lieberkuhn in rat jejunum. *Cell Tissue Kinet* 8 (3) 259-266
- Tytgat KM, Boveland FJ, Opdam FJ, Einerhand AWC, Büller HA, Dekker J (1995a) Biosynthesis of rat MUC2 in colon and its analogy with human MUC2. *Biochem J* 309: 221-229
- Tytgat KM, Klomp LW, Boveland FJ, Opdam FJ, Van der Wurff A, Einerhand AWC, Büller HA, Strous GJ, Dekker J (1995b) Preparation of anti-mucin polypeptide antisera to study mucin biosynthesis. *Anal Biochem* 226: 331-341
- Van Beers EH, Büller HA, Grand RJ, Einerhand AWC, Dekker J (1995) Intestinal brush border glycohydrolases: structure, function, and development. *Crit Rev Biochem Mol Biol* 30:197-262

- Van Beers EH, Rings EH, Posthuma G, Dingemans MA, Taminiau JA, Heymans HS, Einerhand AW, Büller HA, Dekker J (1998) Intestinal carbamoyl phosphate synthase 1 in human and rat. Expression during development shows species differences and mosaic expression in duodenum of both species. *J Histochem Cytochem* 46:231-240
- Van Klinken BJW, Dekker J, Büller HA, de Bolos C, Einerhand AWC (1997) Biosynthesis of mucins (MUC2-6) along the longitudinal axis of the human gastrointestinal tract. *Am J Physiol* 273:G296-302
- Van Klinken BJW, Dekker J, Büller HA, Einerhand AWC (1995) Mucin gene structure and expression: protection vs. adhesion. *Am J Physiol* 269:G613-627
- Van't Land B, Meijer HP, Frerichs J, Koetsier M, Jager D, Smeets RL, M'Rabet L, Hoijer M (2002) Transforming Growth Factor-beta2 protects the small intestine during methotrexate treatment in rats possibly by reducing stem cell cycling. *Br J Cancer* 87:113-118
- Verburg M, Renes IB, Büller HA, Einerhand AWC, Dekker J (2000a) Paneth and goblet cell-mediated protection of the intestinal epithelium during methotrexate-induced mucositis. Supplement to *Gastroenterology* 118:A826
- Verburg M, Renes IB, Meijer HP, Taminiau JA, Büller HA, Einerhand AW, Dekker J (2000b) Selective sparing of goblet cells and paneth cells in the intestine of methotrexate-treated rats. *Am J Physiol Gastrointest Liver Physiol* 279:G1037-1047
- Verburg M, Renes IB, Van Nispen DJPM, Ferdinandusse S, Jorritsma M, Büller HA, Einerhand AWC, Dekker J (2002) Specific responses in rat small intestinal epithelial mRNA expression and protein levels during chemotherapeutic damage and regeneration. *J Histochem Cytochem* 50:1525-1536
- Waseem NH, Lane DP (1990) Monoclonal antibody analysis of the proliferating cell nuclear antigen (PCNA). Structural conservation and the detection of a nucleolar form. *J Cell Sci* 96:121-129
- Werkheiser WC (1961) Specific binding of 4-amino folic acid analogues by folic acid reductase. *J Biol Chem* 236:888-893
- Wershil BK, Castagliuolo I, Pothoulakis C (1998) Direct evidence of mast cell involvement in *Clostridium difficile* toxin A-induced enteritis in mice. *Gastroenterology* 114 (5):956-964
- Wershil BK (2000) IX. Mast cell-deficient mice and intestinal biology. *Am J Physiol* 278 (3):G343-G348
- Westcarr S, Farshori P, Wyche J, Anderson WA (1999) Apoptosis and differentiation in the crypt-villus unit of the rat small intestine. *J Submicrosc Cytol Pathol* 31:15-30
- Wilson CL, Heppner KJ, Labosky PA, Hogan BL, Matrisian LM (1997) Intestinal tumorigenesis is suppressed in mice lacking the metalloproteinase matrilysin. *Proc Natl Acad Sci U S A* 94:1402-1407
- Wilson CL, Heppner KJ, Rudolph LA, Matrisian LM (1995) The metalloproteinase matrilysin is preferentially expressed by epithelial cells in a tissue-restricted pattern in the mouse. *Mol Biol Cell* 6:851-869
- Wilson CL, Ouellette AJ, Satchell DP, Ayabe T, Lopez-Boado YS, Stratman JL, Hultgren SJ, Matrisian LM, Parks WC (1999) Regulation of intestinal alpha-defensin activation by the metalloproteinase matrilysin in innate host defense. *Science* 286:113-117
- Wilson LM, Baldwin AL (1999) Environmental stress causes mast cell degranulation, endothelial and epithelial changes, and edema in the rat intestinal mucosa. *Microcirculation* 6:189-198
- Wilson LM, Baldwin AL (1998) Effects of environmental stress on the architecture and permeability of the rat mesenteric microvasculature. *Microcirculation* 5:299-308
- Wright NA, Irwin M (1982) The kinetics of villus cell populations in the mouse small intestine. 1. Normal villi: the steady state requirement. *Cell Tissue Kinet* 15:595-609
- Xian CJ, Howarth GS, Mardell CE, Cool JC, Familiari M, Read LC, Giraud AS (1999) Temporal changes in TRF3 expression and jejunal morphology during methotrexate-induced damage and repair. *Am J Physiol* 277:G785-G795
- Xu G, Huan LJ, Khatri IA, Wang D, Bennick A, Fahim RE, Forstner GG, Forstner JF (1992) cDNA for the carboxyl-terminal region of a rat intestinal mucin-like peptide. *J Biol Chem* 267:5401-5407
- Yeh KY, Yeh M, Holt PR (1991) Thyroxine and cortisone cooperate to modulate postnatal intestinal enzyme differentiation in the rat. *Am J Physiol* 260:G371-378
- Yeh KY, Yeh M, Holt PR (1989) Differential effects of thyroxine and cortisone on jejunal sucrase expression in suckling rats. *Am J Physiol* 256:G604-612
- Yogalingam G, Doyle IR, Power JH (1996) Expression and distribution of surfactant proteins and lysozyme after prolonged hyperpnea. *Am J Physiol* 270:L320-330
- Yoshida A, Takata K, Kasahara T, Aoyagi T, Saito S, Hirano H (1995) Immunohistochemical localization of Na(+)-dependent glucose transporter in the rat digestive tract. *Histochem J* 27:420-426
- You G, Lee WS, Barros EJ, Kanai Y, Huo TL, Khawaja S, Wells RG, Nigam SK, Hediger MA (1995) Molecular characteristics of Na(+)-coupled glucose transporters in adult and embryonic rat kidney. *J Biol Chem* 270:29365-29371
- Yu LC, Perdue MH (2001) Role of mast cells in intestinal mucosal function: studies in models of hypersensitivity and stress. *Immunol Rev* 179:61-73
- Yusta B, Boushey RP, Drucker DJ (2000a) The glucagon-like peptide-2 receptor mediates direct inhibition of cellular apoptosis via a cAMP-dependent protein kinase-independent pathway. *J Biol Chem* 275:35345-35352
- Yusta B, Huang L, Munroe D, Wolff G, Fantaski R, Sharma S, Demchyshyn L, Asa SL, Drucker DJ (2000b) Enteroendocrine localization of GLP-2 receptor expression in humans and rodents. *Gastroenterology* 119:744-755
- Zhang Y, Shao JS, Xie QM, Alpers DH (1996) Immunolocalization of alkaline phosphatase and surfactant-like particle proteins in rat duodenum during fat absorption. *Gastroenterology* 110 (2):478-488
- Zheng H, Wang J, Hauer-Jensen M (2000a) Role of mast cells in early and delayed radiation injury in rat intestine. *Radiat Res* 153:533-539
- Zheng H, Wang J, Kotliansky VE, Gotwals PJ, Hauer-Jensen M (2000b) Recombinant soluble transforming growth factor beta type II receptor ameliorates radiation enteropathy in mice. *Gastroenterology* 119:1286-1296

The author of this thesis was born in Amsterdam on January 31, 1968. She attended Primary School at the Instituut Schreuder in Amsterdam. In 1986 she received her gymnasium B diploma at the Chr. Scholengemeenschap Buitenveldert, Amsterdam. In 1987 she finished an initial year of French language and letters at the Vrije Universiteit in Amsterdam, followed by a year of Art History and Archeology at the University of Amsterdam (UvA). In 1988 she decided for the study of Biology, also at the UvA. She spent her graduation practice at the department of Cellular Biology & Histology at the UvA, where she was supervised by Prof.dr. C.J.F. van Noorden and Dr. W.J. Geerts in collaboration with the department of Anatomy & Embryology of Prof.dr. W.H. Lamers at the Amsterdam Medical Center. In 1994 she finished her studies of Biology. Following a year of research experience at the department of Cellular Biology & Histology at the UvA. She started her PhD-project at the department of Pediatric Gastroenterology & Nutrition at the AMC, investigating the various functions of the intestinal epithelium during damage and regeneration in response to chemotherapy. This project was supervised by Prof.dr. H.A. Büller, Dr. A.W.C. Einerhand and Dr. J. Dekker. In 1998 this research group moved to the Erasmus University in Rotterdam where they joined the Laboratory of Pediatrics. In 2003, concluding her PhD project she wrote this thesis at the Erasmus University in Rotterdam.

De schrijfster van dit proefschrift is geboren op 31 januari 1968 te Amsterdam. Het basisonderwijs volgde zij aan het Instituut Schreuder in Amsterdam. In 1986 behaalde zij haar gymnasium B diploma aan de Chr. Scholengemeenschap Buitenveldert in Amsterdam. In 1987 rondde zij de propedeuse af van de studie Franse Taal en Letterkunde aan de Vrije Universiteit van Amsterdam. Vervolgens studeerde zij 1 jaar Kunstgeschiedenis en Archeologie aan de Universiteit van Amsterdam (UvA). In 1988 besloot zij het roer om te gooien en begon aan een studie Biologie, eveneens aan de UvA. Haar afstudeerstage volgde zij bij de vakgroep Celbiologie & Histologie van de UvA o.l.v. Prof.dr. C.J.F. van Noorden en Dr. W.J. Geerts in samenwerking met de vakgroep Anatomie & Embryologie van Prof.dr. W.H. Lamers op het AMC. In 1994 heeft zij de studie Biologie afgerond. Na een jaar als vrijwilligster onderzoekservaring opgedaan te hebben bij haar afstudeergroep kreeg zij een baan bij het laboratorium KinderGastro-enterologie & Voeding van het AMC om aan haar promotie-onderzoek te kunnen beginnen o.l.v. Prof.dr. H.A. Büller, Dr. A.W.C. Einerhand en Dr. J. Dekker. In 1998 is deze onderzoeksgroep verhuisd naar de afdeling Kindergeneeskunde van het Erasmus Medical Center te Rotterdam. In 2003 heeft zij deze opleiding afgerond met het schrijven van dit proefschrift aan het Erasmus MC te Rotterdam waarin de resultaten van het onderzoek zijn samengevat.

# List of publications

- M Verburg, IB Renes, HA Büller, AWC Einerhand, J Dekker. Isolation stress increases small intestinal sensitivity to chemotherapy in rats. *Gastroenterology* 124 (3) 660-671 (2003).
- M Verburg, IB Renes, DJPM van Nispen, S Ferdinandusse, M Jorritsma, HA Büller, AWC Einerhand, J Dekker. Specific responses in rat small intestinal epithelial mRNA expression and protein levels during chemotherapeutic damage and regeneration. *J Histochem Cytochem* 50 (11) 1525-1536 (2002).
- IB Renes, M Verburg, NP Bulsing, S Ferdinandusse, HA Büller, J Dekker, AWC Einerhand. Protection of the Peyer's patch-associated crypt/villus epithelium against methotrexate-induced damage is based on its distinct proliferation kinetics. *J. Pathology* 198 (1) 60-68 (2002).
- IB Renes, M Verburg, DJPM van Nispen, JAJM Taminiau, HA Büller, J Dekker, AWC Einerhand. Epithelial proliferation, cell death, and gene expression in experimental colitis: alterations in carbonic anhydrase 1, mucin MUC2, and trefoil factor 3 expression. *Int J Colorectal Dis*, 17 (5) 317-326 (2002).
- IB Renes, M Verburg, DJPM van Nispen, HA Büller, J Dekker, AWC Einerhand. Distinct epithelial responses in experimental colitis: implications for ionuptake and mucosal protection. *Am J Physiol* 283 (1) G169-179 (2002).
- M Verburg, IB Renes, HP Meijer, JAJM Taminiau, HA Büller, AWC Einerhand, J Dekker. Selective sparing of goblet cells and paneth cells in the intestine of methotrexate-treated rats. *Am J Physiol* 279 (5) G1037-1047 (2000).
- J Dekker, J-W Van Klinken, KAMJ Tytgat, GR Van den Brink, JHB Van de Bovenkamp, M Verburg, IB Renes, HA Büller, AWC Einerhand. Regulation of mucin expression in the gastrointestinal tract. In: *Digestive mucus: from research to clinical implications*. J Bara, Y Christen, MT Droy-Lefaix, eds, Irvin Editions, Neuilly-sur-Seine, France, pp19-32 (2000).
- BJW van Klinken, AWC Einerhand, LA Duits, MK Makkink, KM Tytgat, IB Renes, M Verburg, HA Büller, J Dekker. Gastrointestinal expression and partial cDNA cloning of murine MUC2. *Am J Physiol* 276 (1Pt1) G115-124 (1999).
- WJC Geerts, M Verburg, A Jonker, AT Das, L Boon, R Charles, WH Lamers, CJF Van Noorden. Gender-dependent regulation of glutamate dehydrogenase expression in periportal and pericentral zones of rat liver lobules. *J Histochem Cytochem* 44 (10) 1153-1159 (1996).

De afgelopen jaren heb ik met heel veel fijne collega's en vrienden te maken gehad die allen op hun manier een steentje hebben bijgedragen aan de tot standkoming van dit proefschrift. Hen wil ik allen bedanken voor hun steun en gezelligheid.

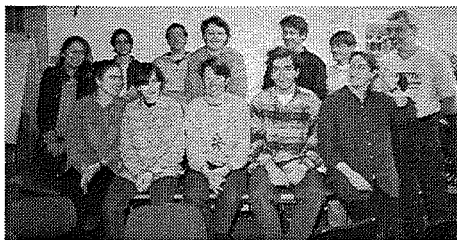
Toen ik eind 1996 aan mijn promotie-onderzoek begon bij de K&G&V telde de groep 3 begeleiders (Jan, Hans, Sandra), 6 AIO's (Kristien, Erik, Jan Willem 1, mijzelf, en korte tijd later Jeroen en Ingrid), en 2 studenten (Jan Willem 3, Helen M). Met heel veel plezier en goede herinneringen denk ik terug aan deze tijd waarin ik samen met Ingrid begon aan het 'schade en regeneratie' project van de groep. Zo klein als de K&G&V indertijd was, hij was nog altijd te groot voor kamer K2-212 waarin we gehuisvest waren. Hoe het ooit allemaal gepast heeft met de steeds groter wordende groep is ondenkbaar, maar gezellig was het zeker. Vooral tijdens de uitstapjes naar Veldhoven met de kadootjes van de farmaceuten, de truc van de consumptiekaart, het bekende diner in Vaeshartelt en (tot aan het vertrek van Erik) de hardlopers. Daarbij schoven na enige tijd ook de klinici Hankje en Rijk aan. Helen M en JW3 hebben na hun stage nog lang als analiste en computer-deskundige in ons midden verkeerd, ware het niet dat ze omwille hun kwaliteiten weggekocht werden door Nutricia (Helen) en (indertijd) Neurozintuigen (JW3). Natuurlijk ook Kristien, terug van weggeweest, en Gijs, jullie allen wil ik bedanken voor de leuke tijd die ik bij de K&G&V op het AMC gehad heb.

De experimenten deden we in de laboratoria van G2 en K2, dat we deelden met de vakgroep Kinder-endocrinologie van Jan de Vijlder en de afdeling Neurozintuigen van Frank Baas. Voor de werkbesprekingen weken we uit naar het Emma kindziekenhuis op de 8e. Daar maakte ik o.a. kennis met Jan Tam, de grondlegger van het methotrexaat-model. Jouw kritische vraag tijdens mijn sollicitatie-voordracht (wat de klinische relevantie was van mijn onderzoek aan de regulatie van genexpressie in de lever) zit nog altijd in mijn hoofd. Altijd bleef jij geïnteresseerd in onze bevindingen en meerdere malen hebben we onze resultaten aan de jouwe getoetst.

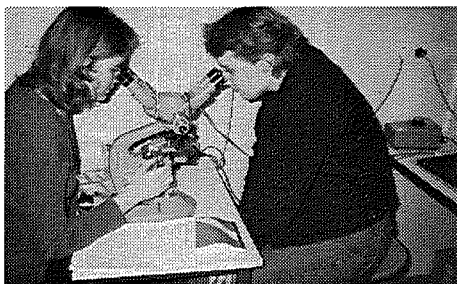
Al voor het project goed en wel op gang was kreeg ik een studente onder mijn hoede. Gelukkig was Ingrid inmiddels ook aan haar onderzoek begonnen en stond ik er niet alleen voor om deze kritische en leergierige Sacha te begeleiden. Uiteindelijk heeft Sacha tijdens haar afstudeerstage bij ons de basis gelegd voor onze publicaties van zowel het mrx- als het dss-model. De door haar tot in de puntjes verzorgde experimenten hebben tot mooie plaatjes geleid die we op menig congres hebben kunnen laten zien. Lieve Sacha, ik ben je erg dankbaar voor je gezelligheid en je werkprestaties. Gefeliciteerd ook met je eigen proefschrift want je bent mij inmiddels ruimschoots voorbij gestreefd. Ook de studentes Esmée en Roos waren in die periode bij onze groep aangeschoven, en niet te vergeten ook Jos, Sandy, Tanja, Chi, Mireille en nog later Louise en Marieke. Marieke heeft ons verder geholpen met de eindeloze reeks kleuringen die nodig was voor een grondige analyse van de schade die we aan de darmen aanbrachten.



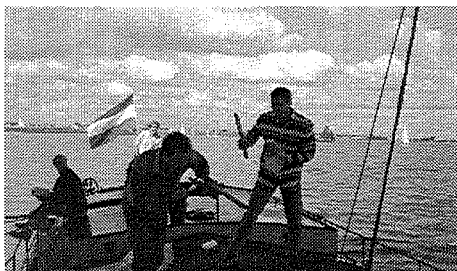
Onze werkkamer K212 in het AMC Amsterdam, 1995-98



De afdeling kindergastroenterologie & voeding (K&G&V) in het AMC Amsterdam, 1997



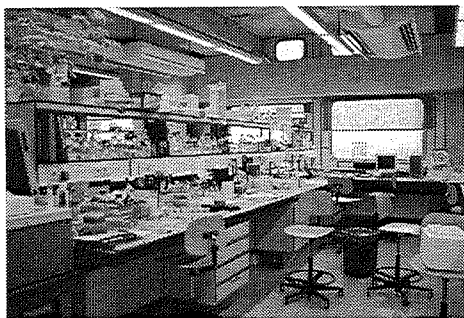
Microscopisch onderzoek met studente Marieke Jorritsma in het AMC Amsterdam, 1998



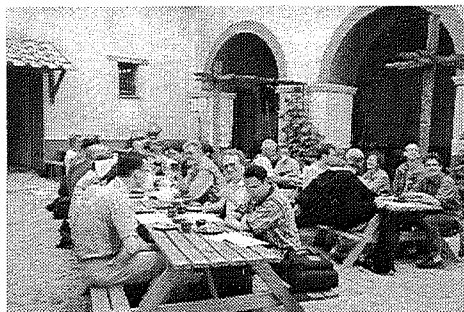
Baguettegevecht (Storm en Erwin) op het IJsselmeer, 1996



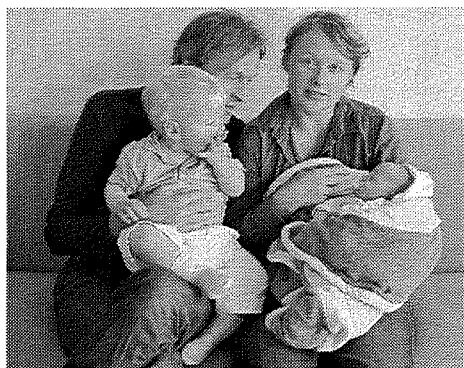




Laboratorium ERASMUS MC, Rotterdam 1998-2003



Labdag kindergeneeskunde in ARCHEON, Alphen 2000



Met Geert, Steven en Florian Thijs, Amsterdam 2003

Heel lief dat je zo met me hebt meegeleefd al die jaren. Dankjewel voor je vriendschap.

Beste Sandra, vooral tijdens de eerste helft van mijn onderzoek heeft jou enthousiasme me vaak opgepept om het vele werk leuk te blijven vinden. Dankzij jou is ook een cruciale fout aan het licht gekomen omtrent de kwantificering van GLUT5. Gelukkig bleef je hardnekkig volhouden dat de onwaarschijnlijke toename van dit eiwit tijdens schade opnieuw gecontroleerd moest worden, alvorens het werk ter publicatie op te sturen. Dankjewel voor de begeleiding die je me door de jaren heen hebt gegeven en voor het bekritisseren en bediscussiëren van mijn manuscripten.

En Beste Hans, het voelt altijd heel vertrouwd om jou kamer binnen te wandelen, ook al gebeurt dat dan weinig. Jou raadgevingen, zoals een 'take home message' geven en 'boven de stof staan', staan in mijn geheugen gegrift. Je hebt me in veel hoedanigheden meegemaakt en ik dank je voor het vertrouwen dat je in me hebt gehouden.

Beste Jan, door de jaren heen ben ik je heel erg gaan waarderen. Toen ik bij de xg&v kwam begreep ik weinig van jou, waaronder je manier van rubriceren en ordenen. Op de computer, in de literatuurmappen, de vriezereinhoud, enz enz. Uren was ik bezig dingen te vinden. Al schrijvende ben ik de logica gaan inzien en ben jou manier van indelen (on)bewust gaan kopiëren. Nu ben ik heel dankbaar dat je mijn begeleider was. Ik heb ontzettend veel van je geleerd. Met een akelige precisie controleerde je mijn formuleringen en met veel geduld heb je me door de manuscripten heen gesleept. Je commentaar was altijd heel duidelijk ('.....snap ik niet!'). Als ik een stuk bij je inleverde, hoopte ik even rust te hebben. Maar helaas had je het vaak de volgende dag al weer gecorrigeerd teruggestuurd. Ook na je verhuizing naar Utrecht bleef je zo accuraat. Jou kwaliteiten in het maken van simpele figuren zijn benut bij het samenstellen van dit proefschrift. Verder zijn jou bijdragen aan de inhoud van dit proefschrift -voor de kenner- op meerdere plaatsen duidelijk terug te vinden. Ik wens je veel geluk met Marja, Mark, Tim, en Iris, bedankt voor alles.

Lieve Jaap, dankzij jou is het proefschrift een prachtig boekwerk geworden. Bij ons thuis werkte je met een krijsend kind op schoot of op de achtergrond onverstoorbaar door aan de vormgeving van dit oeuvre. Ook mijn ouders wil ik bedanken, dat ze er altijd voor me waren. En mijn broer Michiel die mij altijd uitdaagde het onderzoek in begrijpelijke taal uit te leggen. En natuurlijk Geert. Eindelijk krijgt hij een vrouw die niet bezig is met de afronding van haar proefschrift. Lieve Steven en lieve Florian, van binnen en van buiten hebben jullie de rijping van dit proefschrift meegeemaakt, bedankt dat jullie er zijn!